

# Optics in the relativistic regime

Gerard A. Mourou\*

*Center for Ultrafast Optical Science and FOCUS Center, University of Michigan, Ann Arbor, Michigan 48109, USA  
and Laboratoire d'Optique Appliquée, UMR 7639 ENSTA, Ecole Polytechnique, CNRS, Chemin de la Hunière, F-91761 Palaiseau CEDEX, France*

Toshiki Tajima

*Kansai Photon Science Institute, Japan Atomic Energy Agency, 8-1 Umemidai, Kizu, Souraku, Kyoto, 619-0215 Japan*

Sergei V. Bulanov

*Kansai Photon Science Institute, Japan Atomic Energy Agency, 8-1 Umemidai, Kizu, Souraku, Kyoto, 619-0215 Japan  
and A. M. Prokhorov General Physics Institute of Russian Academy of Sciences, Moscow 119991, Russia*

(Published 28 April 2006)

The advent of ultraintense laser pulses generated by the technique of chirped pulse amplification (CPA) along with the development of high-fluence laser materials has opened up an entirely new field of optics. The electromagnetic field intensities produced by these techniques, in excess of  $10^{18}$  W/cm<sup>2</sup>, lead to relativistic electron motion in the laser field. The CPA method is reviewed and the future growth of laser technique is discussed, including the prospect of generating the ultimate power of a zettawatt. A number of consequences of relativistic-strength optical fields are surveyed. In contrast to the nonrelativistic regime, these laser fields are capable of moving matter more effectively, including motion in the direction of laser propagation. One of the consequences of this is wakefield generation, a relativistic version of optical rectification, in which longitudinal field effects could be as large as the transverse ones. In addition to this, other effects may occur, including relativistic focusing, relativistic transparency, nonlinear modulation and multiple harmonic generation, and strong coupling to matter and other fields (such as high-frequency radiation). A proper utilization of these phenomena and effects leads to the new technology of relativistic engineering, in which light-matter interactions in the relativistic regime drives the development of laser-driven accelerator science. A number of significant applications are reviewed, including the fast ignition of an inertially confined fusion target by short-pulsed laser energy and potential sources of energetic particles (electrons, protons, other ions, positrons, pions, etc.). The coupling of an intense laser field to matter also has implications for the study of the highest energies in astrophysics, such as ultrahigh-energy cosmic rays, with energies in excess of  $10^{20}$  eV. The laser fields can be so intense as to make the accelerating field large enough for general relativistic effects (via the equivalence principle) to be examined in the laboratory. It will also enable one to access the nonlinear regime of quantum electrodynamics, where the effects of radiative damping are no longer negligible. Furthermore, when the fields are close to the Schwinger value, the vacuum can behave like a nonlinear medium in much the same way as ordinary dielectric matter expanded to laser radiation in the early days of laser research.

DOI: [10.1103/RevModPhys.78.309](https://doi.org/10.1103/RevModPhys.78.309)

PACS number(s): 41.75.Jv, 52.38.-r, 52.40.Mj

## CONTENTS

|   |     |   |     |
|---|-----|---|-----|
| I. Introduction   | 310 | 2. The petawatt   | 315 |
| II. Ultrahigh-Intensity Lasers: The Chirped Pulse Amplification Technique | 311 | E. Optical parametric chirped pulse amplification   | 315 |
| A. Amplification—the energy extraction condition                          | 312 | 1. Temporal quality: prepulse energy contrast   | 316 |
| B. Amplification—the propagation condition                                | 312 | 2. Pulse cleaning   | 317 |
| C. The CPA concept  | 313 | F. Spatial quality: deformable mirrors  | 318 |
| D. The key element: the matched stretcher-compressor                      | 313 | G. Theoretical power and intensity limits   | 318 |
| 1. New materials for CPA and gain narrowing                               | 315 | H. The smallest relativistic laser—the $\lambda^3$ laser and carrier-envelope phase control         | 318 |
|   |     | I. The largest relativistic laser—the zettawatt laser   | 320 |
|   |     | J. New amplification techniques: plasma compression   | 320 |
|   |     | K. Average power  | 320 |
|   |     | III. Ultrahigh-Intensity Laser Regimes: Extending the Field of Laser Physics from the eV to the TeV | 321 |
|   |     | A. Introduction   | 321 |

\*Electronic address: Gerard.Mourou@ensta.fr

|       |  |     |
|-------|--|-----|
| B.    | Similarities and differences between bound-electron and relativistic nonlinear optics              | 322 |
| C.    | Relativistic rectification or wakefield effect   | 322 |
| D.    | Scattering in the relativistic regime  | 323 |
| IV.   | Relativistically Strong Electromagnetic and Langmuir Waves in a Collisionless Plasma               | 323 |
| A.    | Wakefield generation and relativistic electron acceleration  | 325 |
| B.    | Relativistic self-focusing   | 327 |
| C.    | Relativistic transparency and pulse shaping  | 330 |
| D.    | Relativistic self-induced transparency of short electromagnetic wave packets in underdense plasmas | 332 |
| E.    | Relativistic solitons  | 332 |
| F.    | High-order harmonic generation   | 337 |
| V.    | Interaction of Charged Particles with Electromagnetic Waves in the Radiation-Dominant Regime       | 339 |
| VI.   | Relativistic Engineering   | 341 |
| A.    | Flying mirrors   | 341 |
| B.    | Efficient attosecond phenomena in the relativistic $\lambda^3$ regime                              | 344 |
| VII.  | Nuclear Physics  | 345 |
| A.    | Rutherford, Livermore, Michigan, Osaka, and LULI experiments                                       | 345 |
| B.    | Tridents   | 345 |
| C.    | Superhot plasma and cluster interaction, Coulomb explosion, cluster fusion, neutron sources        | 346 |
| D.    | Fast ignition  | 347 |
| VIII. | High-Energy Physics  | 348 |
| A.    | Large-field-gradient applications  | 348 |
| 1.    | Electron injector  | 348 |
| 2.    | Laser-accelerated ions   | 350 |
| 3.    | High-energy proton beams   | 351 |
| B.    | Laser-produced pions and muons   | 354 |
| C.    | Colliders  | 355 |
| 1.    | Laser-based colliders  | 355 |
| 2.    | Increasing the $\tau$ -lepton lifetime   | 356 |
| 3.    | Photon-photon collider or $\gamma$ - $\gamma$ collider   | 356 |
| IX.   | Astrophysics   | 356 |
| X.    | Ultrahigh Intensity and General Relativity   | 358 |
| XI.   | Nonlinear QED  | 359 |
| XII.  | Conclusions  | 362 |
|       | Acknowledgments  | 363 |
|       | References   | 363 |

## I. INTRODUCTION

Over the past 15 years we have seen optics on the threshold of a new scientific adventure similar to that experienced in the 1960s. Soon after the advent of the laser in the 1960s the first nonlinear optical effects were demonstrated. For the first time the laser field could disturb the Coulomb field that binds the electrons to their nucleus and produce new frequencies (Franken, 1961) or even be rectified (Bass, 1962). It could modify the index of refraction of optical media (Mayer and Gires, 1964; Bloembergen and Lallemand, 1966). Raman scattering in molecules could now lead to stimulated Raman scattering (Woodbury and Ng, 1962). The electrostrictive effect could induce acoustic waves to produce stimulated Brillouin scattering (Chiao, Garmire, and Townes, 1964;

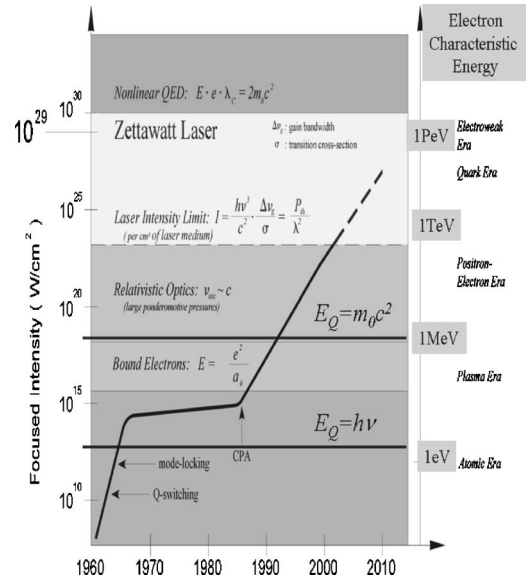


FIG. 1. Laser intensity vs years. This curve is obtained for amplifying beam of around  $\text{cm}^2$  beam size. Note the steep slope in intensities that occurred during the 1960s. This period corresponded to the discovery of most nonlinear optical effects due to the bound electron. We are today experiencing a similar rapid increase in intensity opening up a new regime in optics dominated by the relativistic character of the electron. Note that a few years ago we called it high intensity when the electron in a quiver energy was around 1 eV. Today high intensity corresponds to electron quiver energies of the order of  $mc^2 \sim 0.5$  MeV. The dashed line corresponds to what could be obtained with significant increases in beam size (see Sec. II.I).

Chiao, Townes, and Stoicheff, 1964). Higher-order optical nonlinearities involving the simultaneous absorption of several photons were soon demonstrated, opening the field of multiphoton ionization (Voronov and Delone, 1965; Agostini *et al.*, 1968). Figure 1 shows the strong correlation between the rapid increase in laser intensities produced in the 1960s and the discovery of the major effects in nonlinear optics. This rapid evolution in intensity was due to the introduction of  $Q$  switching (Hellwarth, 1961) and mode locking (Mocker and Collins, 1965). During this period the increase in the intensities that could be reached was so rapid that physicists were already predicting new types of optical nonlinearities dominated by the relativistic character of the free electron (Reiss, 1962; Eberly, 1969; Litvak 1969; Sarachik and Schappert, 1970; Max *et al.*, 1974) or vacuum nonlinearity (Brezin and Itzykson, 1970).

The key to high and ultrahigh peak power and intensity is the amplification of ultrashort pulses in the picosecond and femtosecond time scales. Over the past 40 years laser-pulse durations have continuously decreased from the microsecond domain with free running to the nanosecond regime with  $Q$  switching, and finally to the picosecond and few-femtosecond regime with mode locking (Brabec and Krausz, 2000; see Fig. 2). With the advent of mode locking, the laser-pulse duration became so short that pulses could not be amplified without producing unwanted nonlinear effects. This is

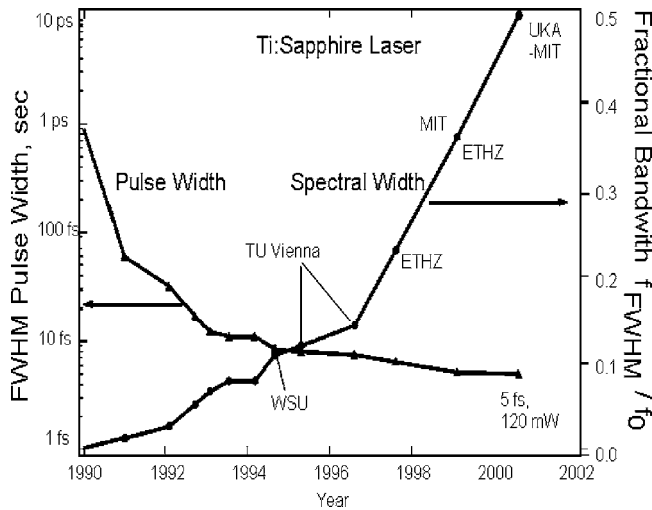


FIG. 2. Pulse duration vs years. The laser-pulse duration has also rapidly changed from microsecond (free running), nanosecond ( $Q$  switched), and picosecond mode locking. Here we show the pulse duration evolution since the 1990s after the invention of Ti:sapphire Kerr lens mode locking (Spence *et al.*, 1991). Courtesy of F. Krausz, TU Vienna.

the reason for the power and intensity plateau seen in Fig. 1 (Mourou, Barty, and Perry, 1998). For reasonable sized systems, i.e., with a beam diameter of the order of 1 cm, the maximum obtainable power stayed around 1 GW and focused intensities at about  $10^{14}$  W/cm<sup>2</sup>. Higher power can be obtained through the use of amplifying media with gain bandwidths that can accommodate the short pulse spectrum and high-energy storage media that have a small transition cross section  $\sigma_a$ . However, this approach also requires the use of input pulses with a high laser fluence (J/cm<sup>2</sup>). As we shall see later, good energy extraction from an amplifier calls for input pulses close to the saturation fluence  $F_{\text{sat}} = \hbar\omega/\sigma_a$ . This level of fluence delivered over a short time will lead to prohibitively large intensities, in excess of TW/cm<sup>2</sup>, far above the limit of  $\sim$ GW/cm<sup>2</sup> imposed by the need to prevent nonlinear effects and optical damage in the amplifiers and optical components. Consequently, the only alternative seemed to be to use low-energy storage materials (dyes and excimers) and increase the laser beam cross section, leading to unattractive, large, low-repetition-rate, high-priced laser systems. Because of the large size of such systems, high-intensity physics research was limited to a few facilities such as the CO<sub>2</sub> laser at Los Alamos National Laboratory (Carman *et al.*, 1981), the Nd:glass laser at the Laboratory for Laser Energetics (Bunkenburg *et al.*, 1981), and excimer lasers at the University of Illinois at Chicago and University of Tokyo (Luk *et al.*, 1989; Endoh *et al.*, 1989).

In 1985 laser physicists at the University of Rochester (Strickland and Mourou, 1985; Maine and Mourou, 1988; Maine *et al.*, 1988) demonstrated a way to simultaneously accommodate the very large beam fluence necessary for energy extraction in superior storage materials while keeping the intensity and nonlinear effects to

an acceptable level. This technique, called chirped pulse amplification (CPA), revolutionized the field in three ways. First table-top systems using the CPA technique became capable of delivering intensities almost  $10^5$ – $10^6$  times higher than those available in the past. Second the CPA technique could be readily adapted to existing large laser fusion systems at a relatively low cost. Today CPA is incorporated in all the major laser systems around the world—Japan (Yamakawa *et al.*, 1991), France (Rouyer *et al.*, 1993), United Kingdom, United States (Perry *et al.*, 1999), etc. The main application in these laboratories is fast-ignition research (Tabak *et al.*, 1994). Third because of their reduced size CPA lasers could be combined with large particle accelerators. In the case of synchrotrons (Wulff *et al.*, 1997; Larsson *et al.*, 1998; Schoenlein *et al.*, 2000), it could be used to study time-resolved x-ray diffraction. With a linear collider such as SLAC one could produce fields higher than the critical field (Bula *et al.*, 1996) and observe nonlinear QED effects like pair generation from vacuum. At the moment all the colliders are considering the incorporation of CPA technology to produce  $\gamma$  rays for photon-photon collisions, i.e., to create a  $\gamma$ - $\gamma$  collider (Tel'nov, 1990, 2000, 2001; Yokoya, 2000).

As we shall describe later, the availability of ultrahigh-intensity lasers has extended the horizon of laser physics from atomic and condensed-matter studies to plasma, nuclear, and high-energy physics, general relativity and cosmology, and physics beyond the standard model. It has also had a major effect in bringing back to university laboratories science that formerly could only be studied with large-scale facilities.

The study of relativistic effects in the interaction of radiation with matter is of course complex. This is due to the extremely rapid dynamics, the high dimensionality of the problem, the lack of symmetry, and the importance of nonlinear and kinetic effects. Fortunately, powerful methods for investigating laser-plasma interactions have become available through the advent of modern supercomputers and special numerical techniques (Dawson and Lin, 1984; Tajima, 1989). In the case of ultrashort relativistically intense laser pulses, simulations with three-dimensional (3D) particle-in-cell codes provide a unique opportunity for properly describing the nonlinear dynamics of laser plasmas, including nonlinear wave breaking, the acceleration of charged particles to high energies, and the generation of coherent nonlinear structures such as relativistic solitons and vortices. In this regard the contribution of three-dimensional computer simulations cannot be overstated.

## II. ULTRAHIGH-INTENSITY LASERS: THE CHIRPED PULSE AMPLIFICATION TECHNIQUE

In this section we review some of the key concepts of amplification and propagation that led to the present chirped pulse amplification architecture.

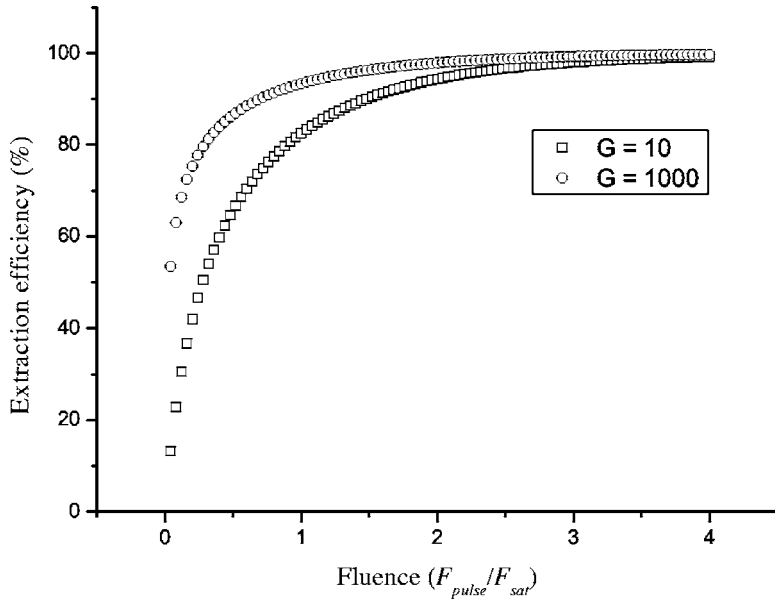


FIG. 3. Amplifier efficiency. This illustrates the importance for the input pulse fluence  $F_{\text{pulse}}$  to be few times the saturation fluence  $F_{\text{sat}}$  to obtain a good extraction efficiency.

#### A. Amplification—the energy extraction condition

Before 1985 all amplifier systems were based on direct amplification. As mentioned in the Introduction, a simple rule for laser amplification is that the maximum energy per unit area extracted from an amplifier is of the order of  $F_{\text{sat}}$ , the saturation fluence of the materials. This value is given by

$$F_{\text{sat}} = \frac{\hbar\omega}{\sigma_a}, \quad (1)$$

where  $\hbar$  is Planck's constant,  $\omega$  is the angular laser frequency, and  $\sigma_a$  is the amplifying transition cross section.  $F_{\text{sat}}$  is 0.9 J/cm<sup>2</sup> for Ti:sapphire and 4 J/cm<sup>2</sup> for Nd:glass and of the order of a mJ/cm<sup>2</sup> for dyes and excimers. It can be shown (Siegman, 1986) that the output fluence  $F_{\text{out}}(t)$  is given by

$$F_{\text{out}}(t) = F_{\text{sat}} \ln \left[ \frac{G_0 - 1}{G(t) - 1} \right], \quad (2)$$

where  $G_0$  is the low signal gain and

$$G(t) = \exp[\sigma N_{\text{tot}}(t)] \quad (3)$$

is the amplifier time-dependent total gain. Here  $N_{\text{tot}}(t)$  is the time-dependent total population inversion. The amplifier efficiency  $\eta$  is given by

$$\eta = \frac{\ln G_0 - \ln G_f}{\ln G_0}. \quad (4)$$

The gain  $G_f$  at the end of the impulsion is given by

$$G_f = 1 + (G_0 - 1) \exp \left[ - \frac{F_{\text{pulse}}}{F_{\text{sat}}} \right]. \quad (5)$$

From Eqs. (4) and (5) we can see that, to reach an efficiency close to unity, the laser input fluence  $F_{\text{pulse}}$  must correspond to few times  $F_{\text{sat}}$ . Figure 3 illustrates this point for two different initial gains  $G_0$  of 10 and 10<sup>3</sup>.

#### B. Amplification—the propagation condition

Prior to CPA the amplifying media were exclusively dyes (Migus *et al.*, 1982) and excimers (Endoh *et al.*, 1989; Luk *et al.*, 1989). Typical cross sections for these media are very large, in the range of 10<sup>-16</sup> cm<sup>2</sup>, implying a  $F_{\text{sat}}$  of only a few mJ/cm<sup>2</sup>, or a power density of 1 GW/cm<sup>2</sup> for subpicosecond pulses. Above this power density level, the index of refraction becomes intensity dependent according to the well-known expression

$$n = n_0 + n_2 I. \quad (6)$$

Due to the spatial variation of the laser beam intensity, this will modify the beam wave front according to the “*B* integral,”

$$B = \frac{2\pi}{\lambda} \int_0^L n_2 I dx. \quad (7)$$

Here  $B$  represents, in units of  $\lambda$ , the amount of wave-front distortion due to the intensity-dependent index of refraction, accumulated by the beam over a length  $L$ . For a perfectly Gaussian beam,  $B$  will cause the whole beam to self-focus above a critical power given by

$$P_{\text{cr}} = \frac{\lambda_0^2}{2\pi n_0 n_2}. \quad (8)$$

For example, the nonlinear index is  $n_2 = 5 \times 10^{-16}$  cm<sup>2</sup>/W for Ti:sapphire. When the laser beam exhibits spatial intensity modulations,  $n_2$  will cause the beam to break up in filaments. In practice the small-scale self-focusing represents the most severe problem in an amplifier system. The maximum growth rate  $g_m$  (Bespalov and Talanov, 1966) will occur for spatial frequencies  $K_m$  given by

$$K_m = \left( \frac{2\pi}{\lambda} \right) \left( \frac{2n_2 I}{n_0} \right)^{1/2}, \quad (9)$$

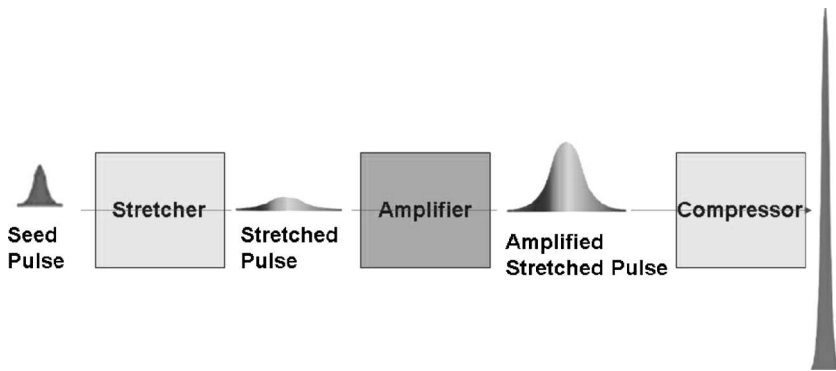


FIG. 4. Chirped pulse amplification concept. To minimize nonlinear effects the pulse is first stretched several thousand times lowering the intensity accordingly without changing the input fluence ( $\text{J}/\text{cm}^2$ ). The pulse is next amplified by a factor of  $10^6$ – $10^{12}$  and is then recompressed by a factor of several thousand times close to its initial value.

$$g_m = \left( \frac{2\pi}{\lambda} \right) \left( \frac{n_2 I}{n_0} \right). \quad (10)$$

For intensities of the order of  $I \sim 1 \text{ GW}/\text{cm}^2$ , in Ti:sapphire,  $K_m \sim 200 \text{ cm}^{-1}$ , corresponding to  $50 \mu\text{m}$ . These wave-front “irregularities” will grow at a rate of  $g_m \sim 3 \text{ cm}^{-1}$ . Note that the exponential growth rate  $G_m$  over the gain length  $L$  is exactly equal to  $B$ ,

$$G_m = B. \quad (11)$$

For laser fusion systems, the beam is “cleaned” with spatial filters every time  $B$  reaches 3. For high-field experiments in which the spatial and temporal beam quality requirements are more stringent,  $B$  must be kept below 0.3 corresponding to a wave-front distortion of  $\lambda/20$ .

### C. The CPA concept

We have seen above that amplifying media with low cross sections offer the benefits of a compact laser system. For instance, Nd:glass has a cross section of  $10^{-21} \text{ cm}^2$ , which means that we can store a thousand to ten thousand times more atoms per unit volume and, consequently, get a thousand to ten thousand times more energy before it self-oscillates, than we can with dye or excimers of cross section  $\sim 10^{16} \text{ W}/\text{cm}^2$ . However, to extract this large amount of energy in a picosecond pulse would require a beam with a fluence  $F_s$  of the order of  $1 \text{ J}/\text{cm}^2$  or an intensity of  $10^{12} \text{ W}/\text{cm}^2$  corresponding to a  $B$  of a few thousand, i.e., a thousand times the limit established in the previous paragraph!

Therefore, in order to utilize superior energy storage materials, the laser scientist is confronted with the seemingly insoluble problem of increasing the input energy needed for energy extraction, while keeping the input intensity at an acceptable level. This problem is solved by the CPA method. The pulse is first stretched by a factor of a thousand to a hundred thousand. This step does not change the input pulse energy (input fluence), and therefore the energy extraction capability, but it does lower the input intensity by the stretching ratio and hence keeps  $B$  to a reasonable level. The pulse is then amplified by 6 to 12 orders of magnitude, i.e., from the nJ to the millijoule-kilojoule level and is finally recompressed by the same stretching ratio back to a duration close to its initial value (see Fig. 4).

### D. The key element: the matched stretcher-compressor

In the first CPA set up of the Rochester group (Strickland and Mourou, 1985) the laser pulse was stretched in an optical fiber that had positive group delay dispersion and was recompressed by a pair of parallel gratings (Treacy, 1969), which could have a negative group delay dispersion. Although this first realization of CPA led to a spectacular 100-fold improvement in peak power, it had the problem that the stretcher and compressor were not matched over all orders. This meant that after recompression the pulse exhibited unacceptable prepulses and postpulses. Following the first CPA demonstration the Rochester group started to look for the ideal “matched stretcher-compressor.” It was realized in 1987, when Martinez (1987) proposed a grating compressor with positive group delay dispersion for communication applications as shown in Fig. 5. In communication systems the wavelength of choice is  $1.5 \mu\text{m}$ , a region where the fiber exhibits negative group velocity dispersion. After propagation in a fiber the communication bits exhibit a negative chirp. It is therefore necessary to use a dispersive delay line with a positive group velocity dispersion to recompress the pulses. After examining this device the Rochester group came to the conclusion that

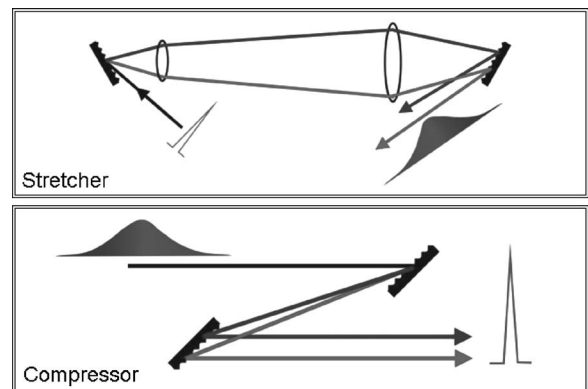


FIG. 5. Treacy and Martinez grating arrangements. The Martinez grating pair used as a stretcher and Treacy grating pair used as a compressor. It was discovered and demonstrated (Pessot *et al.*, 1987) that these two grating arrangements are in fact matched over all orders. The pulse can be stretched and recompressed arbitrarily keeping the initial pulse unchanged. This grating arrangement is used in most CPA systems.

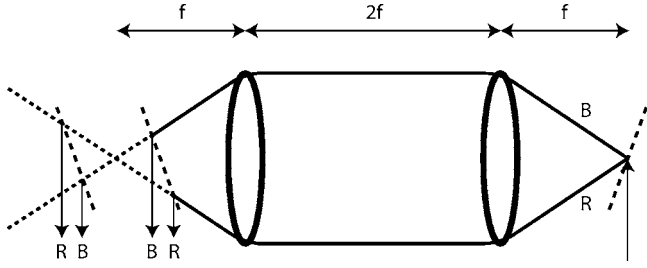


FIG. 6. Matching between the Martinez and Treacy grating pair arrangements. The input grating is imaged by a telescope of magnification 1, to form a “virtual” grating parallel to the second grating. The distance  $b$  between the two gratings, real and virtual, can be continuously adjusted from positive to negative.

the Martinez “compressor” was in fact the matched stretcher of the Treacy compressor that they were seeking. This can be easily shown by considering the arrangement shown in Fig. 6. When one uses a telescope of magnification 1, the input grating located at a distance  $f$  from the first lens will be imaged at the same distance  $f$  of the second lens to form an “imaginary” grating. The second grating can be placed at a distance  $b$  from the imaginary grating. Note that  $b$  can be positive or negative according to the second grating position.

To stretch the pulse we impart a frequency-dependent phase shift  $\phi(\omega)$  that can be expanded in a Taylor series around the central frequency  $\omega_0$ :

$$\phi(\omega) = \phi_0 + \phi_1(\omega - \omega_0) + \phi_2(\omega - \omega_0)^2 + \phi_3(\omega - \omega_0)^3 + \dots, \quad (12)$$

where

$$\phi_n = \frac{1}{n!} \left. \frac{d^n \phi}{d\omega^n} \right|_{\omega_0}. \quad (13)$$

The quadratic phase  $\phi_2$  is also known as the second-order dispersion. It is responsible for stretching the pulse. The higher-order terms  $\phi_3$  and  $\phi_4$ , third- and fourth-order dispersion will distort the pulse shape and give it wings. If  $\phi_{\text{str}}$  and  $\phi_{\text{comp}}$  are the frequency-dependent phases of the stretcher and compressor, a matched stretcher-compressor fulfills the condition

$$\phi_{\text{str}} + \phi_{\text{com}} = 0. \quad (14)$$

The Treacy compressor is composed of a grating pair. It acts as a dispersive delay line that produces negative second-order dispersion, whose value can be shown to be

$$\phi_2 = -\frac{m^2 \lambda^3}{2\pi c^2 d^2 \cos^2 \theta} b, \quad (15)$$

where  $c$  is the speed of light,  $m$  is the diffraction order,  $d$  is the groove spacing, and

$$b = -\frac{G}{\cos \theta(\lambda_0)}. \quad (16)$$

Here  $G$  is the perpendicular grating separation and  $\theta$  is the diffraction angle. The third- and fourth-order dispersion can be easily found, using Eq. (13), to have the form

$$\begin{aligned} \phi_3 &= -\phi_2 \frac{\lambda}{2\pi c} \left[ 1 + \frac{m\lambda \sin \theta}{d \cos^2 \theta} \right], \\ \phi_4 &= -\phi_3 \frac{3\lambda^2}{4\pi^2 c^2} \left\{ 4 + 8 \frac{m\lambda \sin \theta}{d \cos^2 \theta} \right. \\ &\quad \left. + \frac{\lambda^2}{d^2} [1 + \tan^2 \theta (6 + 5 \tan^2 \theta)] \right\}. \end{aligned} \quad (18)$$

Because all these orders are strictly proportional to  $b$  along with its sign, condition (14) can be fulfilled by locating the second grating in a stretcher at a position  $-b$  from its image.

The phase conjugation properties of the two systems were proposed and demonstrated by Pessot *et al.* (1987) by stretching a pulse of 80 fs by a factor of 1000 using Martinez arrangement and then compressing it back to the same value using the Treacy compressor. This demonstration represented a major step in chirped pulse amplification.

This matched stretcher-compressor integrated into a CPA system was to produce a terawatt pulse from a tabletop system—the so-called T<sup>3</sup>—by the Rochester group. It was subsequently used for subpicosecond pulses (Maine and Mourou, 1988; Maine *et al.*, 1988) and for a pulse duration of 100 fs by Pessot *et al.* (1989). This arrangement has become the standard architecture used in most CPA systems.

For shorter pulse systems with large bandwidth, an additional phase term  $\phi_{\text{mat}}(\omega)$ , due to material dispersion in the amplifier, Faraday rotator, Pockels cells, etc., must be added to Eq. (14) to produce the new matching condition

$$\phi_{\text{str}}(\omega) + \phi_{\text{comp}}(\omega) + \phi_{\text{mat}}(\omega) = 0. \quad (19)$$

To calculate  $\phi_{\text{mat}}(\omega)$  we use the familiar Sellmeier expression,

$$n^2(\lambda) = 1 + \sum_j \frac{b_j}{\lambda^2 - \lambda_j^2}, \quad (20)$$

where  $b_j$  and  $\lambda_j$  are material constants. From Eq. (20) the second-, third-, and fourth-order dispersion can be calculated using Eqs. (13) to produce

$$\phi_2 = \frac{\lambda^3 L}{4\pi c^2} \frac{d^2 n}{d\lambda^2}, \quad (21)$$

$$\phi_3 = -\frac{\lambda^4 L}{24\pi^2 c^3} \left[ 3 \frac{d^2 n}{d\lambda^2} + \lambda \frac{d^3 n}{d\lambda^3} \right], \quad (22)$$

$$\phi_4 = -\frac{\lambda^5 L}{192\pi^3 c^4} \left[ 12 \frac{d^2 n}{d\lambda^2} + 8\lambda \frac{d^3 n}{d\lambda^3} + \lambda^2 \frac{d^4 n}{d\lambda^4} \right], \quad (23)$$

where  $L$  is the material length.

Fulfilling condition (19) over a wide spectrum has become one of the most important concerns of ultrafast optics. A number of matched stretcher-compressor arrangements have been demonstrated (Lemoff and Barty, 1993; Tournois, 1993; White *et al.*, 1993; Cheriaux *et al.*, 1996).

Very often not all the terms can be ideally compensated. Trying to minimize the stretching/compression ratio is one approach (Backus *et al.*, 1998). Otherwise, higher-order corrections can be compensated by devices such as the acousto-optic temporal phase corrector known as the Dazzler, introduced by the Fastlite company (Tournois, 1997)

### 1. New materials for CPA and gain narrowing

CPA was demonstrated initially with the two broadband-amplifying media that were available at the time, Nd:glass and alexandrite (Pessot *et al.*, 1989). Shortly after this initial work the concept was extended to Ti:sapphire (Vaillancourt *et al.*, 1990; Kmetec *et al.*, 1991; Squier *et al.*, 1991; Sullivan *et al.*, 1991) as well as Cr:LiSrAlF<sub>6</sub> (Beaud *et al.*, 1993; Ditmire and Perry, 1993) and Yb:glass (Nees *et al.*, 1998). Among these materials Ti:sapphire has the advantage of the largest bandwidth, with a high damage threshold and excellent thermal conductivity, which is enhanced at cryogenic temperatures (Backus *et al.*, 1997).

Parametric amplifiers have also been proposed and demonstrated (Dubietis *et al.*, 1992) and mainly developed for large scale laser applications at the Rutherford Appleton Laboratory (Ross *et al.*, 1997, 2000). This elegant technique, called OPCPA for optical parametric chirped pulse amplification, is able, if the nonlinear propagation effects are kept under control, to provide an extremely large bandwidth that can be pumped by large-scale laser systems. OPCPA can therefore be a companion of any large laser fusion system. A more detailed discussion of the OPCPA method is given in Sec. II.E. In a normal CPA system, one of the limitations in pulse duration comes from the gain narrowing. Because of their wide spectrum, short pulses can be amplified only by materials with a gain bandwidth greater than their spectrum. We note that materials with superior energy storage typically have a low transition cross section and broad gain bandwidth. However, large gain will lead to a reduction of the laser spectrum as it is amplified. In the unsaturated regime—the linear regime—the laser spectrum will be subjected to a narrowing given by

$$\Delta\omega = \Delta\omega_a \sqrt{\frac{3}{G(\omega_a) - 3}}, \quad (24)$$

where  $\Delta\omega_a$  is the gain bandwidth and  $G(\omega_a)$  the exponential gain. A gain of ten orders of magnitude will narrow the gain bandwidth by a factor of 3 to 4. A fraction of

this gain, however, can be recovered in the saturated section of the amplifier.

### 2. The petawatt

As soon as the CPA concept was demonstrated at the millijoule and joule levels, it became clear that it could be extended to much higher energies using existing laser fusion systems to amplify nanosecond pulses in the 100–1000 J range. This means that with remarkably few alterations, that is, by chirping the pulse at the input and compressing it at the output, a laser chain built to produce TW pulses could now produce petawatt (PW) pulses (Maine *et al.*, 1987). The first petawatt pulse was demonstrated (Perry *et al.*, 1999) ten years after the first terawatt. One of the impressive hurdles overcome by Perry's group was the fabrication of meter-size diffraction gratings. At present there are around 20 petawatt systems in the planning stages or being built around the world.

Parallel to the Nd-based petawatt systems we have today a number of high-power Ti:sapphire-based systems. They have much shorter pulses in the 20–30 fs range, and energies in the 5–10 J range and hence produce peak power at 100 TW. A 100 TW class Ti:sapphire laser was first demonstrated at the University of California at San Diego (Barty *et al.*, 1994). The leading laboratories at the present time in this area are the Advanced Photon Research Center (APRC) in Japan with around 500 TW (Aoyama *et al.*, 2002), Janus System at Lawrence Livermore, 200 TW, the Laboratory d'Optique Appliquée (LOA) in France, 100 TW, the Max-Born Institute in Germany, 100 TW, the University of Lund in Sweden, 30 TW, and at the Center for Ultrafast Optical Science University of Michigan, 40 TW. Two PW class systems are under construction at the University of Michigan and LOA.

### E. Optical parametric chirped pulse amplification

In this section we discuss the differences between the CPA and OPCPA methods. Figure 7 shows the conceptual layout of an optical parametric CPA (OPCPA) system (Dubietis *et al.*, 1992; Ross *et al.*, 1997). Because we review only the relativistic intensity laser we will not mention the large number of works related to subrelativistic work using OPCPA. As in CPA the object in OPCPA is to stretch the pulse to a nanosecond and then amplify it to the joule or higher level by optical parametric amplification and recompress it back to close to its initial value. Note that the stretching is essential not only to keep the  $B$  integral low but also to extract energy efficiently. It is only during the stretched pulse that light can be transferred from the pump beam to the signal beam.

The advantages of this technique are as follows:

- (1) large bandwidth that could accommodate few-cycle pulses;

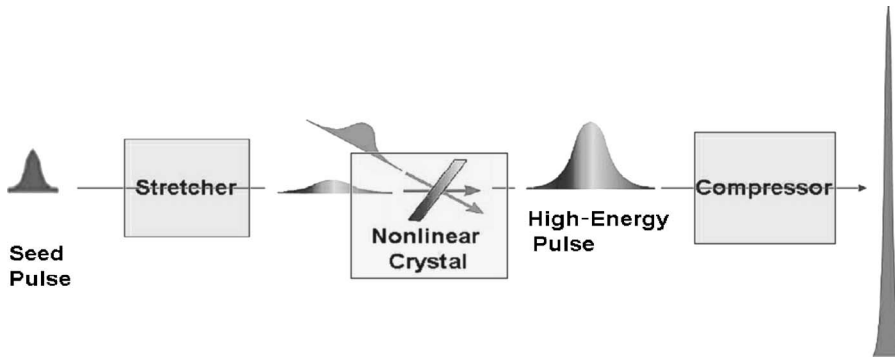


FIG. 7. OPCPA concept. In the OPCPA the pulse is amplified by optical parametric amplification instead of regular optical amplification. Note that for efficiency the pump pulse and the stretched pulse must have approximately the same duration and the same spatial extend.

- (2) ability to benefit from very large KDP crystals ( $100 \times 100 \text{ cm}^2$ ) developed for laser fusion;
- (3) adaptability to existing laser fusion chains, which benefit from low-bandwidth well collimated nano-second laser pulses at 532 nm;
- (4) no heat dissipation in the OPA crystal itself;
- (5) no transverse amplified stimulated emission, which is a major problem for large-aperture Ti:sapphire systems;
- (6) ability to use an iodine laser as a pumping source;
- (7) very simple amplification system.

The disadvantages are as follows:

- (1) Lower efficiency than standard CPA. For a standard Ti:sapphire CPA the efficiency can be as high as 50% from a long green pulse, say, of 50 ns. The energy storage time of Ti:sapphire is  $2 \mu\text{s}$ . So CPA is overall a more efficient system.
- (2) Very large stretching ratio, in the range of  $10^6$  to  $1$  ( $< 10 \text{ fs}$  to  $5 \text{ ns}$ ) necessary for energy extraction. This will make pulse compression down to the 10-fs regime difficult.
- (3) Gain a significant function of the intensity. This means the pump-beam profile may affect the beam quality and needs a high level of control.

In both systems the pulse duration will be ultimately limited by the grating bandwidth. At present no large gratings have the efficiency and the bandwidth required for efficient pulse compression much below 30 fs.

Beam quality from CPA has been demonstrated to be excellent. The latest studies have shown that OPCPA can also provide good spatial beam quality (Collier *et al.*, 1999). The potential of this technique has been demonstrated with the production of a 35-J, 85-fs pulse (equivalent to 0.4 PW) using a 10-cm-diameter beam (Collier *et al.*, 2004). The possibility of reaching high energies seems to be more straightforward with the OPCPA because it can benefit from kJ, ns fusion lasers that are already up and running. The pulse duration, however, will be limited by the grating bandwidth. CPA implementations must wait for large Ti:sapphire crystals grown to  $20 \times 20 \text{ cm}^2$  dimensions. These larger-scale crystals should become available as the demand for

them increases. In the mean time, a matrix of Ti:sapphire crystals could be used, but the crystal positions will need to be interferometrically controlled. For large Ti:sapphire systems, another problem that will need to be addressed is the transverse amplified stimulated emission. A final point to be noted is that both CPA and OPCPA work near the damage fluence threshold for the stretched pulse. Consequently, both systems should produce the same output energy for the same beam cross section.

### 1. Temporal quality: prepulse energy contrast

The characterization of the pulse duration by its full width at half maximum alone is not sufficient for ultrahigh-intensity studies. The peak intensity at present can be as large as  $10^{20} \text{ W/cm}^2$  and in the future will reach  $10^{23} \text{ W/cm}^2$ . Six to ten orders of magnitude below the peak, that is, at  $10^{12}$ – $10^{14} \text{ W/cm}^2$ , plasmas can be generated that will modify the target conditions. Figure 8 gives for the case of solid target interaction the intensity that the laser must not exceed as a function of pulse duration.

There are mainly three sources of prepulse energy. The first is amplified stimulated emission. This is due to amplifier gain and incomplete Pockels cell switching and lasts around 10 ns. The second source is the oscillator background, and the third incomplete compression due to high-order effects and spectral clipping. It is crucial

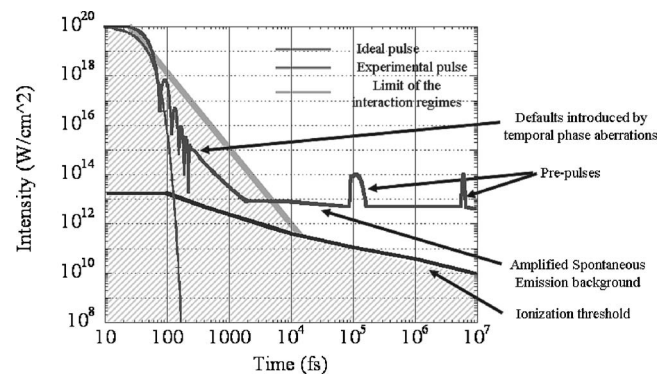


FIG. 8. Pulse contrast. Prior to the main pulse, the base of the pulse needs to stay below a certain intensity level (broad shady line decreasing at  $45^\circ$ ) to avoid the creation of a preformed plasma. Courtesy G. Cheriaux, LOA.

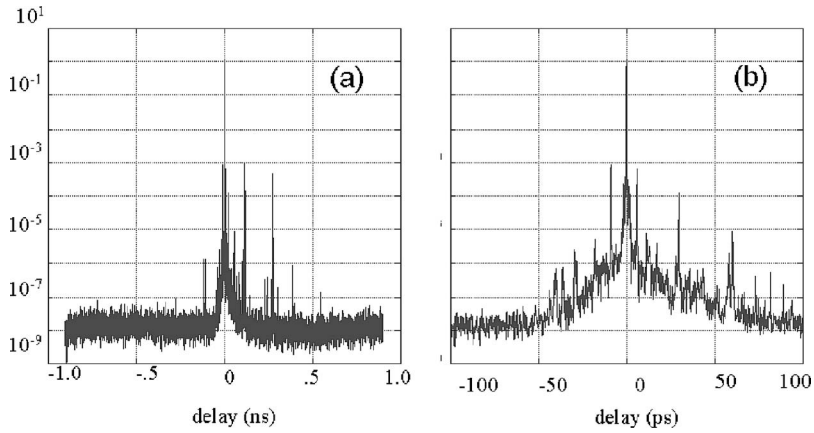


FIG. 9. Third-order autocorrelation of a 27 fs, full width at half maximum from the laser HERCULES at the University of Michigan. Note the very large dynamic range. 1 ns before the main pulse we can see the contribution of the amplified stimulated emission. The two prepulses at  $-100$  ps are due to measurement artifacts in the autocorrelator. The slow pedestal seen in (b) is due to incomplete compression, i.e., higher-order terms.

that the prepulse energy stays at a manageable level. For a long amplified stimulated emission (ns) pulse, the energy level cannot exceed  $1 \text{ J/cm}^2$  for a metallic target and a few  $\text{J/cm}^2$  for a dielectric one. For the short prepulse component, the energy should be less than  $0.1 \text{ J/cm}^2$  in metal and  $1 \text{ J/cm}^2$  in dielectric targets.

A large part of the challenge in studying prepulse effects is that it is not easy to observe an optical pulse over ten decades of intensity with femtosecond resolution. Standard detectors, like streak cameras, have neither the temporal resolution nor the necessary dynamic range. The only adequate technique is based on third-order autocorrelation measurements (Auston, 1971; Albrecht *et al.*, 1981). To make these, we first produce a clean pulse by frequency doubling the pulse under examination in a second-harmonic crystal. The case when the main pulse at  $\omega$  has a contrast of  $10^6$  to 1, the  $2\omega$  pulse will have a contrast of around  $10^{12}$  to 1. This temporally clean pulse at  $2\omega$  will now be mixed with a pulse at  $\omega$  in a third-harmonic crystal. By varying the time delay between the  $\omega$  pulse with respect to the  $2\omega$  pulse a replica of the  $\omega$  pulse at  $3\omega$  will be constructed. The resulting  $3\omega$  radiation can be easily isolated from the  $\omega$  and  $2\omega$  signals, and so we can produce a pulse replica at  $3\omega$  with an extraordinary large dynamic range covering more than

ten orders of magnitude (see Fig. 9). Note that this technique requires many repetitions of the measurement. It can be done only with the “front end” of the system that can operate at a higher repetition rate. We have to be aware that the many prepulses and postpulses seen in Fig. 10 are not necessarily real signals. They can be artifacts produced by Fresnel reflections in the various components of the third-order autocorrelator.

## 2. Pulse cleaning

Pulse cleaning is essential to achieve the contrast compatible with laser solid interactions at intensities above  $10^{19} \text{ W/cm}^2$ . A number of techniques have been tried based on frequency doubling, saturable absorbers, and plasma mirrors. However, all these techniques being intrinsically nonlinear in intensity decrease the beam quality and are only marginally adequate. Polarization rotation in a single-mode fiber (Tapié and Mourou, 1992) has been shown to be the most efficient way to temporally clean pulses while preserving laser beam quality. This works in the following way. When a high-intensity laser propagates in a single-mode birefringent fiber its polarization rotates. The rotation is a function of intensity and it is therefore possible with a polarizer to discrimi-

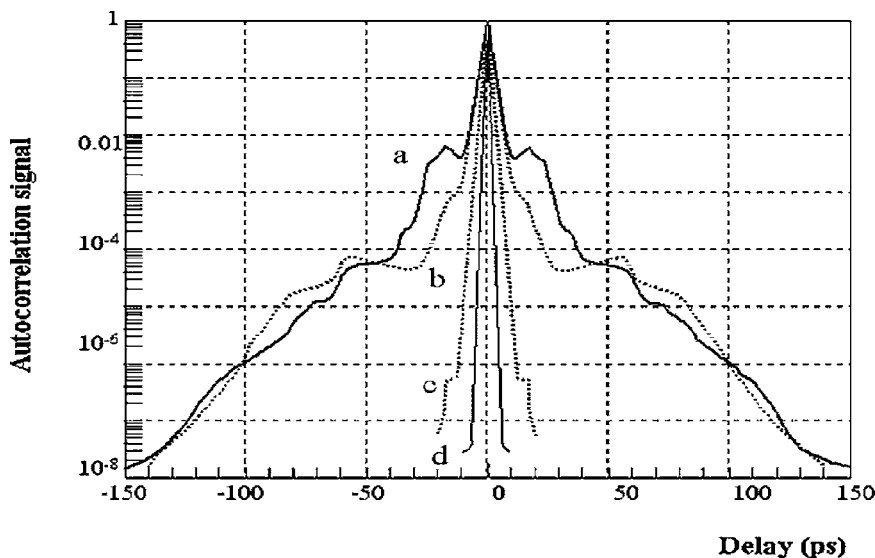


FIG. 10. Polarization rotation used in a single-mode optical fiber to clean the prepulse energy (Tapié and Mourou, 1992). Efficient temporal cleaning can be obtained without sacrificing beam quality. (a) and (b) The second-order autocorrelation of the input under some slightly different conditions. (c) The beam cleaner output. It shows how effective polarization rotation can be. (d) After polarization rotation the pulse has increased its bandwidth. The autocorrelation trace shows the output pulse after recompression.

nate the high-intensity from the low-intensity parts of the pulse (see Fig. 10). This technique has been demonstrated with microjoule-level pulses and used at the front end of a tabletop terawatt ( $T^3$ ) laser system. The dielectric breakdown of the ends of the fiber limits this technique to the microjoule level. Recently the same concept was demonstrated in a hollow-core fiber to the 20- $\mu\text{J}$  level (Homoelle *et al.*, 2002), achieving a contrast enhancement of three orders of magnitude while preserving beam quality. This technique has the potential to clean pulses to the mJ level with good preservation of beam quality. More recently using nonlinear centrosymmetric crystals (Jullien *et al.*, 2005) it has been demonstrated that high contrast could be achieved to the  $10^{10}$  level. Because it is a solid-state technique, this concept seems to become the leading method to produce clean pulses.

#### F. Spatial quality: deformable mirrors

High-intensity CPA laser systems, unlike laser fusion systems working at relatively low intensity ( $10^{14} \text{ W/cm}^2$ ) on target, require very-high-quality wave fronts. Trying to express beam quality in terms of the diffraction limit or  $M^2$  is simply inadequate. For example, a 1.1-diffraction-limit beam can have only 30% of its energy contained in the main focal spot. The rest of the energy is dispersed in a background surrounding the focus.

A better criterion is given by the Strehl ratio, i.e., the ratio of the intensity on axis of the aberrated image to the intensity on axis for a Gaussian image point. Marechal (Born and Wolf, 1964) has developed a formula that gives the Strehl ratio  $R$  as a function of the mean-square deformation  $\overline{\Delta\phi^2}$  of the wave front:

$$R = 1 - \left( \frac{2\pi}{\lambda} \right)^2 \overline{\Delta\phi^2}. \quad (25)$$

From this expression one has to keep  $\Delta\phi$  in the range of  $\lambda/8$  to get 80% of the theoretical intensity limit in the main lobe. A deformable mirror is needed to restore the wave front after amplification, compression, and propagation. With deformable mirrors, not only the laser but also the focusing optics can be corrected to produce the highest intensities. As we shall see in the next section, a relativistic intensity in the so-called  $\lambda^3$  limit was obtained by using only a mJ focused with a paraboloid having a numerical aperture equal to 1 to one single wavelength spot size (Albert *et al.*, 2000). We have applied a deformable mirror in conjunction with a  $f/0.6$  paraboloid and have obtained intensities as high as  $10^{22} \text{ W/cm}^2$  (Bahk *et al.*, 2004) (Fig. 11). Moreover, in the process to correct the wave front we need to measure it accurately. This means that by applying the Fresnel-Kirckhoff integral it is possible to know the laser field and intensity anywhere in the beam and in the focal volume. This is a tremendous side benefit of deformable mirrors.

The gratings used in the system also play a very important role in beam quality. Figure 12 shows the differ-

ence, from a beam quality point of view, between holographic and ruled gratings (Tapié, 1991). Ruled gratings are not perfectly sinusoidal and have some “dephasing” between grooves (ghosts) produced by the long ruling fabrication process. This will clearly produce a far from ideal beam profile. Such dephasing is completely absent in holographic gratings, where all the grooves are close to sinusoidal and strictly in phase.

#### G. Theoretical power and intensity limits

In CPA and OPCPA systems, the pulse maximum energy that can be produced is limited by the damage threshold  $F_{\text{thr}}$  of the stretched pulse and/or the saturation fluence  $F_{\text{sat}}$  (Mourou, 1997) *whichever is the lowest*. In the nanosecond regime the damage threshold scales like  $T^{1/2}$  (Bloembergen, 1974), where  $T$  is the pulse duration.  $F_{\text{sat}}$  is of the order of 20 to 50  $\text{J/cm}^2$  for surface or bulk and depends on the laser wavelength, the material (energy gap), its purity, and preparation. Note that  $F_{\text{sat}}$  is 0.9  $\text{J/cm}^2$  for Ti:sapphire and 40  $\text{J/cm}^2$  for Yb:glass. We have seen in Eq. (5) that to extract energy efficiently from the amplifier the input fluence must be of the order of  $F_{\text{sat}}$ . On the other hand, the minimum pulse duration  $\tau_p$  is imposed by the gain bandwidth of the amplifying medium  $\Delta\omega_a$ . From the relation  $\Delta\omega_a\tau_p \approx 2$ , we can find  $P_{\text{th}}$  the maximum power that can be produced per unit area of beam,

$$P_{\text{th}} = \frac{\hbar\omega}{2\sigma} \Delta\omega_a. \quad (26)$$

From this expression, we find the maximum intensity obtainable by focusing this power on a spot size limited only by the laser wavelength,

$$I_{\text{th}} = \frac{\hbar\omega^3}{8\pi^2\sigma} \frac{\Delta\omega_a}{c^2}. \quad (27)$$

The intensity limits presented in Figs. 1 and 13 are the theoretical power per unit area of beam ( $\text{cm}^2$ ) that could be obtained for different amplifying media: for Ti:sapphire and Yb:glass,  $P_{\text{th}}$  is 200 and 3000 TW, respectively, per  $\text{cm}^2$  of beam size. The corresponding  $I_{\text{th}}$  are of the order of  $0.3 \times 10^{23}$  and  $3 \times 10^{23} / \text{cm}^2$  for Ti:sapphire and Yb:glass, respectively.

#### H. The smallest relativistic laser—the $\lambda^3$ laser and carrier-envelope phase control

Pulses with millijoule energy and duration less than 10 fs when focused to a spot size of a single wavelength can produce intensities above  $10^{18} \text{ W/cm}^2$ , well into the relativistic regime. This type of laser has been demonstrated (Albert *et al.*, 2000) and has the advantage of working at kHz repetition rates. We call this a  $\lambda^3$  laser because all the energy is concentrated with a paraboloid having a numerical aperture equal to 1 into a volume of order  $\lambda^3$ , i.e., one wavelength in the transverse direction and a few wavelengths (cycles) along the propagation

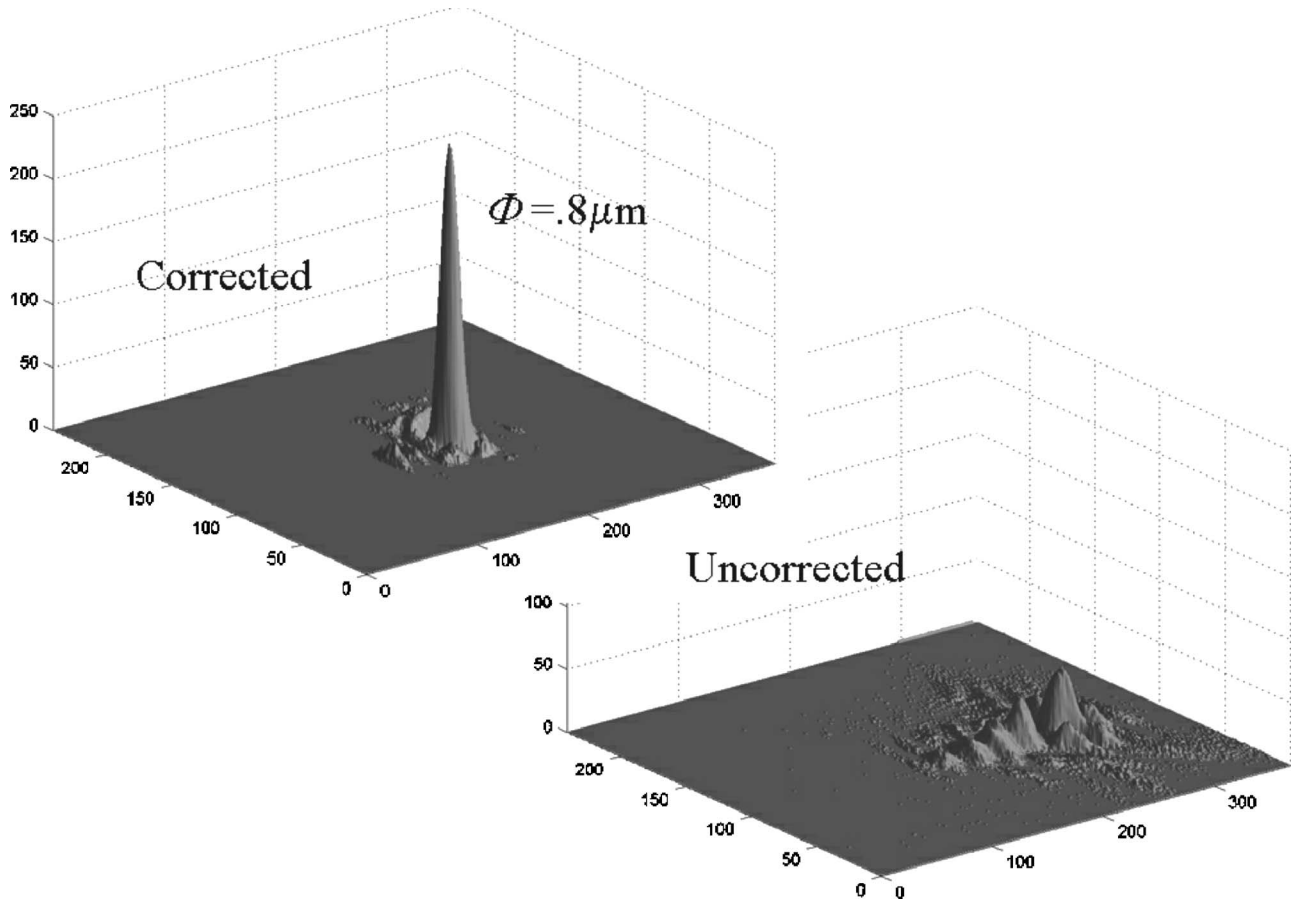


FIG. 11. The use of a deformable mirror (DM) in conjunction with a low  $f/0.6$  ellipsoid mirror can eliminate unwanted aberrations and produce a single-wavelength-focused spot size with a good Strehl ratio. A record intensity of  $10^{22}$  W/cm<sup>2</sup> was obtained. The two figures, DM corrected and uncorrected, show the dramatic effect of a well-corrected laser beam. The additional benefit provided with a deformable mirror is the laser field can be determined anywhere in the beam by using the Fresnel-Kirckhoff integral.

direction. The  $\lambda^3$  laser has a number of significant advantages. First, it is very stable and has a high repetition rate, and therefore is ideal for investigating relativistic effects through the observation of small perturbations

with lock-in detection. Second, the small spot size cuts off instabilities with feature sizes larger than the laser wavelength. Third, x-ray,  $\gamma$ -ray, electron, and proton sources produced using such a laser will have a higher spatial coherence, since spatial coherence scales with the inverse of the spot area. This quality is important for most applications such as x ray, electron and proton im-

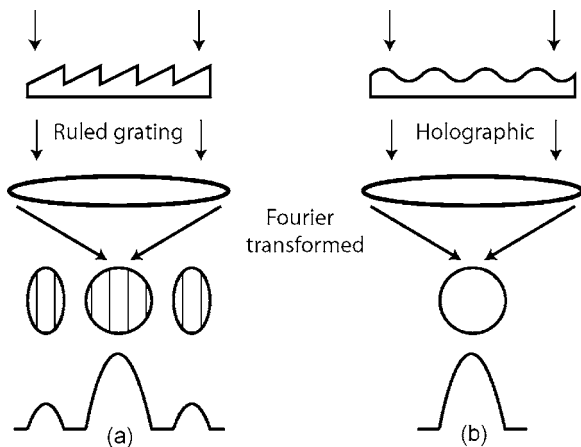


FIG. 12. Comparison between ruled and holographic gratings illustrating the difference in spot quality. In the case of ruled gratings the structure comes from the nonsinusoidal profile and ghosts produced by the imperfect and broken periodicity as they are ruling the grating.

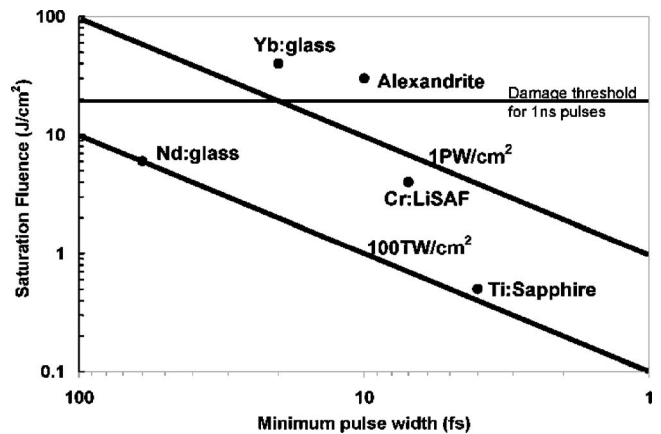


FIG. 13. Theoretical peak power per cm<sup>2</sup> of beams for various amplifying media.

aging, diffraction, and x-ray holography. It is also expected that the shortness of the pulse will produce a coherent interaction between the laser field and the electrons, leading to a more efficient laser-particle coupling. As the pulses get shorter the position of the carrier under the envelope becomes more important. The carrier-envelope phase control has been demonstrated (Hentschel *et al.*, 2001; Baltuska *et al.*, 2003) and is one key element for pulse synthesizer and attosecond pulse generation. In the relativistic regime, especially in the  $\lambda^3$ , carrier-envelope phase control will become very important for reproducible relativistic attosecond pulse generation (Naumova, Nees, Hou, *et al.*, 2004; Naumova, Nees, Sokolov, *et al.*, 2004; Naumova, Sokolov, *et al.*, 2004).

### I. The largest relativistic laser—the zettawatt laser

What is the most powerful laser that we could build with present-day technology? The power of such a laser would be limited by the available pump source. The largest lasers that could be used for a pump at present are the National Ignition Facility (NIF) in the US and the Laser Megajoule in France (Tajima and Mourou, 2002). Working at  $2\omega$  and with 10–20-ns-long pulses these lasers produce 5 MJ of pump light. Using Ti:sapphire as an amplifying medium and working at few times the saturation fluence, we could expect a 50% overall efficiency, or 2.5 MJ before compression. The beam cross section at few  $\text{J}/\text{cm}^2$  would be around 10 m. Assuming that we could compress the beam over 10 fs with a 70% efficiency compressor, we would obtain a power close to  $0.2 \times 10^{21}$  W or 0.2 ZW. If focused by a well-corrected parabola of the same type as the Keck telescope, which has a comparable diameter, this could produce a micrometer spot size with a power density of  $\approx 10^{28}$   $\text{W}/\text{cm}^2$ . This intensity level corresponds to the critical field (Schwinger field) mentioned above. We are therefore in a situation similar to 15 years ago when the first tabletop terawatt laser was demonstrated. At that time a French paper announced “*En route vers le Petawatt*” (Maine, 1987) and predicted that by using the largest developed laser at the time, i.e., Nova at LLNL or Omega at LLE, Rochester, petawatt pulses could be produced. Ten years later the Petawatt was demonstrated by Perry and his co-workers at LLNL, and today around 20 petawatt lasers have been built or are scheduled to be built.

### J. New amplification techniques: plasma compression

New ways are being proposed to overcome the limit of a few  $\text{J}/\text{cm}^2$  imposed by the saturation fluence of the amplifier and/or the dielectric breakdown of CPA system components. Perhaps the most elegant is plasma compression by stimulated Raman backscattering (Shvets *et al.*, 1998; Malkin *et al.*, 1999; see also earlier publications by Nishioka *et al.*, 1993, and by Ueda *et al.*, 1993). Using this concept a long pulse transfers its en-

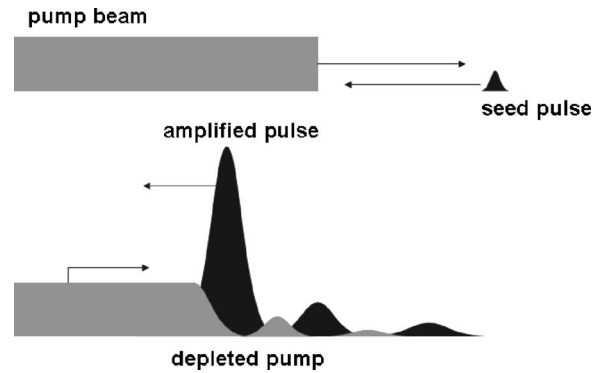


FIG. 14. Plasma compression by Raman backscattering. This scheme is not sensitive to damage as it works with a plasma, a medium that is already broken down.

ergy to a counterpropagating one with stimulated Raman backscattering (Fig. 14). Because the medium, a plasma, is already broken down, it will not be subject to damage and will accept higher fluences. These would be as high as a few  $1000 \text{ J}/\text{cm}^2$  instead of a few  $\text{J}/\text{cm}^2$  as with conventional CPA. Such a system would not also require large and expensive gratings.

### K. Average power

Ultimately most ultrahigh-intensity applications will require high average powers. CPA laser systems, using materials with excellent thermal conductivity such as Ti:sapphire, have improved average laser power by two to three orders of magnitude. Tabletop femtosecond excimer and dye lasers had typical average powers in the mW range. CPA systems have been demonstrated over a wide range of repetition rates from MHz (Norris, 1992) to mHz for petawatt output. Their average power is independent of repetition rate and is typically of 1 W (Fig. 15). Using a thermal lens (Salin and his group, private communication) and cryogenic cooling of the amplifier (Backus *et al.*, 1997) average power in 10-W regimes has been demonstrated. Figure 15 shows relativistic lasers from the kHz to the mHz. We also include for comparison the megajoule/NIF lasers that are not short pulse lasers. Average power is a serious difficulty that will have to be surmounted for real world applications. At cryogenic temperatures the thermal conductivity of Ti:sapphire becomes as good as that of copper. At this power level, however, the absorption in the grating becomes significant. Thermal effects deform the grating surface, leading to a deterioration in beam quality. Applications in high-energy physics, for instance, neutrino-beam production and the  $\gamma$ - $\gamma$  collider, will require average power in the MW range. With advances in laser diode power, high-efficiency gratings, and new broadband materials, we can envisage reaching MW average power in the longer term.

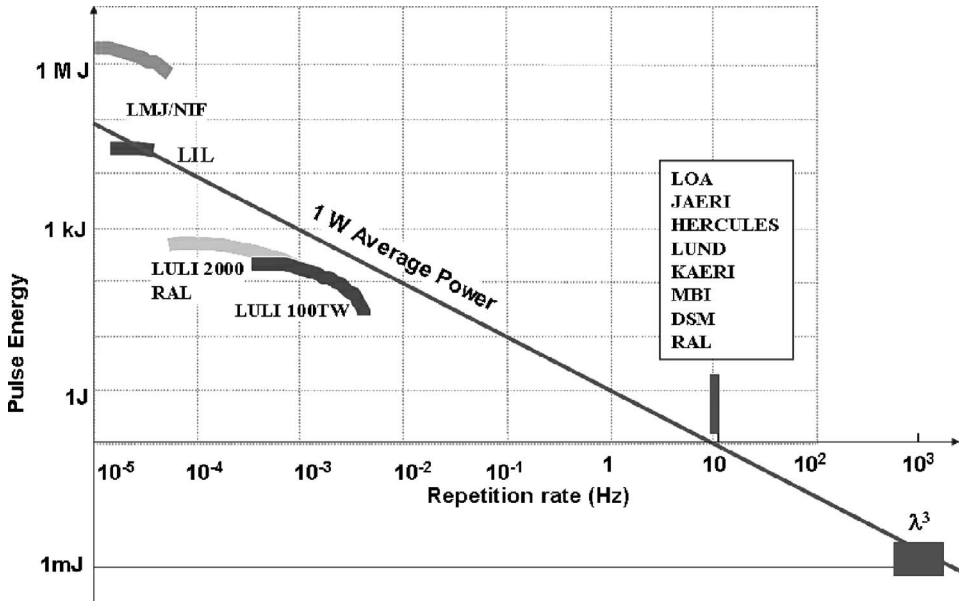


FIG. 15. Average power versus repetition rate. This graph illustrates the fact that the average power is relatively independent of repetition rates over a wide range from Hz for small laser systems to mHz for the very large ones. At present the average power of any CPA systems regardless of their repetition rate is of the order of 1 W. Systems at the 10-W level have been demonstrated. Before CPA it was typically around 10 mW. Many applications will require average powers greater than 1 kW.

### III. ULTRAHIGH-INTENSITY LASER REGIMES: EXTENDING THE FIELD OF LASER PHYSICS FROM THE eV TO THE TeV

#### A. Introduction

At present, focused intensities as high as  $10^{21}$  W/cm<sup>2</sup> are available, and we should soon reach  $10^{23}$  W/cm<sup>2</sup>. These intensities are well above the regime where electron motion starts to be relativistic. If we consider optics to be the science of light-electron interactions, it is natural to use the term relativistic optics for situations in which the light-electron interaction is dominated by relativistic effects. We emphasize the parallel between relativistic optics and “conventional” nonlinear optics. As mentioned previously, the progress in high-intensity lasers makes a change in terminology necessary. We shall refer to “high intensity” when the laser field  $E$  fulfills the following condition:

$$\hbar\omega < m_e c^2 [\sqrt{1 + a_0^2} - 1] < m_e c^2, \quad (28)$$

where the dimensionless amplitude of the laser radiation is given by

$$a_0 = eA/m_e c. \quad (29)$$

Here  $m_e c^2 \sqrt{1 + a_0^2}$  is the ponderomotive potential, and in the limit  $a_0 \gg 1$  it is equal to  $eE_0 \lambda / 2\pi$ , whereas for  $a_0 \ll 1$  it is  $e^2 E_0^2 / 2\omega^2 m_e$ ;  $\hbar\omega$  is the photon energy and  $m_e c^2$  the rest-mass energy of the electron,  $\lambda = 2\pi c / \omega$  the laser wavelength,  $e$  and  $m_e$  the electron charge and mass. This “high-intensity” regime corresponds to intensities between  $5 \times 10^{14}$  and  $10^{18}$  W/cm<sup>2</sup> for 1  $\mu$ m wavelength.

The ultrahigh-intensity regime will be defined as the regime above the  $10^{18}$  W/cm<sup>2</sup> limit, where

$$eE_0 \lambda > 2\pi m_e c^2. \quad (30)$$

For excimer wavelengths around 248 nm the relativistic limit will be at  $10^{19}$  W/cm<sup>2</sup>, while for 10.6  $\mu$ m (CO<sub>2</sub>) this limit is  $10^{16}$  W/cm<sup>2</sup>. Figure 1 shows the nonlinear QED

limit, which is reached for a laser field  $E$  such that

$$eE\lambda_c/2\pi > 2m_e c^2, \quad (31)$$

where  $\lambda_c = \hbar/m_e c$  is the Compton length. Relation (31) corresponds to the situation in which the field can do sufficient work on a virtual electron-positron pair to produce breakdown of the vacuum. This regime corresponds to intensities on the order of  $10^{29}$  W/cm<sup>2</sup> for 1  $\mu$ m light. Such a field,  $m_e c^2 / \lambda_c e$ , is called the Schwinger field. Not surprisingly similar isomorphisms of fields break down a neutral atom, the Keldysh field (see Keldysh, 1965), and semiconductors. We recall that the laser field  $E$  is related to the intensity  $I$  by

$$E^2 = Z_0 I, \quad (32)$$

where  $Z_0 = 377 \Omega$  is the vacuum impedance.

The physics in the high-intensity regime includes high harmonic generation, multiphoton ionization, etc. In essence, it deals with bound-electron nonlinear optics. This regime has been covered extensively by a number of excellent reviews (e.g., Joshi and Corkum, 1995) and will not be discussed in this article.

The ultrahigh-intensity regime has already produced a wealth of scientific results (Mourou, Barty, and Perry, 1998) related to the relativistic character of the electron dynamics (Lindman, 1977). In laser-atom interactions work at high intensity has generally been based on the nonrelativistic Schrödinger equation and dipole approximation. Extending the theory of laser-atom interactions into the relativistic regime requires solving the time-dependent Dirac equation (Popov *et al.*, 1997; Joachain *et al.*, 2000; Keitel, 2001; Chirila *et al.*, 2002; Maquet and Grobe, 2002; Mocken and Keitel, 2003; Popov, 2004). The laser-plasma interaction in the ultrahigh-intensity regime leads to an array of new phenomena like x-ray generation (Kieffer *et al.*, 1992; Kmetec *et al.*, 1992; Beg *et al.*, 1997),  $\gamma$ -ray generation (Norreys *et al.*, 1999), rela-

tivistic self-focusing,<sup>1</sup> high harmonic generation,<sup>2</sup> electron,<sup>3</sup> and proton acceleration,<sup>4</sup> neutron production (Pretzler, 1998; Disdier *et al.*, 1999), and positron production (Gahn *et al.*, 2000), as well as the demonstration of nonlinear QED (Bula *et al.*, 1996; Burke *et al.*, 1997).

### B. Similarities and differences between bound-electron and relativistic nonlinear optics

Classical linear and bound-electron nonlinear optics deal with the electron displacement  $\mathbf{x}(t)$  around the nucleus. This displacement gives rise to the polarizability

$$P(t) = N e \mathbf{x}(t), \quad (33)$$

where  $N$  is the electron density. The force applied to the electron is the Lorentz force

$$F(t) = e E(t), \quad (34)$$

in which in the classical limit we neglect the magnetic-field part due to the smallness of the ratio  $v/c$ . In the linear regime, for electrons bound to their nucleus,  $F(t)$  is proportional to the displacement  $\mathbf{x}(t)$ . As the displacement increases, the proportionality between  $\mathbf{x}(t)$  and  $E(t)$  is no longer respected. This is at the origin of the well-known nonlinear optical effects of bound electron: harmonic generation, optical rectification, etc., mentioned above. As the laser intensity increases to the  $10^{14}$  W/cm<sup>2</sup> level the material will ionize or be damaged and electrons will become free. At the threshold the electron is still bonded and in the process of becoming free high harmonics are created (Joshi and Corkum, 1995). At the same intensity level the deterministic character of the damage threshold in a solid is observed (Joglekar *et al.*, 2003). At a higher intensity level  $\approx 10^{18}$  W/cm<sup>2</sup> the electron is free and its velocity approaches the speed of light. The Lorentz force applied to the electron is

$$F(t) = e \left[ E(t) + \frac{1}{c} v \times B(t) \right], \quad (35)$$

where the term  $v \times B/c$  cannot be neglected. Because of the combined action of the  $E$  and  $B$  fields the electron will follow a complicated trajectory. For linearly polarized light this trajectory is a figure eight in the frame moving at the average electron velocity, as explained in *The Classical Theory of Fields* by Landau and Lifshitz (1980). The normalized vector potential quantity  $a_0 = eA/m_e c$  represents the quivering momentum normalized to  $m_e c$ . Here  $A$  is the electromagnetic vector potential. The longitudinal displacement is proportional to  $a_0^2$  whereas the transverse displacement scales as  $a_0$ . In the reference frame where the charged particle initially is at rest for  $a_0 < 1$  its transverse momentum is larger than the longitudinal one, whereas for  $a_0 > 1$  the situation is reversed and the longitudinal momentum becomes much larger than the transverse one. This complicated electron motion is the source of relativistic nonlinear effects like rectification, self-focusing, harmonic generation, etc.

### C. Relativistic rectification or wakefield effect

This effect known in the literature as the plasma *wakefield effect* was introduced by Tajima and Dawson (1979) as a stable method of exciting large-amplitude fast waves. Previous collective acceleration methods (Budker, 1956; Veksler, 1957) suffered from instabilities involving ions (Mako and Tajima, 1984). Further theoretical work on the field effect was done by Gorbunov and Kirsanov (1987), Sprangle *et al.* (1988), Bulanov, Kirsanov, and Sakharov (1989), and Berezhiani and Murusidze (1990). To underline the similarity of this relativistic process to optical rectification, we shall call it *relativistic rectification*. In a plasma, electrons are strongly accelerated due to the  $v \times B$  force. They drag behind them the much more massive ions, setting up a large electrostatic field parallel to the direction of laser propagation. This field is extremely large and of the order of magnitude of the transverse laser field. The  $v \times B$  term “transforms” the laser field into a longitudinal electrostatic field with an amplitude equivalent to that of the laser transverse field. This is a remarkable result if we consider that laser researchers had long recognized the enormous amplitude of the laser transverse field and tried to flip a fraction of this field along the longitudinal direction using various schemes (see, for example, Apollonov *et al.*, 1998; Bayer, 2002; Schaechter *et al.*, 2002). In the relativistic regime this conversion is done in plasmas automatically and efficiently. Just as harmonic generation is the hallmark of bound-electron nonlinear optics, relativistic rectification seems to be the most prominent effect of relativistic optics.

Optical rectification in classical nonlinear optics is not often used. It occurs only in noncentrosymmetric crystals and is not very efficient. It is due to the fact that in a noncentrosymmetric system the charges are preferentially pushed in the direction normal to the propagation

<sup>1</sup>On relativistic self-focusing, see, for example, Max *et al.*, 1974; Sprangle *et al.*, 1987; Borisov *et al.*, 1992; Gibbon *et al.*, 1995; Monot *et al.*, 1995; Chen, Maksimchuk, and Umstadter, 1998; Chen, Sarkisov, *et al.*, 1998; Fuchs *et al.*, 1998.

<sup>2</sup>On high harmonic generation, see, for example, Bulanov *et al.*, 1994; Lichters *et al.*, 1996; Von der Linde, 1998; Zepf *et al.*, 1998; Tarasevich *et al.*, 2000.

<sup>3</sup>On electron acceleration, see, for example, Clayton *et al.*, 1993; Modena *et al.*, 1995; Nakajima *et al.*, 1995; Umstadter, Chen, *et al.*, 1996; Umstadter, Kim, and Dodd, 1996; Wagner *et al.*, 1997; Chen, Sarkisov, *et al.*, 1998; Gordon *et al.*, 1998; Malka *et al.*, 2002; Bingham, Mendonca, and Shukla, 2004; Faure *et al.*, 2004; Geddes, 2004; Mangles *et al.*, 2004; Tochitsky *et al.*, 2004.

<sup>4</sup>On proton acceleration, see, for example, Esirkepov *et al.*, 1999; Krushelnik *et al.*, 1999; Sarkisov *et al.*, 1999; Bulanov *et al.*, 2000; Clark, Krushelnick, Davies, *et al.*, 2000; Clark, Krushelnick, Zepf, *et al.*, 2000; Maksimchuk *et al.*, 2000; Snavely *et al.*, 2000; Zhidkov, Sasaki, and Tajima, 2000; Umstadter, 2003; Bingham, Mendonca, and Shukla, 2004; Maksimchuk *et al.*, 2004.

axis, to produce a net electrostatic field perpendicular to the direction of propagation. In relativistic optics it is just the opposite. The rectified field is longitudinal. It is efficiently produced in centrosymmetric media—plasmas—and is of the order of the transverse field.

Relativistic intensities can produce large electrostatic fields. For example, for  $I=10^{18}$  W/cm<sup>2</sup> we could produce [see Eq. (34)] an electrostatic field up to 2 TV/m and 0.6 PV/m for  $10^{23}$  W/cm<sup>2</sup>. These values are gargantuan. To put them in perspective, they correspond to a particle acceleration to SLAC energies (50 GeV) over a distance of 100  $\mu$ m. If we were able to maintain this gradient over 1 m, a tabletop PeV accelerator capable of producing a beam that would circle the Earth, as discussed by Fermi in 1954, could be made using conventional technology. One direct consequence of electron acceleration is proton/ion acceleration, as the electron pulse pulls behind it positively charged ions to make a short proton pulse. This aspect of relativistic rectification is further discussed in Secs. VII and VIII, which are devoted to nuclear and high-energy physics.

#### D. Scattering in the relativistic regime

There are two kinds of interactions between photons and charged particles. The first is the single-particle interaction, in its most basic form a collision between a photon and an electron. The other is the collective interaction between photons and particles, or between an intense laser and matter. This may be considered as a stream of photons and a collection of charged particles such as electrons. Both kinds of interaction become more intense as the intensity of the laser is increased, particularly when the intensity enters the relativistic regime.

These two kinds of interaction are analogous to the interaction between wind and the water of a lake. When the wind is slow or gentle, the surface of the lake water is gently swept by the wind, causing a slow stream in the surface water via the molecular viscosity of water by the shearing wind molecules. This interaction arises from collisions between the flowing water molecules and originally stationary water molecules. When the wind velocity picks up, the wind begins to cause ripples on the surface of the lake. This is because the shear between the velocity of the wind and the originally stationary surface water becomes sufficiently large so that a collective instability sets in (Lamb, 1932; Chandrasekhar, 1961; Timofeev, 1979). More detailed studies of wave generation by wind on a water surface (Vekstein, 1998) show an analogy between the Landau damping of plasma waves and the resonant mechanism of wave generation on a water surface by wind. Due to this instability, the wind and water self-organize themselves in such a way as to cause undulating waves on the surface, which cause a greater friction (called *anomalously enhanced viscosity* or *anomalous viscosity* for short) between the wind and water. When this commences, the momentum of wind molecules is much more effectively transferred to that of

water molecules, and the water stream becomes more vigorous.

In the single-particle interaction within a stream of a large number of photons, the photons collide with electrons via Thomson scattering. According to classical physics, an electron scatters the incident electromagnetic wave without any change in the frequency of the radiation in the reference frame where the electron is at rest. The Thomson cross section of the scattering is given by

$$\sigma_T = \frac{8\pi}{3} r_e^2 = 0.665 \times 10^{-24} \text{ cm}^2, \quad (36)$$

where  $r_e = e^2/mc^2 = 2.82 \times 10^{-13}$  cm is the classical electron radius. In quantum theory, under the conservation of energy and momentum, the frequency and the wave vector of the scattered photons change as  $\lambda = \lambda_0 + \lambda_c(1 - \cos \theta)$ . Here  $\lambda_0 = 2\pi\lambda_0$  and  $\lambda = 2\pi\lambda$  are the wavelengths before and after scattering,  $\theta$  is the scattering angle, and  $\lambda_c = \hbar/mc = 3.86 \times 10^{-11}$  cm is the Compton length. The scattering cross section in this limit is given by the Klein-Nishina-Tamm formula (see Berestetskii, Lifshitz, and Pitaevskii, 1982). When a flux of laser photons is directed at an electron, this causes a force on it,

$$F \approx \frac{\sigma_T}{4\gamma^2} \frac{E_0^2}{4\pi}, \quad (37)$$

where  $\gamma$  is the Lorentz factor of the electron, i.e., the electron energy grows as  $E \propto (W\sigma_T t)^{1/3}$  (see Landau and Lifshitz, 1980).

#### IV. RELATIVISTICALLY STRONG ELECTROMAGNETIC AND LANGMUIR WAVES IN A COLLISIONLESS PLASMA

In this section we discuss the basic properties of finite-amplitude electromagnetic and electrostatic waves in plasmas (electrostatic waves are also known as *Langmuir waves*).

In the small-amplitude limit electromagnetic and Langmuir waves propagate through a collisionless plasma with a frequency independent of the amplitude. The frequency of a longitudinal Langmuir wave in a cold plasma,  $\omega_{pe} = \sqrt{4\pi ne^2/m_e}$ , is also independent of the wave vector of the wave, i.e., the phase velocity of a Langmuir wave is equal to  $v_{ph} = \omega_{pe}/k$  and its group velocity  $v_g = \partial\omega/\partial k$  is equal to zero. The frequency of a transverse electromagnetic wave is  $\omega = \sqrt{k^2 c^2 + \omega_{pe}^2}$ , i.e., its group and phase velocity are related to each other as  $v_{ph} v_g = c^2$ . In the case of finite-amplitude waves, the frequency depends on the wave amplitude, as demonstrated by Akhiezer and Polovin (1956), who gave the exact solution to the problem of the propagation of relativistically strong electromagnetic waves in collisionless plasmas.

Assuming an unbounded cold collisionless plasma, as described by Maxwell's equations and by the hydrodynamic equations of an electron fluid, we find that coupled electromagnetic and Langmuir waves are given by (Kozlov *et al.*, 1979; Farina and Bulanov, 2001)

$$\phi'' = \frac{\beta_g}{1 - \beta_g^2} \left( \frac{\psi_e}{R_e} - \frac{\psi_i}{R_i} \right), \quad (38)$$

$$a'' + \omega^2 a = a \frac{\beta_g}{1 - \beta_g^2} \left( \frac{1}{R_e} - \frac{\rho}{R_i} \right). \quad (39)$$

The electromagnetic and electrostatic potentials, normalized to  $m_e c^2 / e$ , depend on  $\xi$  and on  $\tau$  as  $A_y + iA_z = a(\xi) \exp(i\omega\tau)$  and  $\phi = \phi(\xi)$  via the variables  $\xi = x - v_g t$  and  $\tau = t - v_g x$ . The space and time coordinates are normalized to  $c/\omega_{pe}$  and  $1/\omega_{pe}$ , respectively. The primes in Eqs. (38) and (39) denote a differentiation with respect to the variable  $\xi$ . In these equations the normalized group velocity of the electromagnetic wave is  $\beta_g = v_g/c$ , the electron-to-ion mass ratio is  $\rho = m_e/m_i$ , and the functions are  $\psi_e = \Gamma_e + \phi$ ,  $\psi_i = \Gamma_i - \rho\phi$ ,  $R_e = \sqrt{\psi_e^2 - (1 - \beta_g^2)(1 + a^2)}$ ,  $R_i = \sqrt{\psi_i^2 - (1 - \beta_g^2)(1 + \rho^2 a^2)}$ . The constants  $\Gamma_e$  and  $\Gamma_i$  must be specified by the boundary conditions at infinity. If the amplitude of the electromagnetic wave at  $x \rightarrow \pm\infty$  is finite ( $a = a_0$ ,  $\phi = 0$ ), and the plasma is at rest, then we have  $\Gamma_e = \sqrt{1 + a_0^2}$  and  $\Gamma_i = \sqrt{1 + \rho^2 a_0^2}$ . The density and the Lorentz factor (the energy normalized to  $m_a c^2$ ) of the  $\alpha$ -species ( $\alpha = e, i$ ) particles are equal to

$$n_\alpha = \beta_g \frac{\psi_\alpha - \beta_g R_\alpha}{R_\alpha (1 - \beta_g^2)}, \quad \gamma_\alpha = \frac{\psi_\alpha - \beta_g R_\alpha}{1 - \beta_g^2}. \quad (40)$$

Equations (38) and (39) admit the first integral

$$\frac{1 - \beta_g^2}{2} (a'^2 + \omega^2 a^2) + \frac{1}{2} \phi'^2 + \frac{\beta_g}{1 - \beta_g^2} \left( R_e - \beta_g + \frac{R_i - \beta_g}{\rho} \right) = \text{const.} \quad (41)$$

For  $a = a_0 = 0$ , Eqs. (38) and (39) describe a longitudinal plasma wave. In this case the integral (41) gives the relationship between the electric field and the particle energies,  $E^2 + 2(\gamma_e + \gamma_i/\rho) = \text{const.}$  The amplitude of the Langmuir wave cannot be arbitrarily large. It is limited by the condition  $R_\alpha > 0$ . At  $R_\alpha = 0$  the particle density tends to infinity. This is the wave-breaking point. Formally the set of equations (38)–(41) no longer describes the evolution of a Langmuir wave after breaking, and a kinetic description must be used. As shown by Khachatryan (1998) and Gorbunov, Mora, and Ramazashvili (2002), ion motion has little influence on the wave-breaking limit, which is given by terms of the order of  $\rho$ . When the wave is slow, i.e.,  $\beta_g \ll 1$ , the wave-breaking amplitude is equal to  $E_m = \beta_g$ , as discussed by Dawson (1959). In the generic case when  $\gamma_g = 1/\sqrt{1 - \beta_g^2}$  can be arbitrarily large, the maximum value of the electric field in the wave is

$$E_m = \frac{m_e \omega_{pe} c}{e} \sqrt{2(\gamma_g - 1)}. \quad (42)$$

The field here is expressed in dimensional form, also called the Akhiezer-Polovin limiting electric field. Tajima and Dawson (1979) recognized that a fast wave does not (easily) break because the electron momentum

increases while its velocity is still at  $c$ . At wave breaking, the electron velocity becomes equal to the Langmuir-wave phase velocity. This condition is equivalent to the equality  $\gamma_e = \gamma_g$ . The effect of thermal motion of the electrons on Langmuir wave breaking has been discussed by Katsouleas and Mori (1988) and by Khachatryan (1998).

Another important characteristic of nonlinear waves is that their frequency, and hence wavelength, is dependent on wave amplitude. In cold plasmas the wavelength of a weak Langmuir wave is  $\lambda_p = 2\pi\beta_g c/\omega_{pe}$ . In the ultrarelativistic case ( $\gamma_e, \gamma_g \gg 1$ ) the wavelength is about  $4\lambda_p \sqrt{2\gamma_e}$ , where  $\gamma_e \leq \gamma_g$ . We see that relativistic effects lead to an increase of the wavelength. However, the effects of ion motion decrease the wavelength, as discussed by Khachatryan (1998), Bulanov *et al.* (2001), Gorbunov, Mora, and Ramazashvili (2002), and Gorbunov *et al.* (2003).

As seen above, Langmuir wave breaking occurs when the quiver velocity of the electron becomes equal to the phase velocity of the wave. In a plasma with an inhomogeneous density, the Langmuir wave frequency depends on the coordinates. As a result, the wave number depends on time through the well-known relationship (Whitham, 1974)  $\partial_t k = -\partial_x \omega$ . The resulting increase over time of the wave number results in a decrease of the phase velocity and breaking of the wave at the instant when the electron velocity equals the wave phase velocity, even if the initial wave amplitude is below the breaking threshold. In this case wave breaking occurs in such a way that only a small part of the wave is involved. We can use this property to perform an injection of electrons into the acceleration phase, as was shown by Bulanov and co-workers (Bulanov, Naumova, *et al.*, 1998; see also Suk *et al.* 2001; Hemker *et al.*, 2002; Hosokai *et al.*, 2003; Tomassini *et al.*, 2003; Thompson *et al.*, 2004). In a similar way Langmuir wave breaking may occur in non-one-dimensional configurations (see Dawson, 1959; Bulanov *et al.*, 1997), due to the dependence of the wave frequency on its amplitude, as analyzed by Drake *et al.* (1976).

For a circularly polarized transverse electromagnetic wave with  $a = a_0$  and  $\phi = 0$  we can easily obtain from Eq. (39) that the frequency as a function of the wave amplitude and velocity is given by  $\omega^2 = \gamma_g^2 (1/\Gamma_e + \rho/\Gamma_i)$ . This expression may be rewritten in the following dimensional form containing the wave number  $k$ :

$$\omega^2 = k^2 c^2 + \omega_{pe}^2 (1/\sqrt{1 + a_0^2} + \rho/\sqrt{1 + \rho^2 a_0^2}).$$

Here we see that relativistic effects and ion motion modify the plasma frequency. The electron in a transverse electromagnetic wave moves along a circular trajectory with energy  $m_e c^2 \sqrt{1 + a_0^2}$ . Its longitudinal momentum is equal to zero, and the transverse component of the momentum is equal to  $a_0$ .

In a linearly polarized wave in plasmas, the transverse and longitudinal motions of electrons are always coupled, as was shown by Akhiezer and Polovin (1956), Chian (1981), and Smetanin *et al.* (2004). In a small but finite-amplitude  $a_0$  linearly polarized wave, the trans-

verse component of the electric field oscillates with a frequency  $\omega \approx kc + (\omega_{pe}^2/2kc)(1 - a_0^2/2)$ , while the longitudinal component oscillates with twice the frequency, and its amplitude is of the order of  $a_0^2$ .

### A. Wakefield generation and relativistic electron acceleration

Just as a sufficiently strong wind induces instability at the surface of water with subsequent waves and anomalous viscosity, a sufficiently intense laser pulse (or photon flux) induces a plasma wave (or the Langmuir wave or longitudinal wave mentioned above as a relativistic rectification). In this case the photon flux causes a “ripple” in the plasma, which causes a collective force to drag (accelerate) electrons. This wave is called the wakefield, as it appears in the wake of (i.e., behind) the laser pulse. We note here that resonant excitation in a large-amplitude plasma wave by means of sequences of short laser pulses has been analyzed by Dalla and Lontano (1994) and by Umstadter, Esarey, and Kim (1994). An alternative configuration for a laser wakefield accelerator has been proposed by Andreev *et al.* (1992), Antonson and Mora (1992), Krall *et al.* (1993). In this configuration acceleration is enhanced via resonant self-modulation of the laser pulse. This requires laser power in excess of the critical power for relativistic guiding and a plasma wavelength short compared to the laser pulse length. Relativistic and density wake effects strongly modulate the laser pulse at the plasma wavelength, resonantly exciting the plasma wave and leading to enhanced acceleration.

Wakefield excitation, within the framework of a given laser pulse, is described by Eq. (38), where the terms  $\psi_\alpha$  and  $R_\alpha$  on the right-hand side contain the given function  $a(\xi)$ . The wakefield is excited by the nonlinear force of the laser electromagnetic fields, called the *ponderomotive potential*:

$$\Phi = m_e c^2 a_0^2 / e \quad (43)$$

in the case when  $a_0 \ll 1$ . In this “weak-field” limit the ponderomotive force is proportional to the square of the laser field ( $a_0^2$ ) because the force  $\mathbf{v} \times \mathbf{B}$  is proportional to  $\mathbf{v} \times \mathbf{E}$ , where  $\mathbf{E}$  and  $\mathbf{B}$  are the laser electromagnetic fields. When  $a_0$  is sufficiently large (or arbitrary),

$$\Phi = m_e c^2 \gamma_e / e. \quad (44)$$

As we can see from Eq. (38) in the case of immobile ions ( $\rho \rightarrow 0$ ) the electrostatic potential in the wakefield wave is bounded by  $-1 < \phi < a_m$  with  $a_m$  the maximum value of the laser pulse amplitude (see Bulanov, Kirsanov, and Sakharov, 1989). Equation (38) also shows that the effect of ion motion restricts the potential  $\phi$  between the bounds  $-1 < \phi < \min\{a_m, \rho^{-1}\}$ . From this equation we can further find that, behind a short laser pulse, the wavelength  $\lambda_{W-F}$  of the wake and the maximum value of the electric field  $E_{W-F}$  and of the potential  $\phi_{W-F}$  scale as

$$\lambda_{W-F} = 2^{3/2} a_m, \quad E_{W-F} = 2^{-1/2} a_m, \quad \phi_{W-F} = a_m^2. \quad (45)$$

for  $-1 < a_m < \rho^{-1/2}$ , and as

$$\lambda_{W-F} = 2^{1/2} / (\rho a_m), \quad E_{W-F} = 2^{-1/2} a_m, \quad \phi_{W-F} = \rho^{-1} \quad (46)$$

for  $a_m > \rho^{-1/2}$ .

The effects of ion motion modify the transverse electromagnetic wave when its amplitude becomes larger than  $\rho^{-1}$ . For an electron-proton plasma and a 1- $\mu\text{m}$  laser, this corresponds to a radiation intensity of  $I = 4.7 \times 10^{24} \text{ W/cm}^2$ . However, during wakefield generation and evolution, ion motion becomes important at much lower intensities, when  $a_m > \rho^{-1/2}$ . Hence the wakefield wavelength decreases with increasing laser pulse amplitude. This limit corresponds to the substantially lower laser intensity  $I = 2.5 \times 10^{21} \text{ W/cm}^2$ .

We note here that ion evolution leads to late-time ion structures formed in the wake of an ultrashort, intense laser pulse propagating in a tenuous plasma, as observed by Borghesi *et al.* (2005). The ion pattern found in the wake of the laser pulse shows unexpectedly regular modulations inside a long, finite width channel.

In dimensional units the excited wakefield is

$$E_{W-F} = \frac{m_e \omega_{pe} c}{e} f(a_m, \gamma_g). \quad (47)$$

Here  $f(a_m, \gamma_g)$  is a function that depends on the laser pulse shape and amplitude as well as the plasma density. The field  $E_{W-F,0} = m_e \omega_{pe} c / e$  is the Tajima-Dawson field at which a wave with a nonrelativistic phase velocity would break (resulting in so-called “white waves,” similar to those in Hokusai’s immortal landscapes of the “Floating World” School Ukiyoye), acquiring density modulations near 100% or more (Tajima and Dawson, 1979). Sometimes  $E_{W-F,0}$  is called the wave-breaking field, but this is not appropriate in relativistic regimes, where wave breaking is mitigated by the wave’s relativistic phase velocity (Tajima and Dawson, 1979). In this case, since the wakefield phase velocity is equal to the laser pulse group velocity ( $v_g = c \sqrt{1 - \omega_{pe}^2 / \omega^2}$ ), we have  $\gamma_g = \omega / \omega_{pe} = \sqrt{n_{cr} / n_0}$ , where  $n_0$  is the electron density of the plasma and where the critical density is  $n_{cr} = \omega^2 m_e / 4 \pi e^2$ . The intensity of the collective accelerating field is immense and for a given laser pulse amplitude below the wave-breaking limit the wakefield scales as

$$E_{W-F,0} = [n_0 / (10^{18} \text{ cm}^{-3})] \text{ GeV/m}. \quad (48)$$

When the laser pulse amplitude is larger than the wave-breaking limit, i.e., larger than  $(m_e \omega_{pe} c / e) \sqrt{2(\gamma_g - 1)}$ , a stationary wakefield does not exist. However, in this regime for a finite time the laser pulse can generate electric fields substantially higher than the field given by Eqs. (45) and (48). This corresponds to electron acceleration behind the laser pulse in the near-critical plasma, as discussed by Bulanov, Kirsanov, and Sakharov (1989); Tzeng *et al.* (1997); Gordon *et al.* (1998); Liseikina *et al.* (1999); Nagashima, Kish-

imoto, and Takuma (1999); Trines *et al.* (2001); Pukhov and Meyer-ter-Vehn (2002); Pukhov (2003).

The laser pulse ponderomotive potential can exert a strong force on electrons either directly (i.e., by the laser electromagnetic field itself) or via an electrostatic field such as the wakefield. For relativistically strong laser fields ( $a_0 > 1$ ) the accelerating field increases in proportion to the square root of the laser intensity  $I$ . At the same time, the interaction time between the laser and electron increases, as the electron velocity along the direction of laser propagation (the  $x$  direction) approaches  $c$ , which is proportional to  $a_0$ . As a result the energy (or momentum) gain  $E$  of a relativistic particle from a laser-electron interaction in a homogeneous plasma is of the order of

$$E = eE_{W-F}l_{\text{acc}}, \quad (49)$$

where  $l_{\text{acc}}$  is the acceleration length (Tajima and Dawson, 1979),

$$l_{\text{acc}} = \frac{2c}{\omega_{pe}} \gamma_g^2 = \frac{2c}{\omega_{pe}} \left( \frac{\omega}{\omega_{pe}} \right)^2. \quad (50)$$

This length is approximately  $(\omega/\omega_{pe})^2$  times greater than the plasma wavelength. We note that this result was obtained in the limit of a small-amplitude wakefield. In the case of a relativistically strong wakefield, the acceleration length is  $l_{\text{acc}} = (2c/\omega_{pe})\gamma_g^2 a_0$ . The maximum energy of the accelerated particles is constrained by the plasma wave breaking:  $E_{\text{max}} = 4m_e c^2 \gamma_g^2$  (Esarey and Pilloff, 1995; Reitsma *et al.*, 2002). In the case of tailored gas targets the electron energy can be well above this limit [e.g., see Bulanov *et al.* (2001), and references therein].

Wakefield acceleration of electrons has been observed in experiments by Modena *et al.* (1995) and Nakajima *et al.* (1995). Record electron energy has been obtained by Malka *et al.* (2002). In these experiments the quasithermal fast electron spectrum has been observed. However, bunches of relativistic electrons with a narrow energy spread have been demonstrated (Faure *et al.*, 2004; Geddes, 2004; Mangles *et al.*, 2004; Miura *et al.*, 2005; Yamazaki *et al.*, 2005). In these experiments, the fast electron energy is 10–170 MeV, the laser irradiance varies from  $10^{18}$  to  $10^{19}$  W/cm<sup>2</sup>, the pulse length is 30–55 fs, and the density ranges from  $10^{18}$  to  $10^{20}$  cm<sup>-3</sup>. Under these experimental conditions electrons arrive in the acceleration phase as a result of self-injection via Langmuir wave breaking.

As mentioned above, according to Akhiezer and Polovin (1956), the group velocity of the relativistically strong electromagnetic wave given by  $v_g = c\sqrt{1 - \omega_{pe}^2/(\omega^2\sqrt{1+a_0^2})}$ , depends on the wave amplitude  $a_0$ . As a result we find the amplitude of the laser-pulse driver which generates the breaking wake wave:  $a_0 > (2\omega/\omega_{pe})^{2/3}$  (Zhidkov, Koga, Kinoshita, and Uesaka, 2004; Zhidkov, Koga, Sasaki, and Uesaka, 2004). This corresponds to the wave-breaking condition, when the electron displacement inside the wave becomes equal to or larger than the wavelength of the wake plasma wave. Since in order to have a good quality wake wave the

width of the laser-pulse driver must be wider than the plasma wave wavelength, it easy to show that the above condition of wake wave breaking means that the laser power is above the threshold of the relativistic self-focusing.

Wave breaking acquires different features in three-dimensional configurations for a finite width relativistically strong laser pulse propagating in a homogeneous plasma or inside a plasma channel. The 3D wakefield in a plasma has a specific paraboloidal structure. The transverse inhomogeneity of the wake plasma wave is caused by the inhomogeneity of the wake field frequency  $\omega_{W-F}$  due to the relativistic dependence, which in its turn is determined by the transverse inhomogeneity of the laser-pulse driver. The curvature of the constant phase surfaces increases with the distance from the laser-pulse front. The curvature radius of the structure  $R$  decreases until it becomes comparable to the electron displacement  $\xi_{W-F}$  in the wake wave and the wake wave breaks. This is the so-called regime of the transverse wake wave breaking and the electron injection into the acceleration phase (Bulanov *et al.*, 1997).

Under the conditions, when both the nonlinear wave breaking and the self-focusing instability occur simultaneously, the breaking appears in the first period of the wake plasma wave, and electrons are injected within the first wavelength of the wake. It is well known that electrons injected at the breaking point then move along the separatrix in the phase plane,  $x - v_g t, p_x$ . Calculating the energy spectrum of fast electrons (for details, see Bulanov and Tajima, 2005; Bulanov, Yamagiwa, Esirkepov, *et al.*, 2005), we consider electrons whose trajectories lie on the separatrix and electrons are distributed uniformly along the separatrix. Near the top of the separatrix, where the electron momentum dependence on the coordinate can be approximated by  $p_x = p_m(1 - X^2\omega_{pe}^2/2c^2a^2) = p_m(1 - t^2/t_{\text{acc}}^2)$ , where  $X = x - v_g t$  and  $p_m = E_{\text{max}}/c = 4m_e c \gamma_g^3$ , we write the electron distribution function  $f(X, p_x)$  as

$$f(X, p_x) = \frac{n_b \omega_{pe}}{\sqrt{2ca}} \delta \left[ p_x - p_m \left( 1 - \frac{X^2 \omega_{pe}^2}{2c^2 a^2} \right) \right]. \quad (51)$$

Here  $\delta(z)$  is the Dirac delta function. When the laser pulse reaches the end of the plasma, the electrons appear in a vacuum region with their instantaneous energy. The distribution function of the electrons at the target has the form  $f(t, E) = (n_b \omega_{pe} / \sqrt{2ca}) \delta(E - E_m(1 - t^2/t_{\text{acc}}^2))$ . In order to find the energy spectrum of electrons on the target we must integrate over time the  $f(t, E)$  function between  $-t_{\text{acc}}$  and  $t_{\text{acc}}$ . We obtain

$$\begin{aligned} \frac{dN(E)}{dE} &= \frac{n_b \omega_{pe}}{\sqrt{2ca}} \int_{-t_{\text{acc}}}^{t_{\text{acc}}} \delta \left[ E - E_m \left( 1 - \frac{t^2}{t_{\text{acc}}^2} \right) \right] dt \\ &= \frac{n_b \omega_{pe}}{2\sqrt{2ca} \sqrt{E_m(E_m - E)}}. \end{aligned} \quad (52)$$

In Fig. 16 we present the electron energy spectrum given by formula (52).

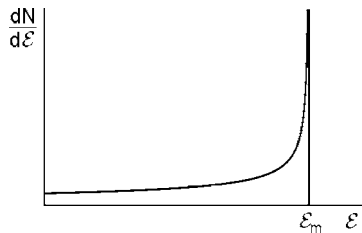


FIG. 16. Quasimonoenergetic energy spectrum of electrons with the energy close to its maximal value.

As follows from Eq. (52) and seen in Fig. 16, the energy spectrum has a maximum at  $E = E_m$  and it has a cut with no particles for  $E > E_m$ . A similar spectrum of fast electrons accelerated by the wake plasma wave in the breaking regime can be seen in experiments by Geddes *et al.* (2004) and Mangles *et al.* (2004).

Plasma inhomogeneity, depending on its shape, can either improve the conditions for acceleration or cause them to deteriorate. In an inhomogeneous plasma with a density that depends on the coordinate as  $n_0(x) = n_0(L/x)^{2/3}$ :  $L \approx (c/3\omega_{pe})(\omega/\omega_{pe})^2$ , the acceleration length becomes formally infinite and the particle energy growth becomes unlimited,  $E = m_e c^2 (\omega/\omega_{pe})^2 (x/L)^{1/3}$ . The electron energy gain in the regime when the wakefield is below the wave-breaking threshold should scale as  $E = m_e c^2 a_0$ .

The snowplow acceleration discussed by Ashour-Abdalla *et al.* (1981) and Tajima (1985) was found to entail an energy gain proportional to  $a_0^2$ . This scaling, as explained above, arises from the ponderomotive potential and has sometimes been called *direct acceleration*.<sup>5</sup> It has also been referred as *Dirac acceleration* (Nakajima, 2002) and other names. However, the basic acceleration kinematics are the same. This scaling offers a tremendous advantage when we increase the laser intensity to the relativistic regime. Instead of the laser quivering energy scaling as  $m_e c^2 a_0$  the longitudinal electron energy scales as  $m_e c^2 a_0^2$ . A similar acceleration mechanism has been considered by Gunn and Ostriker (1969) responsible for the production of ultrahigh-energy cosmic rays in interactions of the strong electromagnetic radiation generated by rotating neutron stars. This mechanism allows the electron motion in a laser plasma to become more coherent with photons. The interaction grows more efficient as the laser intensity increases in the ultrarelativistic regime.

In an infinite plane geometry, even a strong electromagnetic wave interaction provides no energy gain to an electron, according to the Woodward-Lawson theorem (Woodward, 1947; Lawson 1979). However, such effects

do not include three-dimensional geometry (Troha *et al.*, 1999), e.g., in the focus region (Narozhny and Fofanov, 2000; Pang *et al.*, 2002). The wave-guide and wiggler mode structure of the electromagnetic wave (Kong *et al.*, 2003; Singh and Tripathi, 2004) as well as the radiation friction force (Fradkin, 1980; Bulanov *et al.*, 2004) make the resulting energy gain finite. We note that vacuum electron acceleration up to 200 MeV energy has been observed by Malka *et al.* (1997). (See also Banerjee *et al.*, 2005, where the results of the electron interaction with the focused laser pulse in vacuum are reported.) However, the conditions of theorem may break down for a variety of reasons, such as radiation damping due to the intense acceleration or due to the external magnetic field (Davydovskii, 1963; Kolomenskii and Lebedev, 1963; Roberts and Buchsbaum, 1964; Apollonov *et al.*, 1998), or due to extraction of fast particles by means of a thin foil (Vshivkov *et al.*, 1998a, 1998b). It is also worth noting that until the laser intensity exceeds  $10^{22}$  W/cm<sup>2</sup> ions are not considered as too heavy. This leaves the laser-matter interaction in our problem almost entirely due to the electron dynamics, a radically different situation from that in typical plasma physics where both ions and electrons are allowed to move simultaneously. It is the simultaneous motion of these two species that brings on a host of destructive plasma instabilities (Mikhailovskii, 1992). In the relativistic regime, by contrast, the plasma instabilities, as we shall see below, are more often than not self-organizing in nature. This difference in laser-plasma interactions is another very significant distinction between the relativistic and nonrelativistic regimes.

## B. Relativistic self-focusing

Probably the most impressive nonlinear phenomenon in an underdense plasma is the self-focusing of laser radiation. Self-focusing, discovered by Askar'yan in 1962, appears to be due to the nonlinear change of the refractive index of the medium in the region where a high-intensity electromagnetic wave has a transverse intensity distribution (see also Chiao, Garmier, and Townes, 1964). In the relativistic laser pulse-plasma interaction self-focusing appears due to a relativistic increase in electron mass and to plasma density redistribution under the action of the ponderomotive force. This effect was predicted in the 1960s and 1970s by Litvak (1969), Max *et al.* (1974), Schmidt and Horton (1985), but had to wait until the advent of ultrahigh-intensity lasers to be demonstrated (Borisov *et al.*, 1992; Monot *et al.*, 1995). The threshold (critical) power for relativistic self-focusing is (Barnes *et al.*, 1987; Sun *et al.*, 1987)

$$P_{\text{cr}} = \frac{m_e c^5 \omega^2}{e^2 \omega_{pe}^2} \approx 17 \left( \frac{\omega}{\omega_{pe}} \right)^2 \text{ GW.} \quad (53)$$

The laser pulse can be self-focused over a distance much larger than the Rayleigh length

<sup>5</sup>See, for example, Feldman and Chiao, 1971; Landau and Lifshitz, 1980; Lai, 1980; Hartemann *et al.*, 1995, 1998; Rau, Tajima, Hojo, 1997; Salamin and Faisal, 1997; Hartemann *et al.*, 1998; Pukhov and Meyer-ter-Vehn, 1998; Quesnel and Mora, 1998; Narozhny and Fofanov, 2000; Salamin and Keitel, 2002.

$$Z_R = \pi w_0^2 / \lambda, \quad (54)$$

where  $w_0$  is the laser pulse waist at the focus.

The self-focusing of an initially almost homogeneous wave field corresponds to the development of filamentation instability. If the wave amplitude is initially slightly modulated in the transverse direction, then the modulation of the refractive index causes the wave fronts to curve. This results in the transverse redistribution of the electromagnetic-field energy so that the modulation amplitude increases, and instability develops. Filamentation instability can be described by linearizing the set of relativistic electron hydrodynamics equations—Maxwell equations—and assuming the variables to be in the form  $\sim \exp[-i(\omega_0 + \Omega)t + ik_0x + iQ_\perp r_\perp]$ , where the unperturbed wave frequency and wave number are related as  $\omega_0 = \sqrt{k_0^2 c^2 + \omega_{pe}^2}$ . As a result the dispersion equation for the instability growth rate is

$$\Omega = \frac{Q_\perp}{2k_0} \sqrt{Q_\perp^2 c^2 - \omega_{pe}^2 |a_0|^2}. \quad (55)$$

Here  $Q_\perp$  is the transverse wave number of the perturbation. The instability develops (i.e., the perturbation frequency  $\Omega$  is imaginary) if  $Q_\perp < Q_{\perp, \max} = |a| \omega_{pe} / c$ . For  $Q_\perp > Q_{\perp, \max}$ , diffraction prevails and instability is suppressed.

Relativistic filamentation instability leads to relativistic self-focusing of the laser beam. In the weakly relativistic case ( $|a| \ll 1$ ), the condition for relativistic refraction to prevail over diffractive spreading is  $P > P_{\text{cr}}$  [see Eq. (53)]. It is easy to verify that this condition is the analog of the above condition for filamentation instability with  $Q_{\perp, \max} \approx 1/w_{p,0}$ , where  $w_{p,0}$  is the initial laser spot size. For  $P = P_{\text{cr}}$ , diffractive spreading of the laser beam is balanced by the radial inhomogeneity of the plasma refractive index caused by a relativistic increase in electron mass. For  $P > P_{\text{cr}}$ , relativistic self-focusing overcomes diffractive spreading and, in the cubic-nonlinearity approximation, the axially symmetric beam is focused into a field singularity (the transverse size of the laser beam tends to zero and the amplitude of the laser field tends to infinity) in a finite time

$$t_{s-f} = \frac{Z_R}{c} \sqrt{\frac{P}{P_{\text{cr}}} - 1}, \quad (56)$$

where  $Z_R$  is the Rayleigh length given by Eq. (54). If  $P \gg P_{\text{cr}}$ , depending on the initial radial intensity profile, the laser beam can split into several filaments, each of which can undergo catastrophic self-focusing.

The propagation of a relativistically strong ( $|a_0| \gg 1$ ) short pulse (or of a long pulse with a sharp leading edge) is accompanied by excitation of a strong wakefield. In this situation self-focusing cannot be studied separately from other dynamical processes, but must be understood in conjunction with pulse self-modulation, generation of a strongly nonlinear wakefield, erosion of the leading edge, etc. At present, there is no consistent analytical theory of relativistic self-focusing and filamentation of ultrashort superintense laser pulses. The nonlinear evo-

lution of an electromagnetic wave in an underdense plasma has been studied under various simplifying assumptions, such as circularly polarized pulses, the quasistatic approximation, and weak nonlinearity (Litvak, 1969; Sun *et al.*, 1987), or within the framework of the paraxial approximation (Barnes *et al.*, 1987; Bulanov and Sakharov, 1991). Linearly polarized pulses are especially complex because the analytic simplifications that are possible in the case of circularly polarized pulses from their lack of harmonic content do not apply. In addition the intensity of petawatt-power laser pulses is so high that we cannot take advantage of the weak nonlinearity approximation. Much of our information on the dynamics of self-focusing of such pulses is provided by computer simulations (see, for example, Askar'yan *et al.*, 1994, 1995; Pukhov and Meyer-ter-Vehn, 1996; Tzeng, Mori, and Decker, 1996; Chessa and Mora, 1998; Tzeng and Mori, 1998; Naumova *et al.*, 2002a, 2002b).

As is well known, in 3D plasma configurations the role of nonlinearity becomes more important than in 1D and 2D because wave collapse in 3D configurations results in the development of a 3D singularity (Zakharov, 1972; Kuznetsov, Rubenchik, and Zakharov, 1986; Kuznetsov, 1996).

To illustrate specific features of the laser light plasma interaction in three-dimensional regimes, Fig. 17 shows the results of 3D particle-in-cell simulations with the code REMP (Esirkepov, 2001) of laser beam propagation in an underdense plasma (Naumova *et al.*, 2002a, 2002b). Some of these features were described by Honda *et al.* (1999). Pukhov and Meyer-ter-Vehn (1996) have shown that the magnetic interaction, discovered in 2D configurations by Askar'yan *et al.* (1994), plays an important role during relativistic self-focusing in the 3D case for circularly polarized light.

We consider the relativistic self-focusing of a linearly polarized semi-infinite laser beam in an underdense plasma with electric field in the  $y$  direction. The dimensionless amplitude of the laser pulse is  $a=3$ , which corresponds, for a  $1\text{-}\mu\text{m}$  laser, to an intensity of  $I=1.25 \times 10^{19} \text{ W/cm}^2$ . The pulse width is  $12\lambda$ . The plasma density corresponds to  $\omega/\omega_{pe}=0.45$ . The ion-to-electron mass ratio corresponds to the proton mass and it is equal to  $m_i/m_e=1836$ . Figure 17 shows the relativistic self-focusing of a linearly polarized laser pulse in a semi-infinite plasma. We see the formation of a narrow self-focusing channel in the region between the leading part of the pulse, with pronounced filamentation, and the wide trailing part of the pulse. The laser pulse distortion is asymmetric. This anisotropic self-focusing is illustrated by the projections, shown in Fig. 17, of the surface of the constant value of the electromagnetic energy density (a) on the  $x, z$  plane and (b) on the  $x, y$  plane. In the  $x, z$  plane (which corresponds to the  $s$  polarization plane) the distribution of the electromagnetic energy density is up-down symmetric with three filaments in the leading part of the pulse. The self-focusing in the  $s$  plane is very similar to the self-focusing of the  $s$ -polarized laser pulse in the 2D case (Askar'yan *et al.*, 1994). In contrast

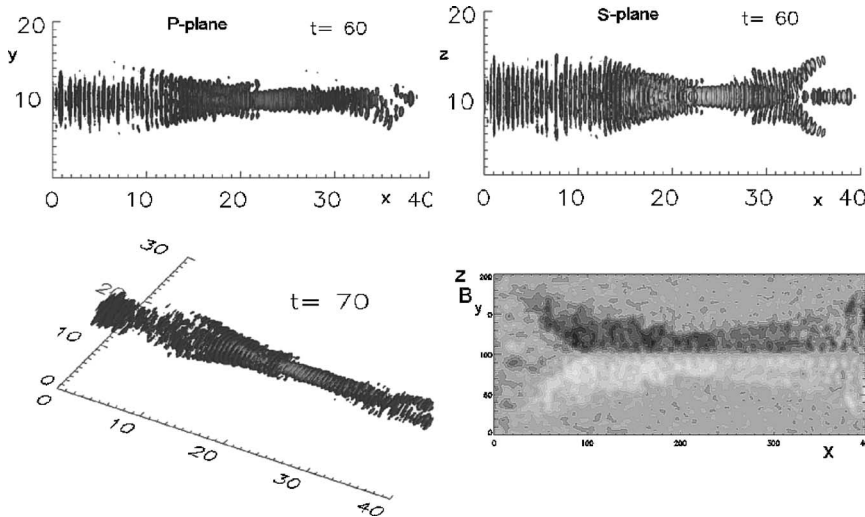


FIG. 17. Relativistic self-focusing. Isosurface of the electromagnetic energy density of a linearly polarized semi-infinite beam in projection to  $p$  and  $s$  plane, and its 3D view; cross section of the magnetic-field component.

the projection on the  $x, y$  plane (in the  $p$ -polarization plane) is asymmetric and we see that the leading part of the pulse starts to bend. The pulse-bending mechanism is discussed by Naumova, Koga, Nakajima, *et al.* (2001).

The asymmetry of the self-focusing leads to a complicated internal structure of the laser pulse channel, as shown in Fig. 17. Here we present two-dimensional cross sections of the magnetic field distribution of the  $y$  component. The self-generated magnetic field changes sign in the symmetry plane, as discussed by Askar'yan *et al.* (1994). Quasistatic magnetic fields have been observed in laser-produced plasmas for moderate intensities of laser radiation (Korobkin and Serov, 1966; Askar'yan *et al.*, 1967; Stamper *et al.*, 1971; Daido *et al.*, 1986). They can affect the thermal conductivity and the long-time-range plasma dynamics (see, for example, Bell, 1994). Several mechanisms of magnetic-field generation are discussed in the literature, including linear and nonlinear processes in plasma waves (Gorbunov, Mora, and Antonsen, 1996; Khachatryan, 2000), baroclinic effects (Shukla, Rao, Yu, and Tsintsadze, 1986), anisotropic electron pressure (Bychenkov, Silin, and Tikhonchuk, 1990), spatial nonuniformity or time variation of the ponderomotive force (Sudan, 1993), inverse Faraday effect in a circularly polarized pulse (Steiger and Woods, 1971; Berezhiani, Mahajan, and Shatashvili, 1997; Gorbunov and Ramazashvili, 1998), and the effect of the current produced by electrons accelerated inside self-focusing channels of electromagnetic radiation (Askar'yan *et al.*, 1994) and at the plasma-vacuum interface in an overdense plasma (Daido *et al.*, 1986; Kuznetsov *et al.*, 2001). In the latter case plasma quasineutrality requires that the fast-electron current be canceled by a cold electron current of opposite sign. These oppositely directed currents repel each other. The repulsion and increase in magnetic field value are the manifestation of current filamentation (Weibel, 1959; Bychenkov, Silin, and Tikhonchuk, 1990; Askar'yan *et al.*, 1994; Pegoraro *et al.*, 1996, 1997; Honda *et al.*, 2000; Califano *et al.*, 2001; Sakai *et al.*, 2002; Honda, 2004). Due to symmetry of the laser pulses, the quasistatic magnetic field reverses its sign at the laser beam axis and hence can

focus charged particles, e.g., fast particles in a laser particle accelerator (Tajima and Dawson, 1979; Bingham, 1994). In addition, in the fast ignitor concept of inertial confinement fusion (Tabak *et al.*, 1994) the quasistatic magnetic field is expected to collimate superthermal electrons and ensure energy transfer from the relatively low-plasma-density region where these electrons are produced by the laser pulse to an overdense plasma in the high-density core where they ignite the fuel.

In the relativistic regime of laser self-focusing, magnetic field generation becomes dynamically important. As a result we see magnetic interaction of the self-focusing channels. Magnetic interaction appears due to the fact that electrons accelerated inside a self-focused laser pulse produce electric currents in the plasma and an associated quasistatic magnetic field. The attraction of electric currents leads to a redistribution of fast electrons. This in turn changes the refractive index, due to the relativistic increase of electron mass, the effective plasma frequency is smallest in regions with the highest concentration of fast electrons. This process causes high-intensity laser radiation filaments to merge and provides a mechanism for transporting laser energy over long distances. In order to estimate the strength of the magnetic field, we note that the velocity of the current-carrying electrons is limited by the speed of light  $c$  and write the channel radius as  $R = \sqrt{a_0} d_e$ , where  $d_e = c / \omega_{pe}$ . We obtain

$$B = \sqrt{a_0} m_e c \omega_{pe} / e, \quad (57)$$

which gives a value of the order of 1 GG for typical values of the laser plasma parameters. A magnetic field over 340 MG has been measured by Tatarakis *et al.* (2002) in the interaction of the linearly polarized  $I = 9 \times 10^{19}$  W/cm<sup>2</sup> laser pulse with a thin solid target. In the case of circularly polarized laser pulse-plasma interaction, a 7-MG magnetic field has been observed in the experiments by Najmudin *et al.* (2001), where its generation was attributed to the inverse Faraday effect.

The merging of self-focused channels and the associated self-generated magnetic field were already seen in the 2D PIC simulations of Forslund *et al.* (1985). The

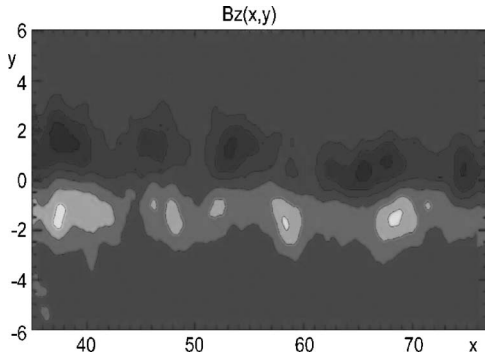


FIG. 18. Vortex row behind the laser pulse seen in the isocontours of the magnetic field.

merging is due to the attraction of the electric currents inside the filaments and the subsequent change of the refractive index due to relativistic electron redistribution (Askar'yan *et al.*, 1994). This mechanism was later called “magnetic lensing” or “electron pinching” and discussed in many papers, including those of Pukhov and Meyer-ter-Vehn (1996), Borghesi *et al.* (1998), and Ruhl, Sentoku, Mima, *et al.* (1999).

The self-generated magnetic field in the laser-plasma interaction evolves into structures that are associated with electron vortices as a consequence of the equation  $\nabla \times B = -4\pi env/c$  (Bulanov, Lontano, Esirkepov, *et al.*, 1996). In this case the electron fluid vorticity is  $\nabla \times v = c\Delta B/4\pi en$ . The vortex row is shown in Fig. 18. Near the laser pulse this vortex row is symmetrical, but unstable against bending and transformed into an antisymmetric configuration. The distance between vortices is comparable to, or in their final stage even larger than, the collisionless skin depth. The vortex row moves as a whole in the direction of laser pulse propagation with a velocity much less than the group velocity of the pulse. The velocity of the vortex row decreases with increasing distance between the vortex chains that form the row (Bulanov, Lontano, Esirkepov, *et al.*, 1996).

Inside a stationary vortex, the radial component of the force due to magnetic pressure and the centrifugal force of electron rotation is balanced by the force due to the charge-separation electric field (Gordeev and Losseva, 1999). The electric current carried by fast electrons forms an electron vortex chain over a time scale typical of the response time of the electron component. During this period ions can be assumed to be at rest. The vortices nevertheless can interact with their neighbor vortices, resulting in a redistribution of the quasistatic magnetic field. A typical time scale in this regime corresponds to scaling, which corresponds to the whistler wave range in magnetized plasmas (see, for example, Ginzburg, 1964).

As seen above, the fast-electron electric current is localized inside self-focused filaments. Since the net electric current of the filament is zero, the electric current inside the filament core and the electric current in the filament shell have opposite signs. Oppositely directed electric currents repel each other. However, inside the

core the dominant force corresponds to self-pinching. These repelling and pinching forces act on the electron component of the plasma. The electrons shift radially, producing an electric field due to electric charge separation. This force in turn balances the repelling-pinching force. The two forces compress the ions in the inner region and push them away towards the outer region of the filament.

We use Eq. (57) to estimate the magnetic field inside the filament. The magnetic pressure is balanced by the electric charge separation field if  $B^2/8\pi = e\delta n\phi$ . Here  $e\delta n$  is the separation electric charge and  $\phi$  is the electrostatic potential, which is equal to  $\phi = 2\pi neR^2$  for  $\delta n \approx n$ . These estimates were done within the framework of the approximation of immovable ions. Ions can be assumed to be at rest during a time approximately equal to  $1/\omega_{pi}$ , where  $\omega_{pi} = \sqrt{4\pi ne^2/m_i}$ . For longer times the ions start to move and are accelerated outwards by the electric field of the charge separation. Their maximum energy equals  $E_{\max} = e\phi = 2\pi ne^2 R^2 = m_e c^2 (R/d_e)^2$ , and it is of the order of  $m_e c^2 a_0$ . Sakai *et al.* (2002) have interpreted the self-focusing and defocusing observed in experiments (Nakajima, 2001) in terms of critically self-organized phenomena.

### C. Relativistic transparency and pulse shaping

The dependence of a relativistically strong electromagnetic wave frequency on its amplitude results in the relativistic transparency of overdense plasmas. A low-frequency wave can propagate through the plasma if the plasma electrons do not screen the electric field of the wave. The condition for wave propagation implies that the convection electric current density  $-env$  is smaller than the displacement current  $\partial_t E/4\pi$  in the wave, i.e.,  $en_0 v \leq \omega E/4\pi$ . In the nonrelativistic limit the electron quiver velocity is proportional to the wave electric field  $v \sim eE/m_e \omega$ , and the condition of transparency is equivalent to  $\omega > \omega_{pe}$ . In the ultrarelativistic limit the electron velocity cannot exceed the speed of light  $v \approx c$  and the plasma becomes transparent if  $\omega > \omega_{pe}/\sqrt{a_0}$ . This corresponds to the cutoff frequency  $\omega_{pe}/(1+a_0^2)^{1/4}$  of the transverse electromagnetic wave described by Eq. (39) in the limit  $a_0 \gg 1$ .

A high-power laser pulse interacting with a very thin foil, modeled as a thin slab of overdense plasma, exhibits features that are not encountered either in underdense or in overdense plasmas (Vshivkov *et al.*, 1998a, 1998b; Shen and Meyer-ter-Vehn, 2002; Cherepenin and Kulagin, 2004) and offers experimental conditions for investigating the basic properties of the laser-plasma interaction (some of these features were discussed by Denavit, 1992). This topic has been the subject of experimental and computer studies (Giulietti *et al.*, 1997; Miyamoto *et al.*, 1997). When the foil thickness is shorter than, or of the order of, both the laser wavelength and the plasma collisionless skin depth, the interaction of the laser pulse and foil can be exploited so as to change the pulse shape. In particular, shaping a laser pulse provides a

method for exciting regular wakefields in a plasma, leading to an effective acceleration of charged particles. The present method is based on the relativistic dependence of the electron mass on the quiver energy. The leading and trailing parts of the pulse are reflected by the foil, which is relativistically transparent for the pulse peak where the intensity is the highest. This process cuts out the outer part of the laser pulse and produces a sharp leading (and trailing) edge, as is needed in order to generate a good-quality wakefield. The conditions for the foil to be transparent depend on the pulse polarization and incidence angle.

In studies of the interaction of relativistically intense electromagnetic radiation with a thin foil, the nonlinear problem can be reduced to the solution of the Cauchy problem for the wave equation with a nonlinear source (Vshivkov *et al.*, 1998a, 1998b). This approach is valid for an arbitrary incident angle of the laser pulse, since a Lorentz transformation to a reference frame moving along the foil can be used to reduce the problem of oblique incidence to that of normal incidence (Bourdier, 1983). In the moving frame all variables are assumed to be time dependent and the coordinate system perpendicular to the foil. This analytical model was used to study the relativistic transparency of the foil and to investigate how the laser pulse shape changes depending on the foil thickness, on the foil plasma density, and on the pulse amplitude. Within this model the foil transparency was found to depend on the relative magnitudes of the pulse dimensionless amplitude  $a$  and of the dimensionless foil parameter  $\varepsilon_0 = 2\pi n e^2 l / m_e \omega c$  as well as on the pulse incidence angle and polarization. Here  $l$  is the foil width and  $n$  is the plasma density inside the foil plasma. The resulting equations do not have high-order derivatives with respect to time, contrary to the case of a three-dimensional point charge, where the equations of motion with the radiation force have unphysical “self-accelerated solutions” [see discussion in the textbooks by Barut (1980), by Landau and Lifshitz (1980), and by Ginzburg (1989)]. A similar approach has been taken by Plaja and Jarque (1998) in order to use relativistic retardation in the relativistic simulation of a plasma.

The resulting nonlinearities will reshape the transmitted and reflected fields through the foil, generate harmonics, including the quasisteady dc current in the case of oblique incidence, and induce polarization changes.

The improvement of the laser pulse contrast (the ratio between the pulse energy and the prepulse energy, including the amplified spontaneous emission energy) is an important problem for various applications. For example, a high contrast is needed to prevent significant plasma formation at the surface of a solid target prior to the arrival of the main pulse. The preplasma formed by the prepulse at the front target surface changes the scenario of fast-ion generation (Nemoto *et al.*, 2001; Dudnikova *et al.*, 2003; Matsukado *et al.*, 2003; Maksimchuk *et al.*, 2004). Possible methods of prepulse reduction were mentioned in Sec. II.B, including an approach to pulse cleaning realized by Tapié and Mourou (1992) and

Homoelle *et al.* (2002). Other methods studied so far include the following:

- (i) electro-optics methods, which remove prepulses of nanosecond length with a regenerative amplifier (Nantel *et al.*, 1998);
- (ii) nonlinear optical processes, such as frequency doubling (Itatani *et al.*, 1998);
- (iii) optical parametric CPA (Kapteyn *et al.*, 1991);
- (iv) self-induced plasma layer shuttering, also known as “plasma mirror” (Pashinin, 1987; Gold *et al.*, 1991; Kapteyn *et al.*, 1991; Backus *et al.*, 1993; Ziener *et al.*, 2003).

The principle of the plasma mirror is to utilize the change in plasma transparency due to thin-target ionization (Pashinin, 1987; Bauer *et al.*, 1998; Bulanov, Macchi, and Pegoraro, 1998; Watts *et al.*, 1999; Dromley *et al.*, 2003; Doumy *et al.*, 2004). In the experimental realization by Watts *et al.* (1999) and Dromley *et al.* (2003) the transparent optical flat was placed at the point where the focused intensity was approximately  $10^{14}$  W/cm<sup>2</sup>. Any prepulse below the plasma formation threshold is transmitted. Above this value a plasma is formed and the light is reflected back with an improved contrast below  $10^{-9}$ . The typical time scale for the laser pulse shaping is determined by the collisional ionization rate and is of the order of 200 fs.

Relativistic transparency provides another way to achieve laser pulse shaping with a much shorter time scale. As noticed above, transmission through the foil depends on the pulse amplitude, the polarization, and the dimensionless parameter  $\varepsilon_0$ . In the simple case of a circularly polarized pulse,  $a(x, t) = a_0(t) \exp[i(x - t)]$ , the solution can be cast in the form  $a(0, t) = a(t) \exp(-it)$ , where we represent the two-dimensional vector  $a(t)$  as a complex-valued function  $a_y + ia_z = A(t) \exp[i\Psi(t)]$ , with amplitude  $A(t)$  and phase  $\Psi(t)$ . If we assume that  $A(t)$  and  $\Psi(t)$  are slowly varying functions of time and if we neglect the time derivatives, we obtain the amplitude and shape of the transmitted and reflected pulses

$$A(t) = A(\varepsilon_0, a_0) = \frac{1}{\sqrt{2}} \sqrt{\sqrt{(1 + \varepsilon_0^2 - a_0^2)^2 + 4a_0^2} - (1 + \varepsilon_0^2 - a_0^2)} \quad (58)$$

and

$$\Psi = \Psi(\varepsilon_0, a_0) = -\arccos(A/a_0). \quad (59)$$

We see that the condition for the foil to be transparent to electromagnetic radiation in the limit of moderate intensity is  $a_0 \ll 1$  and  $\varepsilon_0 \ll 1$ . This can be rewritten as  $\omega \gg \omega_{pe}(l/2d_e)$  which differs from the transparency condition for a uniform plasmas by a factor  $l/2d_e = l\omega_{pe}/2c$ . For relativistically strong waves with  $a_0 \gg 1$ , a foil with  $\varepsilon_0 \gg 1$  is transparent if  $a_0 \gg \varepsilon_0$ . This condition can be written as  $\omega \gg \omega_{pe}(l/2d_e a_0)$ , while according to Akhiezer and Polovin (1956) and to Kaw and Dawson (1970) a uniform plasma is transparent to relativistically strong

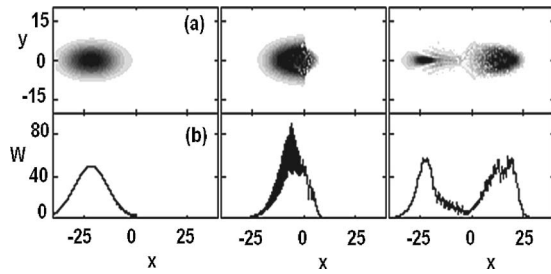


FIG. 19. Laser-pulse shaping.

radiation if  $\omega \gg \omega_{pe}/\sqrt{a_0}$  as discussed above. The relativistic transparency of an overdense plasma slab has also been studied experimentally by Fuchs *et al.* (1997).

Let us now consider a laser pulse whose amplitude varies along  $x$ . The amplitude is zero at the beginning of the pulse, increases up to its maximum value  $a_m$ , and then decreases to zero. If  $a_m > \epsilon_0$ , the portion of the pulse where  $a < \epsilon_0$  is reflected by the foil, while the portion with  $a > \epsilon_0$  propagates through the foil. The model for the foil response used above can also be used to study the dependence of the pulse transmission on incidence angle and polarization. However, this model is based on a number of approximations, and their validity must be checked in the framework of a more detailed description such as particle-in-cell (PIC) simulations. In Fig. 19 we present the results of 3D PIC simulations of a laser-foil interaction (Vshivkov *et al.*, 1998a, 1998b). A circularly polarized pulse, of initial width  $l_{\perp} = 10\lambda$ , is shown before (left column), during (central column), and after (right column) its interaction with the foil. Row (a) gives the  $x, y$  dependence of the pulse electromagnetic energy density and shows that the pulse loses its outer part, where the amplitude is smaller than  $\epsilon_0$ , due to its interaction with the foil. This “peeling” of the pulse provides an example of the nonlinear relativistic transparency of the plasma foil. As a result of this peeling, a pulse with a sharp leading edge is formed, as shown in row (b). The energy absorbed by particles in the foil is only a few percent of the total pulse energy. The pulse curves the foil and makes it concave. The modification of the foil shape acts as a concave mirror and focuses the reflected radiation into a narrow beam with a width much smaller than that of the incident pulse.

#### D. Relativistic self-induced transparency of short electromagnetic wave packets in underdense plasmas

The relativistic transparency of an overdense plasma can be considered as a self-induced nonlinear change of the plasma refractive index. In the limit of relatively low-intensity radiation, McCall and Hahn (1969) first discussed the self-induced transparency of optical beams in the bound-electron regime. They found a regime where the laser pulse propagates with anomalously low energy loss when the laser frequency is tuned while at resonance with a two-quantum-level system. Self-induced transparency is observed once the initial pulse has evolved into a symmetric hyperbolic-secant pulse

function of time and distance, and has the area characteristic of a “ $2\pi$  pulse.” Ideal transparency then persists when coherent induced absorption of pulse energy during the first half of the pulse is followed by coherent induced emission of the same amount of energy back into the beam direction during the second half of the pulse. A relativistic version of this intense laser-matter interaction has been discussed by Mima *et al.* (1986) and Tajima (1987), who found a condition for forming a triple soliton structure that allows no trace of the laser wake behind the pulse. A similar idea was formulated by Kaw *et al.* (1992). The idea is based on two different colored lasers with specific profiles (one peaking at the pulse center and the other lowering at the same point) in such a way as to induce the beat at the front of the rising peak of the first laser, while the beat wave returns its energy to the back of the second laser. Furthermore, through such an arrangement, it was found that the group velocity of photons (and the velocity of the triple soliton) could be increased from less than the speed of light  $c$  to beyond it (superluminal propagation). This idea may be extended by adopting an active lasing medium that is pumped prior to a short pulse laser. If the laser pulse length is set to match the Rabi period of the transition between the lasing electron levels, the laser can absorb energy from the active medium in its front portion, while the back loses its energy back to the medium. In a judicious choice of parameters (Fisher and Tajima, 1993; Schaechter, 1999) one can adjust the laser propagation speed from less than  $c$  in the medium to equal to or greater than  $c$ ; similar proposals of superluminal laser propagation have been made in the atomic physics community (Chiao, 1993).

#### E. Relativistic solitons

In general, in the interaction between an intense short-pulsed laser and matter, a nonlinear interaction acts to enforce (or reinforce) the self-binding forces, be it the longitudinal force (the forward Raman instability) or the transverse force [the self-focusing instability; see Bulanov *et al.* (2001), and references therein]. This is because for ultrashort laser pulses ions have too large an inertia to respond to the laser, and thus the interaction is void of ionic motion. However, nearly all instabilities in a plasma need to involve ions, and their simultaneous motion with electrons follows. When only electrons move in a plasma, there remains a strong electrostatic restoring force from inertial ions. For example, in self-focusing the intense laser creates a density cavity because light accumulates near the axis and evacuates electrons radially outward. However, since ions remain in the central region where electrons are evacuated, this forms an ionic channel. In solitons whose phase velocity is close to the speed of light, this scenario nearly always applies (see Kozlov *et al.*, 1979; Kaw *et al.*, 1992). On the other hand, there is a class of solitons that have slow phase velocity (Marburger and Tooper, 1975; Esirkepov *et al.*, 1998; Farina and Bulanov, 2001; Naumova, Bulanov, *et al.*, 2001; Poornakala, Das, Sen, and Kaw, 2002)

that are coupled with ions. In such a structure, the above general stability scenario is not applicable and we have to consider the problem more carefully. Nonetheless, in general the binding forces that constitute a stable soliton structure are the ponderomotive force of the radiation and the space-charge force set up by electron charge separation.

The ponderomotive force displaces electrons away from the center of the soliton, while the electrostatic force holds electrons to it. On the other hand, ions are driven away from the soliton's center due to this electrostatic force (Naumova, Bulanov, *et al.*, 2001).

The longest-lived solitons have attracted attention because of their resilient and robust behavior (Whitham, 1974). Relativistic solitons have been seen in multidimensional particle-in-cell (PIC) simulations of the laser pulse interaction with underdense plasmas by Bulanov, Inovenkov, Kirsanov, *et al.* (1992), Bulanov *et al.* (1999), Mima *et al.* (2001), Hadzievski *et al.* (2002), Mourou *et al.* (2002). These solitons are generated in the wake left behind the laser pulse. They propagate with a velocity well below the speed of light toward the plasma-vacuum interface. Here they disappear, suddenly radiating away their energy in the form of low-frequency electromagnetic bursts (Sentoku *et al.*, 1999b). Solitons can also be considered as coherent structures forming electromagnetic turbulences. They can be observed via the modification of the plasma density behind the laser pulse and via their low-frequency, broad spectrum of backscattered radiation. The analytical theory of relativistic electromagnetic solitons has been developed by many writers (Gerstein and Tzoar, 1975; Tsintsadze and Tskhakaya, 1977; Kozlov *et al.*, 1979; Shukla *et al.*, 1986; Kaw *et al.*, 1992; Esirkepov *et al.*, 1998; Farina and Bulanov, 2001, 2005; Poornakala, Das, Sen, *et al.*, 2002). In the case of relativistic but relatively low-amplitude solitons (compared to  $a_c = \sqrt{m_i/m_e}$ ) ions can be assumed to be at rest during approximately  $\sqrt{m_i/m_e}$  periods of oscil-

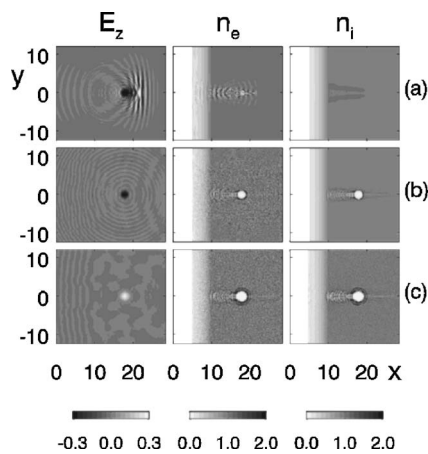


FIG. 20. Soliton formation and its development into the post-soliton in the interaction of an  $s$ -polarized laser pulse with the plasma: the  $z$  component of the electric field (first column), the electron density (second column), and the ion density (third column) in the  $x, y$  plane at (a)  $t=30$ , (b)  $t=70$ , and (c)  $t=120$ .

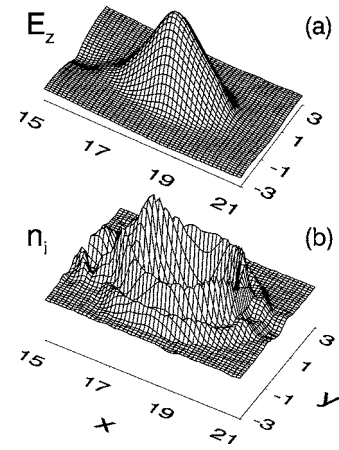


FIG. 21. 3D plot of the  $z$  component (a) of the electric field and (b) of the ion density inside the postsoliton at  $t=120$ .

lations of the electromagnetic field inside the soliton. When the analytical solution for low-frequency, zero-velocity solitons obtained by Esirkepov *et al.* (1998) provides a rather good description, the time  $2\pi/\omega_{pi}$  is substantially longer than the period of the electromagnetic field oscillations inside the soliton, and in the underdense plasma it is much longer than the laser period. However, for a time interval longer than  $2\pi/\omega_{pi}$  the ponderomotive pressure of the electromagnetic field inside the soliton starts to dig a hole in the ion density, and the soliton parameters change (Naumova, Bulanov, *et al.*, 2001). On the ion time scale, therefore, ions move outward and are accelerated to the energy level of  $m_e c^2 a_m$ . As a result, bubbles of ion density depletion are formed (Borghesi *et al.*, 2002).

The post-soliton development is shown in Figs. 20 and 21 (Naumova, Bulanov, *et al.*, 2001; Naumova *et al.*, 2002b). In Figs. 22–24 we present the results of a three-dimensional simulation of laser-induced subcycle relativistic electromagnetic solitons by Esirkepov *et al.* (2002).

In Fig. 22 we see one isolated soliton and a soliton train behind the laser pulse. A substantial part of the laser pulse energy (up to 30%) is transformed into these coherent entities. The soliton consists of oscillating electrostatic and electromagnetic fields confined in a prolate cavity of the electron density. The cavity size is of the order of few laser wavelengths. The cavity is generated by the ponderomotive force and the resulting charge

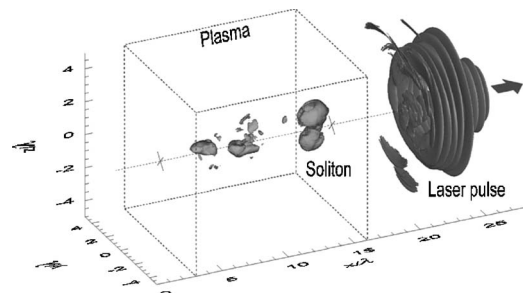


FIG. 22. Isolated soliton and a soliton train behind the laser pulse.

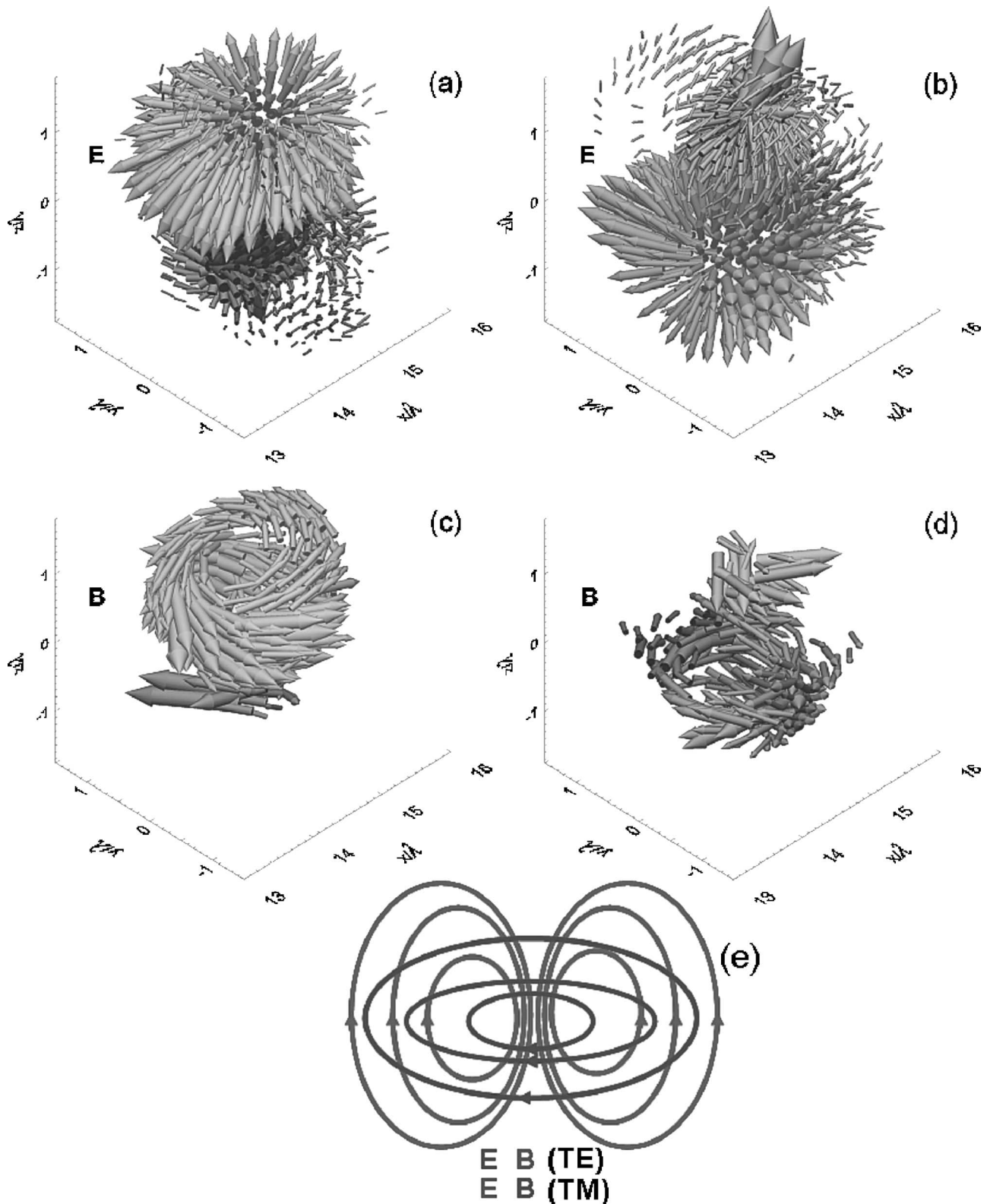


FIG. 23. Structure of (a),(b) electric and (c),(d) magnetic fields inside the soliton at (a),(c)  $t=39.3$  and (b),(d)  $t=40.2$ . (e) The magnetic- and electric-field topology in the TE (with poloidal magnetic field and toroidal electric field) and in the TM (with poloidal electric field and toroidal magnetic field) solitons.

separation induces a dipole electrostatic field. Figure 23 presents the structure of electric and magnetic fields inside the soliton at different times. The soliton resembles an oscillating electric dipole. The oscillating toroidal

magnetic field, shown in Fig. 23, indicates that, besides the strong electrostatic field, the soliton also has an electromagnetic field. The electrostatic and electromagnetic components in the soliton are of the same order of mag-

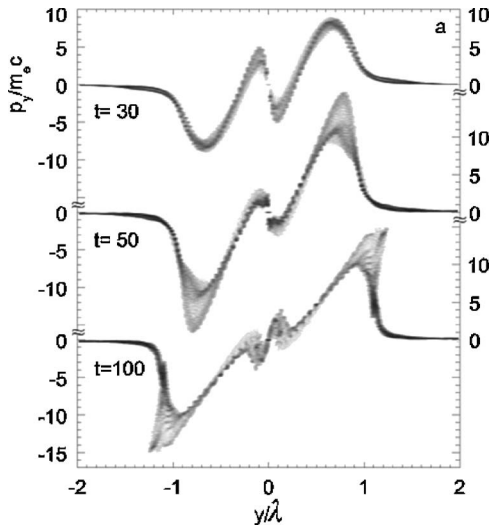


FIG. 24. The postsoliton phase plane at different times.

amplitude. In this figure the structure of electric [(a) and (b)] and magnetic [(c) and (d)] inside the soliton at  $t=39.3$  [(a) and (c)] and  $t=40.2$  [(b) and (d)] is shown. Sketch (e) illustrates the magnetic- and electric-field topology in the TE (with poloidal magnetic field and toroidal electric field) and in the TM (with poloidal electric field and toroidal magnetic field) solitons, i.e., in the observed in the PIC simulations soliton has the TM-mode topology.

We can describe the post-soliton formation scenario as follows. Since the soliton formation time is much shorter than the ion response time  $2\pi/\omega_{pi}$ , ions can be assumed to be at rest during soliton formation. Inside a nonpropagating soliton (a half-cycle soliton according to Esirkepov *et al.*, 1998) the maximum electromagnetic field  $a_m$  and the soliton frequency  $\Omega_S$  are related by  $a_m = 2\sqrt{\omega_{pe}^2 - \Omega_S^2}/\Omega_S$  and the soliton width equals  $c/\sqrt{\omega_{pe}^2 - \Omega_S^2}$ . The ponderomotive pressure of the electromagnetic field inside the soliton is balanced by the force from the electric field produced due to charge separation. The amplitude of the resulting electrostatic potential is given by  $\phi_m = \sqrt{1 + a_m^2}$ . Ponderomotive pressure displaces electrons outward, and the Coulomb repulsion in the electrically non-neutral ion core pushes ions away. The typical ion kinetic energy corresponds to the electrostatic potential energy, which is of the order of  $m_e c^2 a_m$ . This process is similar to a so-called ‘‘Coulomb explosion’’ inside of self-focusing channels (see Esirkepov *et al.*, 1999; Sarkisov *et al.*, 1999; Bulanov *et al.*, 2000; Krushelnick, Clark, Zepf, *et al.*, 2000; Sentoku *et al.*, 2000) and in the case of the cluster targets irradiated by high-intensity laser light (Kumarappan, Krishnamurthy, and Mathur, 2001; Nishihara *et al.*, 2001; Kishimoto, Masaki, Tajima, 2002a, 2002b; Sakabe *et al.*, 2004; Ter-Aoetisyan *et al.*, 2004). In Fig. 24 we show the ion phase plane. We see that ion expansion in the radial direction leads to the digging of a hole in the ion density. The cavity formation in the distribution of the electron and ion densities is shown in Figs. 20 and 21. The plasma cavity forms a resonator for the trapped electromagnetic

field. During cavity expansion, the amplitude and the frequency of the electromagnetic field decrease. Since the cavity radius increases slowly compared to the period of electromagnetic field oscillations, we can use the adiabatic approximation to find their dependence on time, as explained by Landau and Lifshitz (1984). The adiabatic invariant in this case is the ratio between the energy and the frequency of the electromagnetic field:

$$\int E^2 dV / \Omega_S = \text{const.} \quad (60)$$

As a simple analytical model to describe the electromagnetic field inside a post-soliton, we can use the well-known electric or magnetic dipole oscillations inside a spherical resonator (see Landau and Lifshitz, 1984; Jackson, 1998) where the lowest frequency depends on the cavity radius as  $\Omega_S = 2.74c/R$ , for the electric dipole mode and as  $\Omega_S = 4.49c/R$  for the magnetic dipole mode.

From Eq. (60) we obtain that  $E^2 \propto R^{-4}$ . Under the action of the electromagnetic pressure the wall of the cavity moves, piling up plasma like a snow plough. In the ‘‘snow plough’’ approximation (Zel’dovich and Raizer, 1967), the mass of the plasma pushed by the electromagnetic pressure  $E^2/8\pi$  is located inside a thin shell. The mass inside the shell is equal to the mass initially contained inside a sphere of the radius  $R$ :  $M(R) = 4\pi n m_i R^3/3$ . Using Newton’s second law for the motion of the mass  $M$ , we find the time scale of the cavity expansion  $\tau = \sqrt{6\pi n_0 m_i R_0^2 / E_0^2}$ . Asymptotically, when  $t \rightarrow \infty$ , the post-soliton radius increases as  $R \approx R_0(t/\tau)^{1/3}$ , where as the amplitude of the electromagnetic field and its frequency decrease as  $E \propto t^{-2/3}$  and  $\Omega_S \propto t^{-1/3}$ . Postsolitons were observed in the laser plasma by Borghesi, Bulanov, *et al.* (2000).

Analytically relativistic electromagnetic solitons with nonzero propagation velocity in the 1D approximation are described by Eqs. (38) and (39). As shown by Farina and Bulanov (2001), within the framework of the approximation corresponding to Eqs. (38) and (39) there are at least three types of nonlinear waves: bright solitons, dark solitons, and collisionless shock waves.

If we consider fast solitons with a propagation velocity  $\beta_g > \sqrt{\rho}$ , in this case we have bright solitons with amplitudes that reach a maximum and vanish at infinity. This solution to Eqs. (38) and (39) is consistent with the boundary conditions when  $a_0 = 0$ . The bright soliton is described by the well-known expression  $a = a_m / \cosh(\kappa\xi)$  or

$$A_y + iA_z = \frac{a_m}{\cosh[\kappa(x - \beta_g t)]} \exp[-i\omega(t - \beta_g x)]. \quad (61)$$

Here  $\xi = x - \beta_g t$ , the inverse soliton width is  $\kappa = (a_m/2\beta_g)\sqrt{(\beta_g^2 - \rho)/(1 - \beta_g^2)}$ , and the frequency is  $\omega = \sqrt{(1 + \rho)/(1 - \beta_g^2)} - (a_m^2/4\beta_g^2)(\beta_g^2 - \rho)/(1 - \beta_g^2)$ . As we can see, when the soliton propagation velocity approaches  $\beta_{g,c} = \sqrt{\rho}$  the soliton width  $\kappa^{-1}$  tends to infinity for fixed soliton amplitude  $a_m$ . On the other hand, if we assume the soliton width to be fixed, its amplitude becomes in-

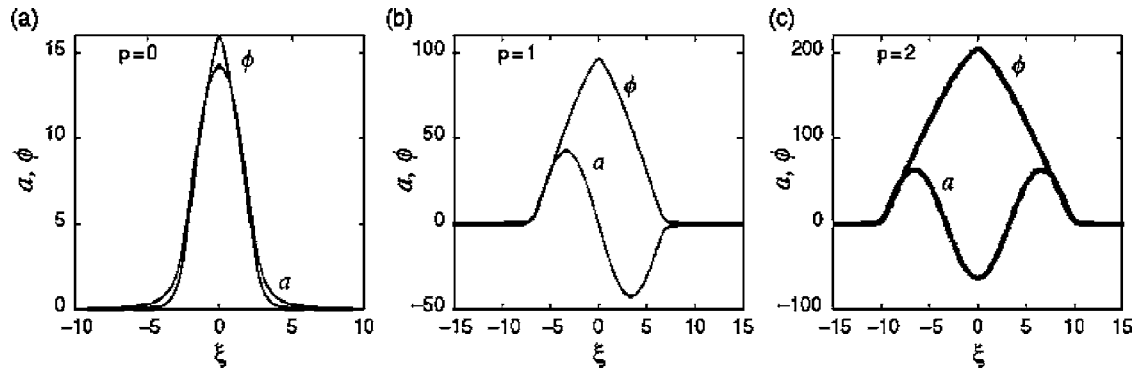


FIG. 25. Electrostatic  $\phi$  and vector potential  $a$  wave forms for bright solitons with  $p=0,1,2$  and velocities close to breaking.

finite as  $\beta_g \rightarrow \beta_{g,c}$ . In this case, we expect breaking of the soliton and the appearance of self-intersection of the charged-particle trajectory.

Figure 25 shows the profile of the soliton vector potential  $a$ , for the propagation velocity close to the breaking velocity  $\beta_{g,br} \approx 0.32$  for the soliton with a node number  $p$  equal to 0, 1, and 2. At  $\beta_g = \beta_{g,br}$  and  $\omega \approx 0.224$ , the solution branch ends since the soliton breaks and a singularity appears in the soliton solution, with the ion density  $n_i$  going to infinity at  $\xi=0$ , i.e.,  $R_i=0$ . From this last condition, we obtain the peak value of the potential  $\phi_{br} = (1 - \sqrt{1 - \beta_{g,br}^2}) / \rho$ . After the break a portion of ions will be injected into the acceleration phase. This shows that soliton breaking can provide an additional mechanism for the generation of fast ions in laser-irradiated plasmas.

If the velocity  $\beta_g$  is smaller than  $\sqrt{\rho}$ , then Eqs. (38) and (39) have a solution that describes a dark soliton. The solution requires the frequency to be equal to  $\omega = \sqrt{(1+\rho)/(1-\beta_g^2) - (a_m^2/2)/(1-\beta_g^2)}$ . The dark soliton is given by

$$A_y + iA_z = a_m \tanh[\kappa(x - \beta_g t)] \exp[-i\omega(t - \beta_g x)], \quad (62)$$

where the soliton inverse width is given by  $\kappa = (a_m/2) \sqrt{(\rho - \beta_g^2)/(1 - \beta_g^2)}$ . These expressions describe a dark soliton (the kink state) of small amplitude: the wave amplitude changes monotonically from  $-a_m$  at  $x = -\infty$  to  $a_m$  at  $x = +\infty$ . In the dark soliton, we have a minimum of the electromagnetic energy density and a minimum of the plasma density, which propagate with the velocity  $\beta_g$  without change of their form. Dark solitons are known in optical systems (Kivshar and Luther-Davies, 1998; Kivshar and Pelinovsky, 2000). Recently, they have been observed in the Bose-Einstein condensate (Burger *et al.*, 1999). We can see that in the limit of low propagation velocity an electron-ion plasma exhibits properties similar to those in Bose-Einstein condensates with positive scattering length (Burnett *et al.*, 1999). In an electron-positron plasma dark solitons are a natural nonlinear mode (Tajima and Taniuti, 1990; Farina and Bulanov, 2001).

Finite plasma temperature effects on soliton properties have been studied by Lontano and co-workers (Lon-

tano *et al.*, 2001, 2002, 2003), while the modification of the soliton structure due to quasistatic magnetic-field effects has been investigated by Farina *et al.* (2000).

Shocks are another type of structure formation in laser-matter interactions. Collisionless relativistic electromagnetic shock waves are described by Eqs. (38) and (39) in the case  $\beta_g \approx \beta_{g,c} = \sqrt{\rho}$ . Their form is given by

$$A_y + iA_z = \frac{a_w \exp[-i\omega(t - \beta_g x)]}{\sqrt{1 + (a_w^2/\sqrt{1 - \beta_g^2}) \exp[\kappa(x - \beta_g t)]}}, \quad (63)$$

where the shock wave amplitude is  $a_w = \sqrt{\rho}$ . A shock wave is compressional, with the carrying frequency of the electromagnetic wave equal to  $\omega = \sqrt{[8(1+\rho) - a_w^2]/[8(1-\beta_g^2)]}$  and its width  $\kappa^{-1} = (2/a_w^2) \sqrt{1 - \beta_g^2}$ . We see that the larger the shock wave amplitude, the steeper is the wave.

A collisionless shock wave corresponds to a nonlinear regime in which relativistically strong electromagnetic waves penetrate into the overdense plasma. Above we have discussed the regimes of relativistic transparency, when the electromagnetic wave could propagate through the overdense plasma due to relativistic correction of the electron mass (see Akhiezer and Polovin, 1956; Kaw and Dawson, 1970; Marburger and Tooper, 1975; Goloviznin and Schep, 1999; Cattani *et al.*, 2000). In our case the effective Lagmuir frequency changes due to both the relativistic correction of the electron mass and a change in the plasma density. The formation of a collisionless shock wave with a stationary and monotonous profile, in contrast to that discovered by Sagdeev (1966), does not require any dissipative process (see also Darmanyan *et al.*, 1998).

When the laser pulse is longer than the wakefield resonant length (Tajima and Dawson, 1979), as in the experiments of Nakajima *et al.* (1995) and Modena *et al.* (1995), the laser pulse is subject to plasma instabilities on electronic time scales. The most effective of these are stimulated Raman scattering instabilities. The forward Raman scattering process modulates the laser pulse in such a way as to reinforce the wakefield resonance as a part of the self-organization of the laser pulse in the plasma. On the other hand, stimulated backward Raman scattering has a greater growth rate than the forward process, though the latter has a longer interaction time

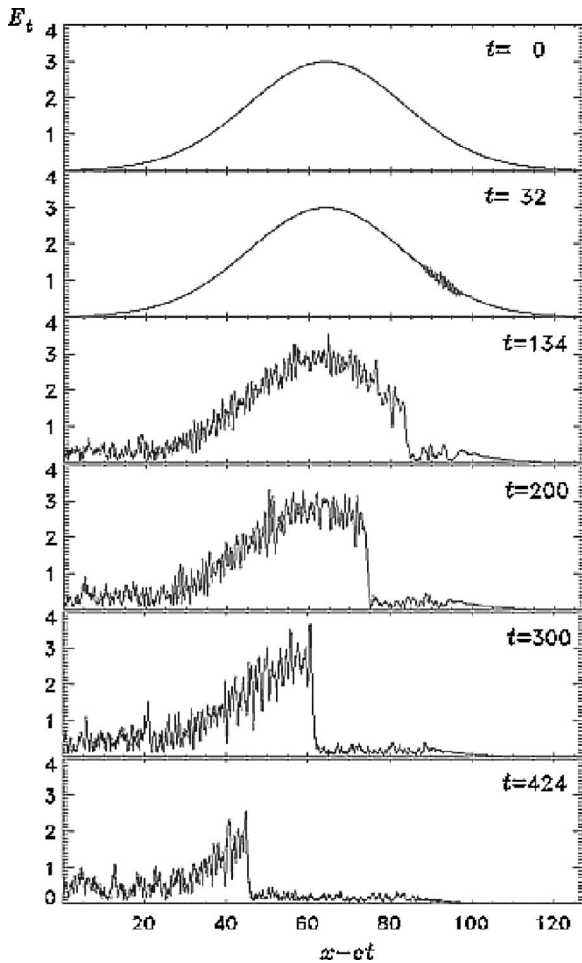


FIG. 26. Shocklike front formation during laser-pulse propagation in underdense plasmas.

because of the copropagating nature of forward scattering. Stimulated backward Raman scattering leads to the erosion of the laser pulse leading edge over a time scale given by  $\omega_{pe}^{-1}(\omega_0/\omega_{pe})^2$  (Bulanov *et al.*, 1992; see Fig. 26). Such a shock front facilitates a sudden and sharp wakefield generation, as described by Bulanov, Lontano, Esirkepov, *et al.* (1996). This mechanism may be employed for electron acceleration as well as ion acceleration (Esirkepov *et al.*, 1999; Koga *et al.*, 2002). See Sec. VIII.A.2, on ion acceleration.

In addition, perhaps as a combination of self-focusing and other nonlinearity, such as the formation of jets, could be observed. Some spectacular jet observations include those of Kando *et al.*, (1997); Ruhl *et al.* (1999); Kodama *et al.* (2000).

#### F. High-order harmonic generation

The interaction of high-intensity laser pulses with underdense and overdense plasmas presents a manifestation of one of the most basic nonlinear processes in physics: high-order optical harmonic generation. High-order optical harmonics have been observed in laser plasma interactions with radiation intensities ranging from moderate up to relativistic intensities. Nonlinear

orders as high as 300 have been reported recently. In addition to its fundamental interest in the theory of nonlinear waves, this radiation presents unique properties of coherence and short pulse duration that makes high-order harmonics a useful XUV source of short coherent radiation such as EUV for lithography, holography, etc. (see Bloembergen, 1965; Shen, 1984; Boyd, 1992; Zhou *et al.*, 1996; Altucci *et al.*, 1999; Villorosi *et al.*, 2000; Salières and Lewenstein, 2001). X-ray generation by lasers has been observed in many laboratory experiments. It can arise as bremsstrahlung and  $K\alpha$  emission, as well as in other forms. x-lasing schemes comprise a huge field of research, beyond the scope of the present review.

The physical generation mechanisms of high-order harmonics have much in common because they rely on the property of nonlinear systems to react in an anharmonic manner under the action of a periodic driving force. On the other hand, the specific realization of this property depends on the laser-matter interaction parameters, mainly on the laser intensity.

At moderate intensity levels (subrelativistic) high-order harmonics occur due to the anharmonicity of the atom response on the finite-amplitude oscillating electric field (see L'Huillier *et al.*, 1992). This anharmonicity is strongly enhanced in atoms and high harmonic generation results (Corkum, 1993; Dietrich *et al.*, 1994; Schafer and Kulander, 1997; Sheehy *et al.*, 1999; Salières *et al.*, 2001). Milosevic, Corkum, and Brabec (2003) draw attention to the formation of attosecond electron wave packets during this process, which are accelerated to many eV energies before refocusing onto their parent ion. The technique of high harmonic generation opens the possibility of imaging attosecond dynamics of nuclear processes. It also has applications in the control of strong-field processes in atomic physics (Schafer *et al.*, 2004). As the intensity of the laser light increases the ionization process acquires complicated properties that include atom stabilization against ionization (see Heneberger, 1968; Fedorov and Movsesian, 1989; Parker and Stroud, 1990; Bestle *et al.*, 1993). Relativistic effects become important at sufficiently high laser intensities. The magnetic-field component of the laser field can strongly influence the stabilization of atoms in the high-frequency regime by inducing a motion along the laser pulse propagation direction (Vázquez de Aldana *et al.*, 2001).

When the laser radiation intensity becomes such that the electron quiver energy is higher than the rest mass energy, relativistic nonlinear optics come into play (Mourou *et al.*, 2002; Tajima and Mourou, 2002; Tajima, 2003). In this regime high-order harmonics generation is due to the nonlinear dependence of the particle mass on the momentum and modulations of the electron density. The first relativistic harmonics were observed with the large-scale CO<sub>2</sub> laser Antares in the early 1980s.

In underdense plasmas high harmonics are produced with the parametric excitation by the laser light of the electromagnetic and electrostatic waves with different frequencies. As mentioned above, linearly polarized electromagnetic waves in an underdense plasma have a

transverse component whose spectrum contains odd harmonics,

$$E_y = -\omega a_0 \cos(\omega t - kx) - \omega a_0^3 \frac{3(8\omega^2 + 3\omega_{pe}^2)}{8(4\omega^2 - \omega_{pe}^2)} \times \cos(3\omega t - 3kx) + \dots, \quad (64)$$

and a longitudinal component with even harmonics,

$$E_x = -ka_0^2 \frac{1}{4\omega^2 - \omega_{pe}^2} \sin(2\omega t - 2kx) + \dots, \quad (65)$$

where the wave frequency depends on the wave number as  $\omega = \sqrt{k^2 c^2 + \omega_{pe}^2}$ .

When laser radiation interacts with overdense plasmas it reflects back at the plasma-vacuum interface in the case of a sharp plasma boundary or at the surface of critical density in the case of a gradual density profile. The plasma reflection layer is driven by the electromagnetic wave back and forth as well as in the plane of the surface of the plasma-vacuum interface (in the plane of the critical surface) forming an oscillating mirror.<sup>6</sup> The spectrum of the light reflected by the oscillation contains odd and even harmonics whose polarization and amplitude depend on the pulse incidence angle, intensity, and polarization.

In the relativistic regime of interactions with a solid target, one of the interpretations is that the large ponderomotive force will drive the critical surface at twice the laser frequency at relativistic velocities and thus provides a new mechanism of harmonic generation. This explanation was first proposed by Bulanov *et al.* (1994) and further studied by Lichters *et al.* (1996). Harmonics up to the 60th have been observed by the Rutherford and Von der Linde groups, Zepf *et al.* (1998) and Tarasevich *et al.* (2000).

Electromagnetic wave reflection by a mirror moving with constant velocity,  $V = c\beta$ , has been described by Einstein (see a detailed description of this phenomenon in the book by Pauli, 1981). If the electric field in the incident wave is given by the function  $f[\omega_0(t-x/c)]$ , in the reflected wave we have  $J(\beta)f[\omega_0 J(\beta)(t-x/c)]$ , where  $J(\beta) = (1-\beta)/(1+\beta)$ . The problem of electromagnetic wave reflection at a uniformly accelerating mirror has been solved using the Rindler transformation to the accelerating reference frame by Van Meter, Carlip, and Hartemann (2001). They noticed that to find the reflected wave from the accelerating mirror one can use the subsequent Lorentz transforms into a reference frame moving with the instantaneous velocity calculated at the proper time of the reflection.

A basic phenomenon responsible for high harmonic generation at the plasma-vacuum interface is the change

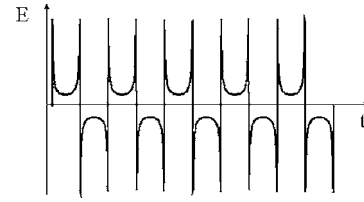


FIG. 27. The reflected-wave electric field vs time.

in frequency and amplitude of the electromagnetic wave during its interaction with the moving electron layer. The electric field transverse component in this case is given by

$$E_{\perp}(x,t) = \frac{2\pi n e l v_{\perp}(t')}{c - v_{\parallel}(t') \operatorname{sgn}[x - x(t')]}, \quad (66)$$

and the magnetic field is given by  $B_{\perp} = E_{\perp} \times n$ . Here  $n$  is the unit vector normal to the electron layer surface,  $v_{\perp}$  and  $v_{\parallel}$  are the transverse (perpendicular to the vector  $n$ ) and longitudinal (parallel to  $n$ ) components of the electron layer velocity. The retarded time  $t'$  is determined from  $t' = t - [x - x(t')]/c$ , with  $x$  the coordinates of the observation point and  $x(t')$  that of the electron layer.

In Eq. (66) we can see that high-order harmonic generation stems from (a) the nonlinear dependence of the electron quiver velocity on the electromagnetic wave, (b) the Doppler shift which is described by the term in the denominator of Eq. (66), and (c) the nonlinear dependence of the retarded time  $t'$  on  $t$ .

To find a qualitative form of the reflected electromagnetic wave we approximate the motion of the electron layer by using expressions that describe the orbit of an electron in a linearly polarized plane wave. It is well known that the electron performs a figure-eight motion in a plane spanned by the electric field vector and the wave vector. Substituting expressions from Landau and Lifshitz (1980) into Eq. (66), we can easily plot the electric field dependence vs time as presented in Fig. 27 (see also Naumova, Nees, Hou, *et al.*, 2004; Naumova, Nees, Sokolov, *et al.*, 2004; Naumova, Sokolov, *et al.*, 2004). We can see that the reflected wave has a form of a train of ultrashort pulses. A characteristic width of a spike is of the order of  $\delta t \approx 1/\omega_0 a_0$ , i.e., the typical harmonic number is about  $2\pi a_0$ .

In the case of oblique incidence the reflected light spectrum has both odd and even harmonics, with different polarization, which depend on the polarization of the incident pulse. According to the selection rules of harmonic generation at a solid target surface (see Lichters *et al.*, 1996; Vshivkov *et al.*, 1998a, 1998b), the  $s$ -polarized incident pulse generates  $s$ -polarized odd harmonics and  $p$ -polarized even harmonics. The  $p$ -polarized incident pulse generates only  $p$ -polarized odd and even harmonics. Macchi *et al.* (2001, 2002) have shown that parametric instability development at the vacuum-plasma interface results in nonlinear distortion of the oscillating mirror in the transverse direction and

<sup>6</sup>See, for example, Bulanov *et al.*, 1994; Gibbon, 1996; Gibbon and Förster, 1996; Lichters *et al.*, 1996; Von der Linde and Rzàzewski, 1996; Von der Linde, 1997; Vshivkov *et al.*, 1998a, 1998b; Zepf *et al.*, 1998; Il'in *et al.*, 1999; Tarasevich *et al.*, 2000; Bulanov, Esirkepov, Naumova, and Sokolov, 2003; Bulanov, Esirkepov, and Tajima, 2003; Pirozhkov *et al.*, 2005.



FIG. 28. Progress in laser development. The target chamber of the Helios system, the first laser that has shown relativistic effects like harmonic generation. This CO<sub>2</sub> laser had  $a_0^2 \sim 1$  with a repetition rate of 1 mHz. Courtesy LANL.

provides an additional mechanism for high-order harmonic generation.

As we can see, low-density, but overdense plasmas can produce large-amplitude modulations of the critical surface, yielding an efficient harmonic generation. Relativistic harmonic generation can also be the source of sub-femtosecond pulses. An interesting approach has recently been demonstrated by the Michigan group with their  $\lambda^3$  laser. In order to reach relativistic intensities this group uses single millijoule pulses delivered over a few optical periods, i.e., 6–20 fs at kHz repetition rates. An  $f/1$  paraboloid combined with a deformable mirror is able to focus the beam on a spot diameter of a single wavelength. Intensities in the  $5 \times 10^{18}$  W/cm<sup>2</sup> or  $a_0^2 \sim 2$  range have been demonstrated at 1-kHz repetition rates. We believe that these truly compact relativistic lasers will make relativistic studies accessible to a much larger community. The progress in this field can be appreciated when we contrast the building size of LANL, and the few shots a day one could manage with the CO<sub>2</sub> laser used in the first relativistic intensity experiments and the Michigan kHz relativistic laser (Figs. 28 and 29).



FIG. 29. Progress in laser development. The target chamber of the University of Michigan  $\lambda^3$  laser. This compact laser has  $a_0^2 \sim 1$  with a repetition rate of 1 kHz. This university-size system is the smallest relativistic intensity laser.

Esirkepov, Bulanov, *et al.* (2004) have shown that coherent synchrotron radiation can be emitted by relativistic electromagnetic subcycle solitons dwelling in a collisionless plasma. Using three-dimensional particle-in-cell simulations they have demonstrated that solitons, left in a wake of a relativistically intense short circularly polarized laser pulse in the plasma, emit spiral electromagnetic waves, as a result of charge density oscillations in the wall of the soliton cavity. This high-frequency afterglow persists for tens of Langmuir periods.

In addition to harmonic radiation, there is an additional radiation called Larmor radiation or nonlinear Thomson scattering. Larmor radiation is the classic radiation due to the acceleration of electrons by laser electric and magnetic fields, in circular orbits. Ueshima *et al.* (1999) have evaluated this radiation. The radiation intensity increases in proportion to  $a_0^2$ , while the peak frequency increases as  $a_0^3$ :

$$\omega_{\max} \approx a_0^3 \omega_0. \quad (67)$$

This type of laser-driven Larmor radiation has been observed by Chen and co-workers (Chen, Maksimchuk, and Umstadter, 1998; Chen, Sarkisov, Maksimchuk, *et al.*, 1998).

In the next subsection we discuss in detail the effect of radiation on charged-particle (electron) dynamics.

## V. INTERACTION OF CHARGED PARTICLES WITH ELECTROMAGNETIC WAVES IN THE RADIATION-DOMINANT REGIME

Investigations of free-electron radiation during its interaction with electromagnetic waves has always, starting from the works of J. J. Thomson, been of great significance. The literature devoted to studies of the electromagnetic wave-particle interaction is vast (see, for example, Nikishov and Ritus, 1964; Sarachik and Schappert, 1970; Zel'dovich, 1975; Waltz and Manley, 1978; Landau and Lifshitz, 1980; Jackson, 1998).

Below we consider the interaction of a relativistic electron with a circularly polarized electromagnetic wave. In the case of a circularly polarized electromagnetic wave, the charged particle moves along a circular trajectory, and one may borrow from the theory of synchrotron radiation (Ginzburg and Syrovatskii, 1965a, 1965b; Sokolov and Ternov, 1968; Ginzburg, 1989) the expressions for the properties of the radiation emitted by the particle.

The intensity of charged-particle radiation in the non-relativistic limit is given by the well-known Larmor formula  $W = -\partial_t E = 2e^2 |\dot{v}|^2 / 3c^3$ . In the relativistic limit, Heaviside (1902) obtained  $W = (2e^2 / 3m_e^2 c^3) (dp_\mu / d\tau)^2$ , where  $p_\mu$  is the particle four-momentum and  $\tau$  is its proper time. When an ultrarelativistic charged particle moves along a circular trajectory, as in a synchrotron, the radiation intensity is proportional to the fourth power of the particle energy  $W = (2e^2 c / 3R^2) \beta^4 \gamma^4$ . Here  $R$  is the radius of the orbit. Using the theory of synchrotron radiation, Ivanenko and Pomeranchuk (1944) pre-

dicted a maximum energy for an electron accelerated in a betatron. Synchrotron radiation was for the first time seen as a blue light of “luminous electrons.” During several revolutions along the orbit the electron loses approximately an MeV of energy in the form of synchrotron radiation. In the case of a charged-particle interaction with a circularly polarized electromagnetic wave in a plasma, where the radiation pressure is balanced by the electric charge-separation field, the radius of the electron orbit is  $R=c/\omega=\lambda/2\pi$  and its momentum is about  $p=m_e c a_0$ , where  $a_0$  is the wave amplitude. This yields for the radiation intensity

$$W = \left( \frac{4\pi r_e}{3\lambda} \right) \omega_0 m_e c^2 a_0^4. \quad (68)$$

We see that the radiation damping force is determined by a dimensionless parameter  $\varepsilon_{\text{rad}}$ :

$$\varepsilon_{\text{rad}} = (4\pi r_e / 3\lambda). \quad (69)$$

By comparing the energy losses given by Eq. (68) with a maximal energy gain of an electron interacting with the electromagnetic wave  $\partial_t E = \omega m_e c^2 a_0$ , we find that radiation effects become dominant at  $a_0 \geq \varepsilon_{\text{rad}}^{-1/3}$ . As was shown by Zel'dovich (1975; see also Bulanov *et al.*, 2004), in the limit of relatively low amplitude of the laser pulse, when  $1 \ll a_0 \ll a_{\text{rad}} = \varepsilon_{\text{rad}}^{-1/3}$ , the momentum of an electron moving in a circularly polarized electromagnetic wave in a plasma depends on the laser pulse amplitude as  $p = m_e c a_0$ , and in the limit  $a_0 \gg a_{\text{rad}}$  the momentum dependence on  $a_0$  is given by  $p = m_e c (a_0 / \varepsilon_{\text{rad}})^{1/4}$ .

Quantum physics effects become important when the photon, generated due to Compton scattering, has energy of the order of the electron energy, i.e.,  $\hbar \omega_m \approx E_e$ . (We do not discuss here quantum fluctuations of the electron orbit similar to quantum fluctuations of the trajectory of the moving electron in a magnetic field; Sokolov, Ternov, and Loskutnov, 1962.) An electron of energy  $E_e = \gamma m_e c^2$  rotates with frequency  $\omega$  in a circularly polarized wave propagating in a plasma and emits photons with the frequency  $\omega_m = \gamma^3 \omega$  (see Landau and Lifshitz, 1980). Quantum effects come into play when

$$\gamma \geq \gamma_q = \sqrt{\frac{m_e c^2}{\hbar \omega}}. \quad (70)$$

For an electron interacting with 1- $\mu\text{m}$  laser light, we find  $\gamma_q \approx 600$ . From the previous analysis of radiation effects, we obtain for the electron a gamma factor imposing a quantum limit given by

$$a_q = \frac{2e^2 m_e c}{3\hbar^2 \omega} = \frac{1}{3\pi} \frac{r_e \lambda}{\lambda_c^2}. \quad (71)$$

For the equivalent electric field of the electromagnetic wave this yields

$$E_q = \frac{2em_e^2 c^2}{3\hbar^2} = \frac{2}{3} \frac{r_e}{\lambda_c} E_{\text{Schw}}. \quad (72)$$

Here

$$E_{\text{Schw}} = \frac{m_e^2 c^3}{e\hbar} \quad (73)$$

is the Schwinger electric field (Schwinger, 1951). The quantum limit electric field  $E_q$  is in a factor  $2\alpha/3$ , with  $\alpha = e^2/\hbar c = 1/137$ , i.e., approximately 200 times smaller than the Schwinger electric field.

In the quantum limit, the radiation energy losses are given by  $\omega m_e c^2 \varepsilon_{\text{rad}} (p/m_e c)^4 I(\zeta)$ , with  $\zeta = (\hbar \omega / m_e c^2) (p/m_e c)^2$ . When  $\zeta \gg 1$ , the function  $I(\zeta)$  is given by (see Ritus, 1979; Berestetskii, Lifshitz, and Pitaevskii, 1982)

$$I(\zeta) \approx \frac{32\Gamma(2/3)}{243} \frac{e^2 m_e^2}{\hbar^2} (3\zeta)^{2/3}. \quad (74)$$

Equalizing the energy losses and the energy gain  $\omega m_e c^2 a_0$ , we find the electron momentum as a function of the electromagnetic wave amplitude in the limit  $a_0 > a_q$ :

$$p \approx m_e c \left( \frac{\hbar \omega}{m_e c^2} \right)^{1/2} \left( 0.34 \frac{a_0}{\varepsilon_{\text{rad}}} \right)^{3/8}. \quad (75)$$

When the electromagnetic wave packet interacts with the charged particle in a vacuum, and the particle is at rest before the interaction, the particle momentum and the Lorentz factor are given by (Lai, 1980; Landau and Lifshitz, 1980)  $p_x = m_e c a_0^2 / 2$ ,  $p_\perp = m_e c a_0$ ,  $\gamma = 1 + a_0^2 / 2$ . In the ultrarelativistic limit, when  $a_0 \gg 1$  the longitudinal component of the particle momentum is much larger than the transverse component. The particle drift velocity along the  $x$  direction is  $v_\parallel = p_x / 2m_e \gamma = c a_0^2 / (2 + a_0^2)$ . Performing a Lorentz transformation along the reference frame moving with the particle drift velocity  $v_\parallel$ , we find that the dimensionless amplitude value of the laser pulse is the same as its value in the laboratory reference frame:  $a'_0 = a_0$ . This is a consequence of the Lorentz invariance of the transverse component of a four-vector. However, the parameter  $\varepsilon_{\text{rad}}$ , given by Eq. (69), is not Lorentz invariant. We find that

$$\varepsilon'_{\text{rad}} = \frac{4\pi r_e}{3\lambda'} = \frac{\varepsilon_{\text{rad}}}{\sqrt{1 + a_0^2}}, \quad (76)$$

where the wavelength of the laser pulse in the moving reference frame is  $\lambda' = \sqrt{(c + v_\parallel)/(c - v_\parallel)} \lambda = \sqrt{1 + a_0^2} \lambda$ . The limit of the radiation-dominant regime now reads as  $a_0^3 \gg \varepsilon'_{\text{rad}}^{-1}$  or  $a_0 \gg \varepsilon_{\text{rad}}^{-1/2}$ . It is easy to show that quantum effects, in the case of a charged-particle interaction with the electromagnetic wave in a vacuum, become important when the wave electric field reaches the Schwinger limit.

For a 1- $\mu\text{m}$  laser pulse interaction with a plasma, as is well known, relativistic effects become important for  $a_0 \geq 1$ , which corresponds to the radiation intensity

above  $I_{\text{rel}}=1.38 \times 10^{18}$  W/cm<sup>2</sup>. The radiation-dominant regime begins at  $a_0 \approx a_{\text{rad}}$  with  $a_{\text{rad}} \approx 400$ , i.e., for a laser light intensity of the order of  $I_{\text{rad}}=3 \times 10^{23}$  W/cm<sup>2</sup>. Quantum physics effects come into play at  $a_0 \approx a_q = 2500$ , which gives  $I_q=1.38 \times 10^{26}$  W/cm<sup>2</sup>. We reach a limit when nonlinear quantum electrodynamics effects with electron-positron pair creation in the vacuum come into play, when the laser pulse electric field becomes equal to the Schwinger electric field  $E_{\text{Schw}}=m_e^2 c^3 / e \hbar$ , which corresponds to  $a_{\text{Schw}}=m_e c^2 / \hbar \omega = 5 \times 10^5$  and  $I_{\text{Schw}} = 3 \times 10^{29}$  W/cm<sup>2</sup>.

For an electron freely accelerated by an electromagnetic wave in a vacuum, the radiation-dominant regime is reached at a 1- $\mu\text{m}$  laser light intensity of the order of  $I_{\text{rad}}=10^{26}$  W/cm<sup>2</sup>, i.e., for an electron energy of the order of 50 TeV. Quantum effects become important at a laser pulse electric field equal to the Schwinger electric field, i.e., at an intensity  $I_{\text{Schw}}=3 \times 10^{29}$  W/cm<sup>2</sup>.

Radiation loss effects can be weakened for a copropagating electron beam accelerated by a laser pulse. It is easy to show that in this case the kinetic energy of an ultrarelativistic electron is equal to  $p_{\parallel} c a_0^2$ , where  $p_0$  is the longitudinal component of beam electrons before interaction with the laser pulse. The limit of the radiation-dominant regime corresponds to  $a_0 \gg \sqrt{2 p_{\parallel 0} / m_e c \epsilon_{\text{rad}}}$ . For 50-GeV electrons, i.e.,  $p_{\parallel 0} / m_e c \approx 10^4$ , this gives  $I_{\text{rad}} = 10^{28}$  W/cm<sup>2</sup>. In the radiation-dominant regime a substantial part of the laser energy is transformed into hard (x-ray) radiation (see Zhidkov *et al.*, 2002).

Another approach to the study of radiation-dominant regimes for the laser-plasma interaction, realized theoretically by Bulanov *et al.* (2004), is connected with use of cluster targets. The laser-cluster interaction is accompanied by the efficient transformation of laser light energy into the energy of the scattered electromagnetic wave (Kishimoto and Tajima, 1999; Kishimoto *et al.*, 2002a, 2002b), and by ion acceleration (Nishihara *et al.*, 2001; Kishimoto *et al.*, 2002a, 2002b; Fukuda *et al.*, 2003; Sakabe *et al.*, 2004). In typical situations the cluster size is smaller than the wavelength of the laser light. In this case scattering occurs in the collective regime and the scattering cross section increases in  $N^2$  times. Here  $N$  is a number of electrons involved in the scattering process. The typical electron number in the cluster can be estimated to be  $N=10^8$ . We can see that the parameter  $a_{\text{rad}}=(4\pi N r_e / \lambda)^{-1/3}$  becomes  $\approx 500$  times larger. It corresponds to a laser intensity of the order of  $I_q = 10^{18}$  W/cm<sup>2</sup>. Thus in this regime we can model the radiation-dominant laser-plasma interaction using moderate-power lasers to provide a source of powerful ultrashort electromagnetic bursts in a process similar to that discussed by Kaplan and Shkolnikov (2002).

## VI. RELATIVISTIC ENGINEERING

The systematic and painstaking study of the processes described above has brought us to a new era. We may soon witness the emergence and maturation of techniques using intense lasers (and other tools such as rela-

tivistic electrons) to control the dynamics of matter so drastically that the dynamics of relativistic effects become of paramount importance. Such an endeavor could rightfully be called *relativistic engineering*. The marriage of laser technology with accelerator technology could conceivably result in applications in a  $\gamma$ - $\gamma$  collider or via the inverse Compton scattering process of the laser. Here, we look at some examples of what we call relativistic engineering and their implications. At least three elements of relativistic engineering need to be considered: (1) longitudinal pulse-length compression (or pulse compression, for short), (2) upshifts in frequency, and (3) angular focusing. These three features in combination may lead to the “manufacture” of laser pulses in an unprecedented parameter regime. Imagine that a first laser pulse induces a laser wakefield. The wakefield has phase velocity  $v_{\text{ph}}$  and associated Lorentz factor  $\gamma_{\text{ph}}$ . The nonlinearity of a strong wakefield amounts to a nonlinear wave profile, including the steepening of the wave and what is called cusp formation in its density. It can be shown that, because of this steep cusp effect, substantial optical effects emerge. For example, the cusp acts as a relativistic mirror. By properly designing the wakefield and thus the relativistic mirror (or mirrors), we should be able to modify the properties of the second laser pulse that is now injected toward them.

With the ideal realization of these features, we should be able to compress the pulse length by  $\gamma_{\text{ph}}^2$ . At the same time, the frequency of the laser increases by the same factor. Because the wavelength is also shortened, it is possible to focus (to the diffraction-limited size) down to a spot that is smaller by the factor  $\gamma_{\text{ph}}$  for the two transverse dimensions. This amounts to the compactification of the original laser pulse in three dimensions to new higher-energy photons by a factor of  $\gamma_{\text{ph}}^6$  in the most optimistic scenario. Take as an example wakefield excitation in a gas of density  $10^{19}$  cm<sup>-3</sup>. This means the Lorentz factor associated with the phase velocity of the wakefield is related to  $\omega / \omega_{\text{pe}}$ , which is on the order of 10. Thus a laser pulse compactification of the order of  $10^6$  could be realized. If one has a laser of 1 PW and focuses it down to an intensity of  $10^{22}$  W/cm<sup>2</sup>, upon relativistic engineering a compactification intensity of  $10^{28}$  W/cm<sup>2</sup> could be reached, close to the Schwinger intensity of  $10^{29}$  W/cm<sup>2</sup>. Admittedly, this is an astounding energy density. How well such relativistic engineering may be accomplished remains to be seen. But it surely offers immense promise if the challenge can be met.

### A. Flying mirrors

We note that laser frequency upshifting and pulse compression can also be achieved using a broad variety of configurations. In particular, wave amplification reflected from a moving relativistic electron slab has been discussed by Landecker (1952) and Ostrovskii (1976). Backward Thompson scattering from a relativistic electron bunch was considered by Arutyunian and Tumanian (1963) and Li *et al.* (2002), and photon acceleration

by Wilks *et al.* (1989). Reflection at the moving ionization front has also been studied by Semenova (1967), Mori (1991), Savage *et al.* (1992), Mori *et al.* (1995), Bakunov *et al.* (2001), and Dias *et al.* (2002). The use of counterpropagating laser-electron pulses in a plasma was discussed by Shvets *et al.* (1998, 1999) and by Ping *et al.* (2000).

As discussed above, the limit of ultrahigh-intensity electromagnetic radiation can be reached as a result of sequential laser radiation frequency upshifting followed by focusing into a one-wavelength focus spot. Within the framework of this scheme we use the properties of the wakefield generated in an underdense plasma by an ultrashort, relativistically strong laser pulse driver. The electron density modulation within a nonlinear wake plasma wave can be regarded as high-density plasma shells moving with the velocity  $v_{ph}$  close to the speed of light in a vacuum. A second laser pulse, which counterpropagates with respect to the driver pulse, may be reflected back from these relativistic electron shells followed by a frequency upshifting and compression of the reflected pulse (see Fig. 30). We say that in a wake behind the laser-pulse driver we see a “flying relativistic mirror.” As a result the wavelength of the reflected wave becomes shorter by a factor  $4\gamma_{ph} \gg 1$ , where  $\gamma_{ph} = 1/\sqrt{1-v_{ph}^2/c^2}$ , as is well known.

Within the framework of the scheme under consideration it is important to realize that the relativistic dependence of the Langmuir frequency on the wave amplitude results in the formation of wake waves with curved fronts that have a form close to paraboloid, as discussed above. The reflection of the electromagnetic wave at the paraboloid flying mirror leads to electromagnetic wave focusing. In the reference frame moving with the mirror velocity the reflected light has a wavelength equal to  $\lambda_0/2\gamma_{ph}$ . It can be focused into a spot of transverse size  $\lambda_0/2\gamma_{ph}$ , which can result in an increase in the light intensity by a factor of  $4\gamma_{ph}^2(R_0/\lambda_0)^2$ , where  $R_0$  is the radius of the incident laser beam. The resulting intensity in the laboratory frame increases by a factor  $64\gamma_{ph}^6(R_0/\lambda)^2$ . This value must be multiplied by the reflection coefficient, which must be smaller than 1.

This scheme of laser-pulse compactification is illustrated in Fig. 30. The topmost row corresponds to the laboratory frame ( $L$ ) before reflection of the laser pulse from the flying mirror. The laser pulse propagates from right to left. The middle row corresponds to the comoving reference frame ( $K$ ). Here laser-pulse reflection and focusing occur producing a focus spot with the size  $\lambda' \approx \lambda_0/2\gamma_{ph}$ . The bottom row corresponds to the laboratory frame ( $L$ ) after reflection: the reflected electromagnetic radiation has the wavelength  $\lambda_f \approx \lambda_0/4\gamma_{ph}^2$  and propagates in a narrow angle  $\theta \approx 1/\gamma_{ph}$ . Because of this steep cusp effect, substantial optical effects emerge. For example, this cusp acts as a relativistic mirror. The interaction of a probe laser pulse with a counterpropagating wakefield corresponds to the reflection of light by a mirror moving at relativistic velocity  $v_{ph}$ . As is well known, the frequency of the reflected light is

$$\omega_R = \omega_0 \frac{1 + \beta_{ph}}{1 - \beta_{ph}} \approx 4\gamma_{ph}^2 \omega_0, \quad (77)$$

where  $\beta_{ph} = v_{ph}/c$ ,  $\omega_0$  is the frequency of the incident electromagnetic wave, and  $\omega_R$  is the frequency of the reflected wave.

The Lorentzian compression of the pulse length as well as the wavelength is by a factor  $\gamma_{ph}^{-2}$ . This is in contrast to the high-order harmonic generation technique, in which the compression of the pulse length and wavelength occurs by the factor of  $n^{-1}$  ( $n$  is the typical highest harmonic number) (Corkum, 1993; Tamaki, Midorikawa, *et al.*, 1999; Kienberger, Krausz, *et al.*, 2004; Sekikawa, Watanabe, *et al.*, 2004). It is also conceivable in this relativistic engineering that the higher harmonic generation can be further incorporated in addition to the Lorentzian compression, which leads to the compression factor  $n^{-1}\gamma_{ph}^{-2}$ . This is a linear (or one-dimensional) compression. As remarked earlier, three-dimensional (volumetric) compression is further possible. In addition, the Lorentzian compression by relativistic engineering does not suffer from the so-called Corkum limit (Corkum, 1993), which is due to the destruction of atomic electron states by too intense laser fields.

This relativistic “effective mirror” can be formed during the wave breaking of a Langmuir wake that propagates in a plasma with phase velocity close to the speed of light in vacuum. In a nonlinear Langmuir wave near the breaking threshold, when the electron quiver velocity  $v_E$  approaches the phase velocity of the wave, the dependence of the electron density on the coordinate  $\xi = x - v_{ph}t$  is given by  $n(\xi) = n_0[1 + \lambda_p \delta(\xi)]/2$ , where  $\lambda_p$  is the Langmuir wavelength and  $\delta(\xi)$  is the Dirac delta function. The electron density distribution corresponds to an integrable singularity [ $\int_{-\infty}^{+\infty} n(\xi) d\xi \neq \infty$ ]. However, this breaks the geometrical optics approximation and leads to the reflection of a portion of the laser pulse in the backward direction and to the upshifting of the frequency of the reflected pulse.

In order to calculate the reflected radiation, we consider the interaction of an electromagnetic wave with an electron density spike formed in a breaking Langmuir wave. Bulanov, Esirkepov, and Tajima (2003) found that the reflection coefficient in the comoving frame is  $\kappa \approx 1/2\gamma_{ph}^3$ . Taking into account the change in volume where the reflected laser pulse is localized we find that the intensity of the reflected electromagnetic wave increases by

$$\frac{I_R}{I_0} \approx 8 \left( \frac{R_0}{\lambda_0} \right)^2 \gamma_{ph}^3, \quad (78)$$

with the reflected energy

$$\frac{E_R}{E_0} \approx \frac{1}{2\gamma_{ph}}, \quad (79)$$

and the power  $P \approx 2P_0\gamma_{ph}$ .

Take as an example the wakefield excitation in a gas of  $10^{18} \text{ cm}^{-3}$  density, by the electromagnetic wave with the amplitude  $a_0 = 15$ . The Lorentz factor associated with

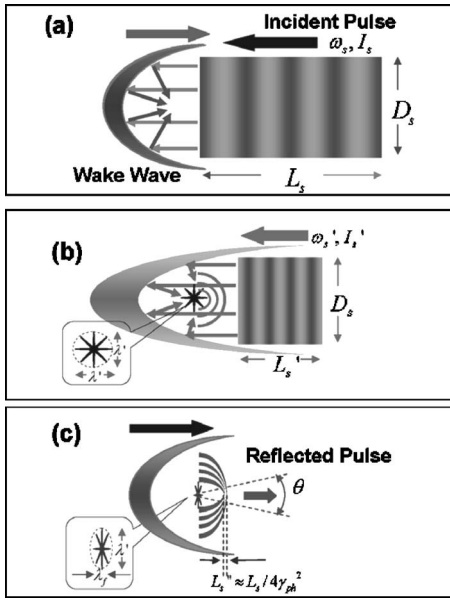


FIG. 30. Laser-pulse compactification scheme. (a) The laboratory frame ( $L$ ) before reflection of the laser pulse from the “flying mirror.” The laser pulse propagates from right to left. (b) The comoving reference frame ( $K$ ). Laser-pulse reflection and focusing occurs in the focus spot with  $\lambda' \approx \lambda_0/2\gamma_{ph}$ . (c) The laboratory frame ( $L$ ). The reflected electromagnetic radiation has  $\lambda_f \approx \lambda_0/4\gamma_{ph}^2$ , and it propagates in a narrow angle  $\theta \approx 1/\gamma_{ph}$ .

the phase velocity of the wakefield is related to  $\omega/\omega_{pe}$ , as  $a_0^{1/2}(\omega/\omega_{pe})$ , where we have taken into account the relativistically strong electromagnetic wave group velocity dependence on its amplitude (Akhiezer and Polovin, 1956), which is on the order of 125. Thus a laser pulse intensification of the order of 465 may be realized. A counterpropagating 1- $\mu\text{m}$  laser pulse of  $2 \times 10^{19} \text{ W/cm}^2$  intensity is partially reflected and focused by the wakefield cusp. If the efficiently reflected beam diameter is 40  $\mu\text{m}$ , then, according to Eq. (78), the final intensity in the focal spot is  $5 \times 10^{28} \text{ W/cm}^2$ . The driver pulse intensity should be sufficiently high and its beam diameter sufficiently broad to give such a wide mirror, say,  $4 \times 10^{20} \text{ W/cm}^2$  with the diameter 40  $\mu\text{m}$ . Thus if both the driver and source are one-wavelength pulses, they carry 6 kJ and 30 J, respectively. We see that the reflected radiation intensity can approach the Schwinger limit. In this range of electromagnetic field intensity it becomes possible to investigate the fundamental problems of modern physics using as a tool the already available laser.

We note here that the above approximation for the electron density in the nonlinear Langmuir wave in the form  $n(\xi) = n_0[1 + \lambda_p \delta(\xi)]/2$  corresponds to the assumption that a substantial part of the electrons is involved into the multistream motion. At the breaking threshold, as it has been demonstrated by Bulanov, Inovenkov, Kirsanov, *et al.* (1991), the electron density has the form  $n(\xi) \approx n_0 \gamma_{ph} / (3k_p \xi/2)^{2/3}$ , and the reflection coefficient calculated in the comoving mirror frame of reference

scales as  $\kappa \approx 1/\gamma_{ph}^4$ . As a result, the intensity of the reflected electromagnetic wave becomes  $I_R \approx I_0 (R_0/\lambda_0)^2 \gamma_{ph}^2$ . This expression can be rewritten as  $I_R \approx \gamma_{ph}^2 P_0/\lambda_0^2$ . We see that the intensity, which corresponds to the critical QED electric field, can be reached for 10 PW laser pulse focused into the 100- $\mu\text{m}$  spot in the  $2 \times 10^{17} \text{ cm}^{-3}$  density plasma.

Laser pulse reflection from flying mirrors has been simulated by Bulanov, Esirkepov, and Tajima (2003) in 3D PIC simulations. The results of the simulations are presented in Fig. 31. Figure 31(a) shows the paraboloid modulations of the electron density in the wake behind the driver laser pulse at  $t=16$ . Their transverse size is larger than that of the reflecting (incident from the right-hand side along the  $x$  direction) laser pulse wavelength. In Fig. 31(b) we present projections of the electric-field components. The  $x$  component of the electric field in the wake wave is shown as a projection onto the  $x, y$  plane. The projection of the  $y$  component of the electric field onto the  $x, z$  plane shows the electric field of the reflected laser pulse. The driver laser pulse is shown by the contours on the right-hand side of the computation box. In Fig. 31(b) we see that the wavelength of the reflected laser light is substantially shorter than that of the incident wave. Moreover its focus spot is also much smaller than the wavelength of the incident pulse. In these simulations the phase velocity of the wake wave corresponds to  $\beta_{ph} = 0.87$ , corresponding to a Lorentz gamma factor equal to  $\gamma_{ph} = 2$ . The frequency of the reflected light is 14 times higher than that of the incident radiation, in perfect agreement with Eq. (77), because in this case  $(1 + \beta_{ph})/(1 - \beta_{ph}) \approx 14.4$ . The electric field of the reflected radiation is about 16 times higher than that in the incident pulse, corresponding to an increase in intensity of 256 times.

These results provide a proof in principle of the concept of electromagnetic field intensification during reflection of laser radiation from flying paraboloidal relativistic mirror in the wake of a plasma wave.

Weinacht *et al.* (1998) were able to observe Rydberg states of electrons in an atom by coherent laser. We discuss further the idea that the generation of attosecond coherent x rays can lead to the direct observation of coherent quantum states of matter. We note that the typical time scale of electron fluctuations (or phase factors) in an atom or in a condensed matter is of the order of attoseconds. In typical matter these phase factors are said to be arbitrary, or more accurately random. Therefore what we learn in quantum mechanics is that the wave function  $\psi$  of an electron itself is usually not measurable, but only  $|\psi|^2$  is. Even with attosecond coherent x rays the scattering of many electrons results in the summation of random phase factors and thus no information is gained. However, we note that when attosecond coherent x rays on a system of a coherent state in which each electron has specifically assigned phase relationship to each other, the scattered coherent photon phases preserve their coherent phase relationships. Thus it should show not a blurred, but a distinct pattern. We

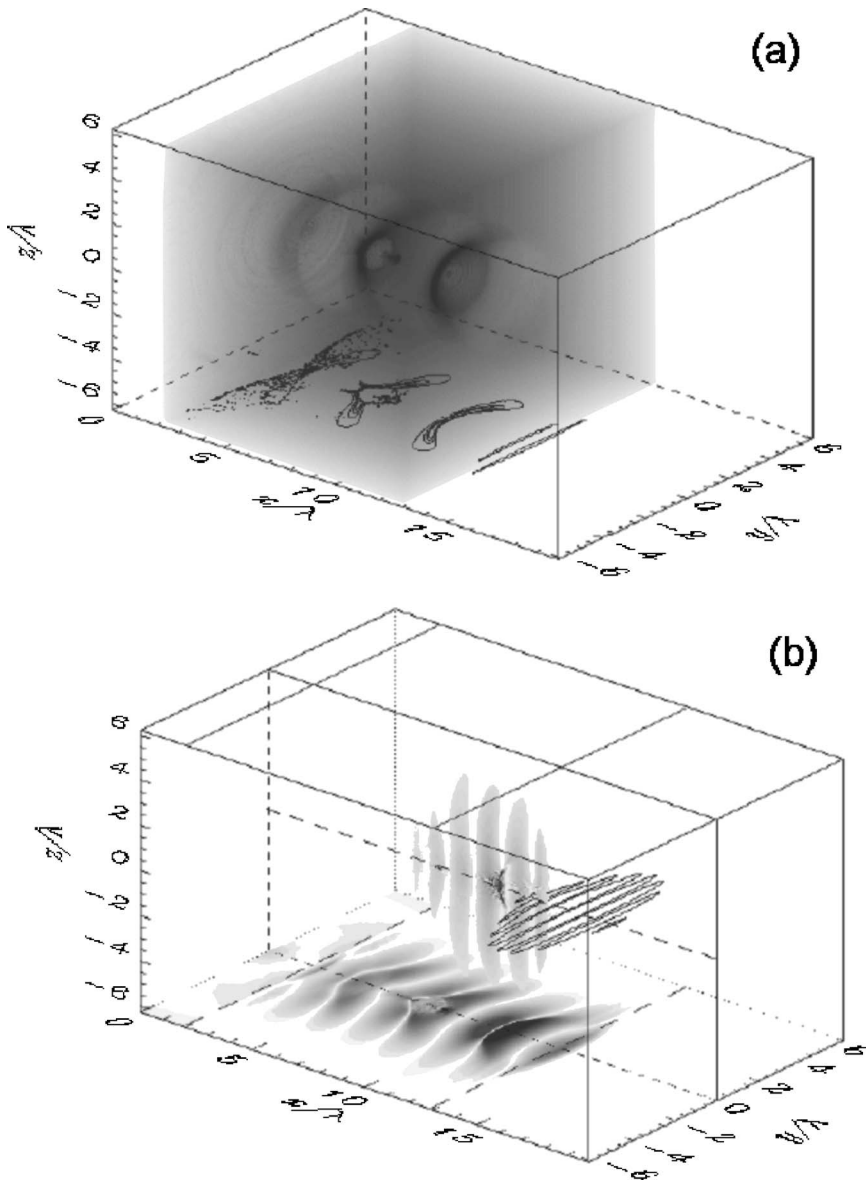


FIG. 31. (a) Paraboloidal modulations of the electron density in the wake behind the driver laser pulse. Projections of the electric-field components in the  $x,y$  plane (the  $x$  component of the wake wave) and in the  $x,z$  plane of the  $y$  component of the reflected pulse at  $t = 20$ . (b) The laser-pulse driver is shown by contours on the right-hand side of the computation box.

thus suggest that attosecond coherent x rays thus generated will give rise to a new experimental discipline of observation of coherent quantum states such as electrons in high-temperature superconductivity.

### B. Efficient attosecond phenomena in the relativistic $\lambda^3$ regime

The generation of subfemtosecond pulses was proposed (Corkum, 1993) and demonstrated (Hentschel *et al.*, 2001) using laser-atom interactions in the nonperturbative regime in gases at intensities of the order of  $10^{14}$  W/cm<sup>2</sup>. Even with quasiperiodic phase matching (Paul *et al.*, 2003), the efficiency achieved with this approach is orders below a percent. An alternative was recently demonstrated by 2D and 3D PIC simulations in which it was shown that ultrashort relativistic laser pulse intensity coupled with overdense plasma could generate isolated attosecond pulses with very high efficiency (Naumova, Nees, Sokolov, *et al.*, 2004).

Relativistic effects in supercritical plasmas have been discussed in their application to the generation of harmonics (Bulanov *et al.*, 1994, 2003; Lichters *et al.*, 1996; Vshivkov *et al.*, 1998a, 1998b) and attosecond pulse trains (Roso *et al.*, 2000) by weakly and tightly focused long pulses (Bulanov *et al.*, 2003). Mourou and co-workers (Mourou *et al.*, 2004; Naumova, Nees, Hou, *et al.*, 2004; Naumova, Nees, Sokolov, *et al.*, 2004) proposed to generate *isolated* attosecond pulses in the regime of tight focusing and ultrashort pulse duration (the  $\lambda^3$  regime; Mourou *et al.*, 2002) in reflection from near-critical plasma, via relativistic deflection and compression. The smaller transverse size ( $\lambda$ ) of the focal region reduces the instabilities and creates stronger slopes in the plasma density that separate subsequent half cycles in the reflected radiation. The shorter pulse duration causes the electrons to move coherently, so that relativistic motion of electrons in the direction of the reflected pulse creates Doppler compression, forming attosecond pulses.

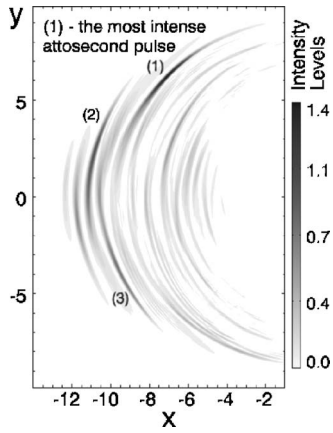


FIG. 32. The electromagnetic energy density of the reflected radiation ( $E^2 + B^2$ ) at  $t=11$ . Numbers (1), (2), and (3) indicate the most intense pulses in the reflected radiation. Parameters of the simulation:  $a=3$ ,  $\tau=5$  fs,  $n_0=1.5n_{cr}$ .

To demonstrate these effects 2D PIC simulations were performed for 5-fs linearly polarized laser pulses incident normally to a plasma layer of near-critical density. On the plot of the reflected radiation (Fig. 32) one may observe deflection at each half cycle of the pulse. The most intense pulse is clearly separated. It contains 10% of the input optical pulse energy within 50% isointensity contour, and its duration is 200 as. Simulations show that this interaction is sensitive to the carrier-envelope phase, and that efficient attosecond pulses are formed for different angles of incidence and exponential plasma profiles (Nees *et al.*, 2005). This technique of efficient generation of isolated attosecond pulses could also be scaled to the joule level, and even shorter pulses could be produced for higher intensities. The target, shaped by the laser pulse at attosecond pulse generation, can focus these attosecond pulses simultaneously to much higher intensity (Naumova *et al.*, 2005). This technique may enable us to reach *extreme* fields.

An analytic model involving only one nonlinear input to the electron velocity component, which is parallel to the plasma gradient, from the  $p$ -polarized electric field component of an incident plane wave has been presented by Mourou *et al.* (2002) and Naumova, Nees, Sokolov, *et al.* (2004). Consider the reflection of a short, relativistically strong, obliquely incident,  $p$ -polarized plane electromagnetic pulse arriving at a foil. It is known that the problem for nonzero angle of incidence  $\theta_0$  can be reduced to the problem for  $\theta_0=0$  (Bourdier, 1983) by using the reference frame  $M$  moving at the velocity  $V_y=c \sin \theta_0$ , with respect to the laboratory frame of reference  $L$ . In the  $M$  frame the incident electric field has only one component,  $E_y$ , the only component of the vector potential being  $A_y$ . While in the laboratory frame of reference  $L$  the plasma was at rest, in the absence of the incident wave, all the particles move with the velocity  $-V_y$  in the  $M$  frame. The Lorentz force driving the electrons in the  $x$  direction (normal to the foil) involves the term  $-V_y B_z$ , where  $B_z$  is the wave magnetic field. The Lorentz force, and consequently the

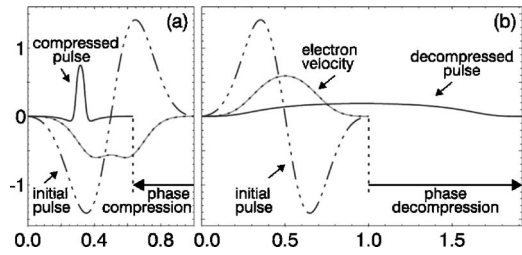


FIG. 33. The incident electric field  $E_\xi$  (dash-dotted line), electron velocity  $v_x(\xi)$  (dotted line), and the reflected electric field  $E_r(\xi_r)$  (solid line) for the parameters  $a_0=2.5$ ,  $\theta=\pi/3$ , and  $\varepsilon_0=0.5$  in the analytical model for pulse (a) compression and (b) decompression. The arrow shows the phase change for the reflected pulse.

electron velocity  $v_x$ , can be negative (directed outwards), so the radiation field produced by the electron at that time has a significantly shorter time scale due to the Doppler effect. For short driving pulses, the total electron displacement can be *negative*, from the plasma towards laser pulse, resulting in an extremely sharp reflected pulse [Fig. 33(a)]. When the sign of  $E_\xi$  is changed, the reflected pulse becomes longer than the driving cycle [Fig. 33(b)].

Simulations demonstrate that for large angles of incidence the relativistic electrons driving the radiation into attosecond pulses can be synchronously extracted from the target through narrow regions with minimal pressure forming efficiently ( $\sim 15\%$ ) dense attosecond electron bunches (Naumova, Sokolov, *et al.*, 2004; Naumova *et al.*, 2005). These electron bunches have the ability to scatter counterpropagating electromagnetic radiation, generating extremely bright attosecond x-ray pulses.

Finally, the efficiency derived from working with overdense plasmas in the relativistic  $\lambda^3$  regime enables a new *microelectronics* and *photonics* based on relativistic effects and operating in the attosecond domain.

## VII. NUCLEAR PHYSICS

### A. Rutherford, Livermore, Michigan, Osaka, and LULI experiments

In intense laser regimes beyond  $10^{17} Z^6$  W/cm<sup>2</sup>, electrons are stripped from atoms with charge number  $Z$ . For certain elements the removal of inner-shell electrons changes the nuclear bound state so much that it destabilizes the nucleus itself. An example of this is <sup>163</sup>Dy (Jung *et al.*, 1997), in which the removal of inner-shell electrons destabilizes the nucleus.

### B. Tridents

The trident process is a process in which a nucleus plays the role of an additional “photon” in the interaction among electrons and photons. This may be shown in a Feynman diagram as a gamma photon initiating electron-positron pair creation.

This process allows us to contemplate the positron production by an intense laser with the currently available technology. If it were only a matter of vacuum pair creation, the necessary electric field would need to reach the Schwinger field strength (see Sec. XI). With the presence of the trident process, this condition is greatly relaxed (Shearer *et al.*, 1972; Mima *et al.*, 1991; Liang *et al.*, 1998) to a level where it can be directly accessed with today's relativistic lasers and may be achievable at laser intensities around  $10^{22}$  W/cm<sup>2</sup>.

In experiments conducted on solid targets (Cowan *et al.*, 2000a) high-energy electrons were generated, leading to the creation of high-energy gamma photons in the solid by the bremsstrahlung process. These gamma rays appear to have induced a nuclear transmutation (Cowan *et al.*, 2000a, 2000b, 2000c). The production of energetic electrons as well as acceleration of other particles may provide for the creation of substantial numbers of isotopes. Isotope production by laser acceleration has been demonstrated by Yamagiwa and Koga (1999), Ledingham *et al.* (2001a, 2003), Leemans *et al.* (2001), and Nemoto *et al.* (2001). Transmutation in the minor actinides may be carried out via a new fission decay mechanism in which the vibrational levels created by the hyperdeformation of nuclei (as in the formation of isomers) are populated (Shizuma *et al.*, 2002). Such a process may be initiated by gamma rays generated by inverse Compton scattering of the laser pulse off of a high-energy electron beam. Gamma rays produced by this means induce various  $(\gamma, n)$  nuclear processes, as opposed to the more common  $(n, \gamma)$  processes seen in nature and demonstrated in prior nuclear experiments.

### C. Superhot plasma and cluster interaction, Coulomb explosion, cluster fusion, neutron sources

Nanoclusters and microclusters have attracted strong interest over the years. In particular their interaction with intense laser beams (Ditmire *et al.*, 1996; Shao *et al.*, 1996; Ditmire, Smith, *et al.*, 1997; Ditmire, Tisch, *et al.*, 1997; Ditmire *et al.*, 1998, 1999, 2000; Zweiback *et al.*, 2000; Zweiback and Ditmire, 2001) has sparked recent interest. The interaction of clusters with a laser has many salient features. One of them is that it is more intense than an interaction with conventional materials such as gas or solid and results in superhot matter and much higher laser absorption.

Cluster targets irradiated by laser light show properties of both underdense and overdense plasmas, as well as novel optical properties (Tajima, Kishimoto, and Downer, 1999). Very efficient absorption of laser energy has been demonstrated by Ditmire *et al.* (1996, 1999) and Lezius (1998), with the formation of underdense plasmas with very high-temperature and x-ray emission. Such high-temperature plasmas make possible tabletop fusion experiments (Zweiback *et al.*, 2000; Last and Jortner, 2001; Parks *et al.*, 2001) and provide a mechanism for ion injection into accelerators.

The regimes of laser-cluster interaction, in which fast ions are generated (Ditmire *et al.* 1996; Krainov and

Smirnov, 2000, 2002), are dominated by collisional absorption and by heating of the cluster plasma. In this case a hot cluster plasma expansion occurs in the ablation regime. With an increase of laser pulse intensity up to the range of  $10^{21}$ – $10^{22}$  W/cm<sup>2</sup>, we expect to see the laser light ripping the electrons away from atoms almost instantaneously, instead of going through secondary processes of heating and collisions. In the petawatt range the laser radiation has such a high intensity that it can blow off all the electrons and prepare a cloud made of an electrically non-neutral plasma. Provided the cluster has large enough size and the density of a solid, the ions are accelerated up to high energy during the Coulomb explosion of the cloud (Last, Schek, and Jortner, 1997; Eloy *et al.*, 2001; Kumarappan *et al.*, 2001, 2002; Nishihara *et al.*, 2001; Kishimoto *et al.* 2002a, 2002b; Kaplan *et al.*, 2003).

An electrostatic potential appears in the plasma formed by a cluster irradiated by a laser pulse. The value of this electrostatic potential, which is due to the separation of the electric charges, can be at most equal to the value of the potential at the surface of a charged sphere with a radius  $R$  and density  $n$ :  $\varphi_{\max} = 4\pi n e^2 R^2 / 3$ .

Let us consider the motion of the ion component under the Coulomb repulsion in this second phase. Assuming the ions to be cold and to move radially, we obtain the energy integral  $E_i - \Pi(r_0, t) = \text{const}$ , where the ion kinetic energy is  $E_i = \sqrt{m_i^2 c^4 + p_i^2 c^2} - m_i c^2$  and the potential energy is  $\Pi(r_0, t) = 4\pi e^2 Q(r_0) / [r_0 + \xi(r_0, t)] - 1/r_0$ , where  $r_0$  is the initial ion position,  $\xi(r_0, t)$  is the ion displacement at time  $t$ , and  $Q(r_0) = \int_0^{r_0} n_i(r_0) r_0^2 dr_0$ . During the expansion of the cloud the ion kinetic energy increases, for  $\xi \rightarrow \infty$ , up to the value  $4\pi e^2 Q(r_0) / r_0$  which depends on the initial position of the ion inside the cloud. Assuming a homogeneous distribution of the ion density inside the cloud,  $n_i$ , we find that an ion acquires a final energy  $E_i = 2\pi e^2 r_0^2 / 3$ , which is limited by  $E_{i\max} = 2\pi e^2 R^2 / 3$ .

Since the ion energy is proportional to  $r_0^2$  we can calculate the ion energy spectrum  $df/dE_i$  which, due to the flux continuity in phase space, is proportional to  $4\pi r_0^2 dr_0 / dE_i$ . We obtain (Nishihara *et al.*, 2001)

$$\frac{df}{dE_i} = \frac{3R}{e^2} \theta(E_{\max} - E_i) \sqrt{\frac{E_i}{E_{\max}}}, \quad (80)$$

where the unit step function is  $\theta(x) = 1$  for  $x > 0$  and  $\theta(x) = 0$  for  $x < 0$ . This form of the fast-ion energy spectrum has been observed by Nishihara *et al.* (2001) in 3D PIC simulations of the Coulomb explosion of a cluster exposed to high-intensity laser radiation.

When the ion energy is smaller than  $m_i c^2$ , we can use a nonrelativistic description of the Coulomb explosion. In this approximation we write the following system of equations of motion:

$$\ddot{\xi} = \frac{\omega_{pe}^2}{3} \frac{r_0^3}{(r_0 + \xi)^2}. \quad (81)$$

Here  $\omega_{pi} = \sqrt{4\pi n_e e^2 / m_i}$  is the ion plasma frequency. Integrating Eq. (81) with the initial conditions  $\xi(0)=0$  and  $\dot{\xi}(0)=0$  yields

$$\frac{1}{2} \ln \left( \frac{2\xi + r_0 + 2\sqrt{\xi^2 + r_0\xi}}{r_0} \right) + \frac{\sqrt{\xi^2 + r_0\xi}}{r_0} = \sqrt{\frac{2}{3}} \omega_{pi} t. \quad (82)$$

When the displacement is small,  $\xi \ll r_0$ , ions move with constant acceleration  $\xi \approx r_0 (\omega_{pi} t)^2 / 6$ , while for  $\xi \rightarrow \infty$ , we have  $\xi \approx \sqrt{2/3} r_0 \omega_{pi} t$ . In the latter case ions move with constant velocity. The typical time of the ion cloud expansion is of the order of  $\omega_{pi}^{-1}$ . Above we assumed that the Coulomb explosion of the cluster is spherically symmetric. The effects of cluster asymmetry were discussed by Askar'yan and Bulanov (1983), Nishihara *et al.* (2001), and Kumarappan *et al.* (2001, 2002).

For the case of deuteron clusters, because of the superhigh temperatures of matter, copious neutrons of fusion origin have been observed (Ditmire *et al.*, 1999). Kishimoto and Tajima have shown that the enhanced interaction of the laser and cluster arises from the nonlinearity of electron orbits from clusters (Kishimoto and Tajima, 1999). When the cluster size is sufficiently small or the laser intensity sufficiently strong, electrons in the cluster execute spatial oscillations whose excursion length  $\xi$  is greater than the size of the cluster  $a$ . Polarization of the cluster by oscillating electrons induced on its surface becomes nonlinear. Electrons see their own strong polarization fields and can no longer come back to their original spot. The electron orbits exhibit remarkable chaos within a single optical cycle (Kishimoto and Tajima, 1999). This strong orbital nonlinearity is responsible for absorbing much of the laser energy within an ultrashort time of less than 10 fs. Some or many of the electrons wander out of their original cluster. When this happens, the cluster is depleted of its electrons, leading to a Coulomb explosion. The energy of the exploding ions is high and takes an almost shell distribution with the predominant population on the high-energy side. The energy of these ions approximately scales as  $E_i \propto a_0^2$  and reaches about 1 MeV at  $a_0=10$  (Kishimoto *et al.*, 2002a, 2002b).

Fast ions accelerated during cluster explosions have also been observed in the experiments of Springate *et al.* (2000). These results open the way for construction of a tabletop neutron source as well as for nuclear fusion devices on a tabletop scale (Last and Jortner, 2001; Parks *et al.*, 2001; Kishimoto *et al.*, 2002a, 2002b).

Laser interactions with foam targets also exhibit the Coulomb explosion mechanism of ion acceleration. Energetic proton generation in low-density plastic ( $C_5H_{10}$ ) foam by intense femtosecond laser pulse irradiation has been studied experimentally and numerically by Okihara *et al.* (2004). Plastic foam was successfully produced by a sol-gel method, achieving an average density of

10 mg/cm<sup>3</sup>. The foam target was irradiated by 100-fs pulses of a laser intensity 10<sup>18</sup> W/cm<sup>2</sup>. A plateau structure extending up to 200 keV was observed in the energy distribution of protons generated from the foam target, with the plateau shape well explained by the Coulomb explosion of lamella in the foam. The laser-foam interaction and ion generation were studied qualitatively by two-dimensional particle-in-cell simulations, which indicated that energetic protons are mainly generated by the Coulomb explosion. From these results, the efficiency of energetic ion generation by Coulomb explosion in a low-density foam target is expected to be higher than in a gas-cluster target. In addition, these neutrons could be controlled by lasers (Tajima *et al.*, 2000).

#### D. Fast ignition

The conventional approach of laser fusion is to compress and heat the target to thermonuclear conditions by one set of laser beams simultaneously. The thermonuclear burn is given by

$$\phi = \rho r / [\rho r + \xi(T)], \quad (83)$$

where  $\xi(T) = 8m_i c_s / \langle \sigma v \rangle$  and  $m_i$  is the ion mass. At a value of  $\rho r = 3 \text{ g/cm}^3$  we obtain 1/3 of burnup. The confinement time (or more precisely the disassembly time of the fuel capsule)  $\tau$  and the density of the fuel  $n$  are related to the value of  $\rho r$ , to yield a Lawson-criterion-like condition,

$$n\tau = \rho r / 4c_s m_i, \quad (84)$$

yielding an approximate criterion for ignition as  $2 \times 10^{15} \text{ s/cm}^3$  (Lindl, 1998; Lindl *et al.*, 2004). In order to achieve this energetically most favorably (i.e., with the least amount of compression energy), one approaches through (or near) the Fermi degenerate state. The laser pulse needs to be smoothly increasing in order to make the shock minimize the entropy increase upon compression. In addition to the adiabatic compression, one wants to make sure that toward the end of the compression phase (i.e., the decreasing phase), the Rayleigh-Taylor instability does not lead to detrimental effects on the fuel (Lindl *et al.*, 2004). These considerations lead to the well-known strategy of the smooth and slow rise of the laser pulse over some 20 ns with a sharp rise toward the end of the pulse, going about 10 times the pulse height in about 2 ns. In this standard approach it is clear that fuel compression is related to the temperature rise through the adiabat. By incorporating the driver energy requirement and the fusion energy gain, one arrives at a scaling law of energy gain as a function of the driver energy  $E_{dr}$  in the high-gain area (Kozaki, 1998) given by

$$G = 100(E_{dr}/E_0)^{1/3}. \quad (85)$$

Here  $E_0$  (in MJ) is the normalizing driver energy that achieves  $G=100$  in "direct drive," which is about 4 MJ according to Kozaki (1998).

In 1994 Tabak *et al.* proposed to decouple the condition for fuel compression and heating to the thermonuclear temperature. In this scheme, they propose to first compress the fuel in a smooth adiabatic fashion without achieving the thermonuclear temperature at the core, which allows a far smaller energy for the laser, because the laser energy is directly tied to the final pressure in compression. One can choose a much lower entropy adiabat in this case. When we achieve the density dictated by Eq. (84), a short intense laser is injected to heat the core. In Tabak's proposed scheme, this short-pulse laser (with a duration of the order of a ps) interacts with the plasma surrounding the compressed target at its resonant surface (with a density  $\sim 10^{21}$  cm $^{-3}$ ). Here, according to the scheme of Tabak *et al.* (1994) electrons are heated and turn into an energetic beam with  $\sim$ MeV energy. With a judicious choice of electron beam energy (i.e., the laser absorption process by the target) and the linear density of the fuel, we can deposit this electron energy in the fuel core. The condition for the electron range not to exceed the target size may be written as

$$\rho r = 0.5 \text{ g/cm}^2, \quad (86)$$

with a laser pulse duration given by

$$\tau_l = 40[(100 \text{ g/cm}^2)/\rho] \text{ ps}. \quad (87)$$

This yields a pulse duration between 10 and 20 ps for a compressed fuel density of 200–300 g/cm $^2$  (Key *et al.*, 1999). According to Atzeni (1999; Atzeni *et al.*, 2002; Temporal *et al.*, 2002), the required laser energy for the fast-ignition drive is

$$E_{\text{las}} = 80[(100 \text{ g/cm}^3)/\rho]^{1.8} \text{ kJ}. \quad (88)$$

This sets the laser energy for fast ignition at about 50 kJ, while 10–20 kJ of electron energy needs to be delivered at the hot spot. The gain with the assist of fast ignition is scaled as a function of the compression driver energy as in the standard “direct drive” scaling (Kozaki, 1998) as

$$G^{fi} = G^{fi0}(E_{\text{dr}}/E_{fi0})^{1/3}, \quad (89)$$

where  $G^{fi0}$  is between 100 and 300 and  $E_{fi0}=0.5$  MJ (Kozaki, 1998). Thus given compression driver energy (even with a modest increase of fast-ignition driver energy and added complexity) the fusion gain is greatly enhanced over the standard method. The crucial question is how the laser energy is transferred to electrons and how this electron beam can be transported to the fuel core and deposit most of its energy in the core. It is expected that a straightforward electron-beam propagation, first created at the resonant surface, will reach the small core spot. There are several expected instabilities in both plasma and beam along the way. They consist of a dense hot plasma with density ranging from  $10^{21}$  to  $10^{26}$  cm $^3$  and have names like the hose instability, the sausage instability, and the filamentation instability. The expected current far exceeds the Alfvén current, above which the induced magnetic field of the electron beam itself bends the electron orbits severely. Thus a strong return current is expected, nearly canceling the

initial electron current. This return current can give rise to secondary plasma instabilities.

A recent target design with a cone access may alleviate some of the major difficulties seen above (Kodama *et al.*, 2001).

To overcome the difficulty of electron beam transport over long distances, Mourou and Tajima have proposed to use lasers with an even shorter pulse (of the order of 10 fs) with much higher intensity,  $10^{25}$  W/cm $^2$ . Such an intense laser pulse will penetrate the dense plasma beyond the ordinary critical density because of relativistic transparency (see Sec. IV.D). It remains to be seen whether the resultant electron energy in the  $\sim$ MeV range is the main constituent of the electron energy distribution. A different embodiment of the fast-ignition concept has been proposed by Roth *et al.* (2001) and Bychenkov, Sentoku, *et al.* (2001), where instead of fast electrons the laser beam accelerates ions that will ignite the precompressed target.

## VIII. HIGH-ENERGY PHYSICS

When can we ascertain that a reaction is a high-energy reaction? One way is simply to examine the ratio

$$R = \frac{\Delta E}{Mc^2} > 1. \quad (90)$$

This expresses, for a given reaction, the ratio between the binding energy ( $\Delta E$ ) and the rest mass energy ( $Mc^2$ ) of the constituents. For instance, for a chemical reaction where  $\Delta E \sim 1$  eV,  $Mc^2 \sim 10$  GeV, so the ratio is  $R \sim 10^{-9}$ . For a nuclear reaction where  $\Delta E \sim 10$  MeV and  $Mc^2 \sim 10$  GeV,  $R \sim 10^{-3}$ . In high-energy physics  $R$  is of the order of, or greater than, 1. The production of a positron, for instance, from the scattering of a relativistic electron with an energy of a few  $mc^2$  from the nucleus by the trident process leads to  $R \sim 1$ . The observation of the positron by Anderson in early 1932, predicted by Dirac, is considered to be the birth of the field of high-energy physics. Similarly, we could argue that the laser-produced positrons demonstrated a few years ago by the Garching group (Gahn *et al.*, 2000) and Livermore groups (Cowan *et al.*, 2000a, 2000b, 2000c) could be considered as the entry of optics into high-energy physics.

Since the first electron acceleration experiments demonstrating the high-field gradients (Clayton *et al.*, 1993; Modena *et al.*, 1995; Nakajima *et al.*, 1995; Umstadter, Chen, *et al.*, 1996), we have seen an increasing number of novel potential applications of ultrahigh-intensity lasers in high-energy physics.

### A. Large-field-gradient applications

#### 1. Electron injector

Already a large body of work has demonstrated the generation of gargantuan electrostatic field gradients. Large numbers of electrons (nC) have been accelerated over only a few tens of  $\mu\text{m}$  to energies above 200 MeV (Malka *et al.*, 2002) and corresponding to gradients of

200 GeV/m. As mentioned above, the quasimonoenergetic electron bunches accelerated in the wakefield have been observed (Faure *et al.*, 2004; Geddes *et al.*, 2004; Mangles *et al.*, 2004; Miura *et al.*, 2005; Yamazaki *et al.*, 2005). It is worth noting that these large gradients confer to the beam a low transverse emittance. The transverse emittance expresses the quality of a beam. It is the product of the beam waist area and the beam solid angle in the far field. It needs to be as low as possible, with a minimum given by  $\lambda^2$ . Laser accelerator beams have already been shown to have a better transverse emittance than those of conventional accelerators. Various methods to induce lower-emittance electron beam sources driven by a laser have been introduced by utilizing large electric fields of laser-plasma interaction to kick the electrons from the plasma into the beam. These include self-modulated laser wakefield acceleration (SMLWFA), LILAC (laser-injected laser accelerator), beat wave, and subcyclic injectors. Possible extractions by applying a rf acceleration of these beams have been considered by Chao *et al.* (2003). They have discussed the space charge effects that play a role in emittance growth and control. A series of recent experiments using the self-modulated laser wakefield acceleration generated quite remarkable results (Modena *et al.*, 1995; Nakajima *et al.*, 1995; Amiranoff *et al.*, 1998; Assamagan *et al.*, 1999; Chen *et al.*, 1999; Kodama, 2000; Amiranoff, 2001; Malka *et al.*, 2001; Leemans *et al.*, 2002; Faure *et al.*, 2004; Geddes, 2004; Mangles *et al.*, 2004). When the plasma density is sufficiently high, the laser pulse is longer than the resonant length given by Tajima and Dawson. However, the self-modulating instability of the plasma electrons via the forward Raman instability (see, for example, Kruer, 1988) can give rise to an undulating laser profile with the plasma period of induced plasma waves. The phase velocity of the plasma wave is equal to the laser group velocity (Tajima and Dawson, 1979)

$$v_{\text{ph}} = c\sqrt{1 - \omega_{pe}^2/\omega^2} \approx c(1 - \omega_{pe}^2/2\omega^2). \quad (91)$$

Because of the large amplitude and relatively slow phase velocity due to the high plasma density in these experiments, electrons in the plasma can be easily picked up and trapped in the plasma wave (Esarey and Piloff, 1995). The general features of these experiments are as follows.

First, a large number of electrons (on the order of 1 nC) are trapped and accelerated. Second, the transverse emittance is surprisingly small, though it is far from clear how accurately the emittance may have been measured so far, amounting to the order of 0.1 mm mrad, at least an order of magnitude smaller than the rf-based electron injector's emittance. Third, the longitudinal energy spread is rather large (up to 100%), because electrons are picked up from background electrons.

The product of the bunch length and the energy spread is the longitudinal emittance. This is comparable to conventional rf-based sources. The tiny transverse spot size of the bunch corresponds to the laser spot size and therefore a small transverse emittance. For ex-

ample, in the study of Assamagan *et al.* (1999) at least  $5 \times 10^8$  electrons were accelerated to an average energy of 7 MeV with a transverse emittance as low as  $10^{-7}$  mrad. It should be noted that though this energy spread is substantial, the relative energy spread  $\Delta E/E$  for high-energy applications is certainly tolerable as  $E$  gets larger. Meanwhile, there have been many theoretical proposals to reduce the energy spread and thus the longitudinal emittance in general (Umstadter, Chen, *et al.*, 1996; Rau *et al.*, 1997; Esarey *et al.*, 1999; Nagashima *et al.*, 1999). Because the experiments of Assamagan *et al.* were first-generation experiments without particular consideration for laser beam handling and dynamics, their low transverse emittance was a surprise as well as a puzzle. It would now be highly desirable to measure the beam properties more precisely. One can understand that the laser-driven electron source has low emittance to begin with, as the laser is focused to a small (say,  $<10 \mu\text{m}$ ) spot and electrons are promptly accelerated to relativistic energies. It is still puzzling, however, that during the beam transport, after the electron bunches emerge from the plasma, space-charge effects can blow up the emittance, despite the quite low values of emittance.

It has been pointed out (Chao *et al.*, 2003) that the coupling between longitudinal and transverse dynamics can be important. This is because in the early experiments (a) the longitudinal bunch length is much smaller than that of conventional beams; (b) the longitudinal energy spread is much larger than that of the conventional ones. The longitudinal emittance (the product of the bunch length and the energy spread) is in fact very similar to those of conventional accelerators, i.e., MeV ps = keV ns. These two characteristics of laser-driven sources make the bunch length change rapidly as soon as the beam emerges from the plasma wave. This bunch lengthening has an influence on transverse space-charge effects. Bunch lengthening gives rise to the dilution of space charge. On the other hand, transverse beam spread can also mitigate the longitudinal bunch lengthening, as it too reduces space-charge effects. It is, therefore, crucial to incorporate the coupling between longitudinal and transverse dynamics in order to evaluate the properties of laser-driven bunches and to control and utilize this new technology in high-energy accelerators. The incorporation of this coupling has been shown to explain the experimentally measured (apparent) emittance's being quite small. The emittance at the plasma source is estimated to be as small as  $10^{-8}$  m rad (Chao *et al.*, 2003).

A good way to balance the desire to have small emittance and beam size and the wish to have a large number of electrons is to use a fairly long pulse (up to 1 ps) and to extract it into a traditional rf (such as the X band) cavity to accelerate electrons to higher energies (beyond 100 MeV) before their space charge can exert its influence on the emittance. If and when such a beam is extracted and injected (with emittance  $10^{-7}$  m rad) into an x-ray free-electron laser (FEL), the undulator length of

the FEL may be greatly reduced, from 100 to 30 m in the example of the LCLS, the proposed x-ray FEL at SLAC, according to Chao *et al.* (2003).

In order to use laser-accelerated beams as injectors in rf accelerators, it is important to understand whether rapid dynamical changes will allow us to properly insert the bunches into the accelerator structure and how to do so. Since longitudinal bunch lengthening happens quickly, we have to capture the beam before it becomes too long. Since the transverse beam spread takes place rapidly as well, we may need to focus the beam with a magnetic field.

This is a direct benefit of abrupt acceleration. In a particle beam the emittance grows at the front end of the beam, where the particles are not yet relativistic and can be easily subject to Coulomb interaction. With the Coulomb interaction scaling as  $1/\gamma^2$ , it is important for the particles to reach the relativistic regime as fast as possible.

Electron bunch production in foil physics poses its own problems, such as electron energy versus  $a_0$ . When the laser intensity is modest ( $a_0$  less than unity), the main electron acceleration is in the direction opposite to the incident laser. As the laser intensity increases, more and more electrons are accelerated in a forward direction through the foil. The ionization process is a combination of Coulomb barrier suppression, above-threshold ionization, and multiphoton ionization. The level of ionization of high- $Z$  atoms has been qualitatively studied (Zhidkov, Sasaki, Tajima, *et al.*, 1999). When the peak intensity of a laser pulse enters the target, electrons stripped from target atoms will be accelerated to high energies. The electron acceleration process in a relatively low- $Z$  target by an ultrashort-pulse laser is related to wakefield generation and associated processes. Here the electron energy spectrum tends to exhibit a power-law behavior (Modena *et al.*, 1995; Nakajima *et al.*, 1995) with a spectrum index between 0 and 2. In the nonrelativistic regime, the wakefield amplitude is proportional to the intensity, while the acceleration length is multiplied by it to get the energy gain. The maximum electron energy is proportional to the laser intensity in the relativistic regime, if based on ponderomotive acceleration.

When the pulse length is sufficiently short and the metallic foil surface sharp enough to send the electron orbit out of the foil surface, the removal of electrons from the uniform medium gives rise to rapid loss of electron memory and to electron heating. This is the mechanism of the so-called Brunel heating or the vacuum heating of electrons by short-pulse lasers (D'yachenko and Imshennik, 1979; Brunel, 1987). On the other hand, if the pulse is long enough to cause the surface to ablate to form a gentle density gradient with a small density gradient to start with, electron orbits are buried in the preformed plasma. In this case, the primary absorption mechanism is resonant absorption. The relevant criterion between the two regimes is the comparative lengths between the electron excursion in the laser field  $\xi = eE/m_e\omega^2$  and the density gradient scale length  $L_n$ . A clear experimental demonstration of this has been car-

ried out by Grimes *et al.* (1999). In the nonrelativistic regime, a rapid rise of the electron energy from the irradiated foil has been observed. The energy of electrons continues to rise after it becomes relativistic. This is due primarily to ponderomotive acceleration at the front of the laser when the foil is thin enough for the laser to burn through the solid target (Denavit, 1992; Gibbon, 1996; Zhidkov, Sasaki, *et al.*, 1999). When the laser is longer and the surface of the foil is ablated, the plasma is heated by resonant absorption, leading to a two-temperature distribution (Kishimoto *et al.*, 1983). Recent work by Nakamura and Kawata (2003) implies that if the pulse is long and the foil is thick enough, the laser front becomes filamentarily fragmented and will result in stochastic acceleration. This leads to heating. Such heating may have taken place in a thick-target large-energy experiment at the LLNL Petawatt experiment (Cowan *et al.*, 2000a, 2000b, 2000c). When the laser is irradiated obliquely with  $p$  polarization, electrons are driven directly into the foil, yielding excitation of large-amplitude longitudinal plasma waves in a solid-state density, which results in ultrashort pulses of high-energy electrons (Ueshima *et al.*, 1999). Similarly, Grimes *et al.* (1999) have considered the extraction of electrons with high density and low emittance from the laser input surface. Sometimes, prepulse induced electron heating can be beneficial to accelerate electrons. Using these hot electrons, one can make a large space-charge separation (Ueshima *et al.*, 2000). There is a possibility of extracting and accelerating polarized electrons. Polarized electron sources have been studied, including GaAs laser irradiation (Nakanishi *et al.*, 2001). In addition to this method, we can think of a new approach based on the intense laser irradiation of a thin magnetized target. The relatively small angular spread of picked up electrons (combined with their small spot size) provides the basis for the small source emittance, just as in the case of the gas-target laser acceleration considered earlier. Moreover, if we magnetize a metallic target (such as Fe), outer-shell electrons get their spins polarized. As the spin depolarization is smaller by the factor of  $g$  ( $\ll 1$ ) over the orbital divergence, such a beam should preserve the spin as well as the (orbital) emittance (Chao *et al.*, 2003).

## 2. Laser-accelerated ions

Laser accelerators of ions are based on the high conversion efficiency between the energy of a laser and that of fast ions. This efficiency was first observed in petawatt laser-plasma interactions at LLNL. Collimated beams of fast ions were recorded in experiments on laser pulse interactions with solid targets (Clark *et al.*, 2000; Maksimchuk *et al.*, 2000; Snively *et al.*, 2000; Mackinnon *et al.*, 2001). A fast-ion isotropic component was also observed during the interaction of laser radiation with gas targets by Fritzier *et al.* (2002). The ion acceleration processes have also been investigated theoretically and

numerically<sup>7</sup> by means of two- and three-dimensional particle-in-cell (PIC) computer simulations. In the experiments mentioned above, electrons were accelerated to energies of several hundred MeV while the proton energy was tens of MeV, the number of fast protons ranged from  $10^{12}$  to  $10^{13}$  per pulse, and there was a 12% efficiency of conversion from the laser energy to the fast-ion energy. The generation of fast ions becomes highly effective when the laser radiation reaches the petawatt power limit as it was shown by Bulanov *et al.* (2001). PIC computer simulations show that by optimizing the laser-target parameters it becomes possible to accelerate protons up to energies of several hundreds of MeV.

The mechanism of laser acceleration of ions (protons and other ions) by the electric field is set up by space-charge separation of hot or energetic electrons and ions. Thus the temperature or the energy of electrons that are driven by the laser determines the energy of ions (Snively *et al.*, 2000; Clark, Krushelnick, Davies, *et al.*, 2000; Clark, Krushelnick, Zepf, *et al.*, 2000; Tajima, 2002). The exact mechanisms in the energy transfer between the fast electron in the ion energy depends on the specific conditions of the laser-target interaction. Koga *et al.* (2002) have shown that a strong solitary density pileup coupled with an associated density cavity provide some 500 TeV/m acceleration gradient. This can happen even at a “modest” intensity level of  $10^{21}$  W/cm<sup>2</sup>.

Bulanov *et al.* (2001) have shown that an intensity of  $10^{22}$  W/cm<sup>2</sup> can accelerate ions to 1 GeV. Before these experiments that showed laser-driven ion acceleration, Rau and Tajima (1998) have suggested a graded density for Alfvén shocks to gradually increase the phase velocity so that ions acceleration can be accomplished at a laser intensity level of  $10^{18}$  W/cm<sup>2</sup> to reach energies beyond 100 MeV. Ions at the 100-MeV energy level offer important applications in proton therapy (Tajima, 1998).

### 3. High-energy proton beams

It has been shown that laser–thin-target interactions can produce plentiful MeV protons in a beam with superior transverse emittance (Roth *et al.*, 2002). The proton generation is a direct consequence of electron acceleration. Electrons that are violently accelerated in the laser field can draw behind them protons that are on either the front or back surface of the target. Highly energetic proton beams have been demonstrated at Livermore, LULI, CUOS, and Rutherford with an intensity of  $10^{18}$ – $10^{20}$  W/cm<sup>2</sup>. They could lead to important applications such as fast ignition for inertial confinement fusion as was pointed out by Roth *et al.* (2001), proton therapy (Bulanov and Khoroshkov, 2002; Fourkal *et al.*,

2002, 2003), fast ion-beam injection to conventional accelerators (see Krushelnick, Clark, Allot, *et al.*, 2000), and proton imaging (Borghesi, Campbell, *et al.*, 2002; Borghesi *et al.*, 2004)

Proton use in radiotherapy and oncology provides several advantages. First, proton beam scattering on atomic electrons is weak and results in low irradiation of healthy tissues surrounding the tumor. Second, the slowing down length for the proton with given energy is fixed and avoids irradiation of the healthy tissues at the rare side of the tumor. Third, the Bragg peak of the energy losses provides substantial energy deposition in the vicinity of the proton stopping point (see, for example, Khoroshkov and Minakova, 1998). Currently, proton beams with the required parameters are produced with conventional charged particle accelerators: synchrotron, cyclotron, and linear accelerators (Scharf, 1994). The use of the laser accelerator is very attractive because its compactness is associated with additional possibilities for controlling proton beam parameters. The typical energy spectrum of laser-accelerated particles observed both in experiments and in computer simulations can be approximated by a quasithermal distribution with a cut-off at a maximum energy. The effective temperature attributed to fast ion beams is within only a factor of a few from the maximum value of the particle energy. On the other hand, the above-mentioned applications require high-quality proton beams, i.e., beams with sufficiently small energy spread  $\Delta E/E \ll 1$ . For example, for hadron therapy it is highly desirable to have a proton beam with  $\Delta E/E \leq 2\%$  in order to provide the conditions for a high irradiation dose being delivered to the tumor while sparing neighboring tissues. In the concept of fast ignition with laser-accelerated ions presented Roth *et al.* (2001), the proton beam was assumed to be quasimonoenergetic. An analysis carried out by Atzeni *et al.* (2002) and by Temporal *et al.* (2002) has shown that ignition of the thermonuclear target with the quasithermal beam of fast protons requires several times larger laser energy. Similarly, in the case of the ion injector, a high-quality beam is needed in order to inject the charged particles into the optimal accelerating phase. Bulanov and Khoroshkov (2002) and Esirkepov, Nishihara, *et al.* (2002) have shown that such a beam of laser-accelerated ions can be obtained by using a double-layer target. Multilayer targets have been used for a long time in order to increase the efficiency of the laser energy conversion into plasma and fast-particle kinetic energy (see, for example, Badziak *et al.*, 2001, 2003). In contrast to the previously discussed configurations, the use of a double-layer target was proposed in order to produce fast proton beams with controlled quality. In this scheme the target is made of two layers with ions of different electric charge and mass. Its sketch is shown in Fig. 34(a). The first (front) layer consists of heavy ions with electric charge  $eZ_i$  and mass  $m_i$ . This is followed by a second (rear) thin proton layer. The transverse size of the proton layer must be smaller than the size of the pulse waist since an inhomogeneity in the laser pulse causes an inhomogeneity of the accelerating electric field and thus a degradation of beam quality, as

<sup>7</sup>See, for example, Gurevich *et al.*, 1966, 1972; Gitomer *et al.*, 1986; Denavit, 1992; Esirkepov *et al.*, 1999; Bulanov *et al.*, 2000; Sentoku *et al.*, 2000; Ueshima *et al.*, 2000; Kuznetsov *et al.*, 2001; Pukhov, 2001; Ruhl *et al.*, 2001; Mackinnon *et al.*, 2002; Sentoku *et al.*, 2002; Kovalev and Bychenkov, 2003; Mora, 2003; Passoni *et al.*, 2004.

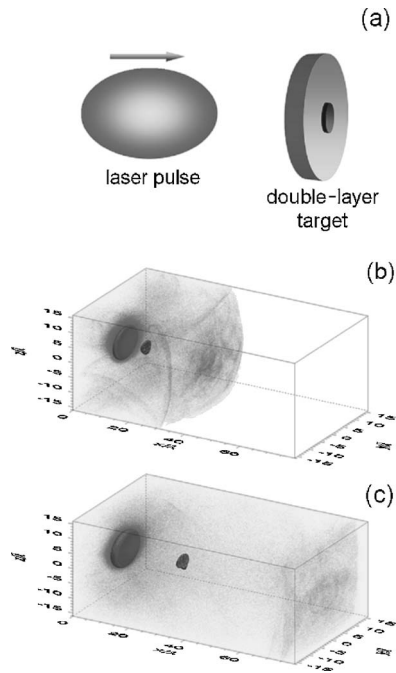


FIG. 34. High-quality proton beam generation. (a) Sketch of the double-layer target. Distribution of the electric charge inside the computation region at (b)  $t=40$  and at (c)  $t=80$ .

seen in experiments in which targets exposed to the laser light had a thin proton layer on their surface.

When an ultrashort laser pulse irradiates the target, heavy atoms are partly ionized and ionized electrons abandon the foil, generating an electric field due to charge separation. Because of the large value of the ratio  $\mu/Z_i$ , where  $\mu=m_i/m_p$ , heavy ions remain at rest while lighter protons are accelerated. In order to achieve  $10^{10}$  fast protons per pulse from the two-layer target required for the applications, it is enough to have a proton layer approximately  $0.02 \mu\text{m}$  thick and a laser pulse focused onto a spot with diameter equal to two laser wavelengths. The first layer is made of heavy ions and the target is sufficiently thick so as to produce a large enough electric field due to charge separation. This electric field has opposite sign on the two different sides of the target, has a zero inside the target, and vanishes at a finite distance. The number of protons is assumed to be sufficiently small so as not to produce any significant effect on the electric field. The most important requirement is that the transverse size of the proton layer be smaller than the pulse waist so as to decrease the influence of the laser pulse inhomogeneity in the direction perpendicular to propagation. The pulse inhomogeneity causes an inhomogeneity of the accelerating electric field, which results in an additional energy spread of the ion beam seen in experiments. The effect of the finite waist of the laser pulse also leads to an undesirable defocusing of the fast ion beam. In order to compensate for this effect and to focus the ion beam, we can use deformed targets, as suggested by Bulanov *et al.* (2000), Ruhl *et al.* (2001), and Wilks *et al.* (2001).

In order to estimate the typical energy gain of fast ions, we assume that many free electrons produced by ionization in the irradiated region of the foil are expelled. In this case the electric field near the positively charged layer is equal to  $E_0 \approx 2\pi n_0 Z_i e l$ , where  $l$  is the foil thickness. The region of strong electric field has a transverse size of the order of the diameter  $2R_\perp$  of the focal spot. Thus the longitudinal size of this region where the electric field remains essentially one dimensional is also of order  $2R_\perp$  and the typical energy of the ions accelerated by the electric field due to charge separation can be estimated as  $\Delta E_{\text{max}} \approx 4\pi n_0 Z_a e^2 l R_\perp$ .

The energy spectrum of protons can be found by taking the electric field in the vicinity of the target to be of the form of the electric field near an electrically charged prolate ellipsoid (see Landau and Lifshitz, 1984). On the axis the  $x$  component of the electric field is given by

$$E_x(x) = \frac{4E_0}{3} \frac{R_\perp^2}{R_\perp^2 - l^2 + x^2}. \quad (92)$$

The distribution function of fast protons  $f(x, v, t)$  obeys the kinetic equation, which gives  $f(x, v, t) = f_0(x_0, v_0)$ , where  $f_0(x_0, v_0)$  is the distribution function at the initial time  $t=0$ . The number of particles per unit volume in phase space  $dx dv$  is  $dn = f dx dv = f v dv dt = f dE dt / m_p$ . We assume that at  $t=0$  all particles are at rest, i.e., their spatial distribution is given by  $f_0(x_0, v_0) = n_0(x_0) \delta(v_0)$ , with  $\delta(v_0)$  the Dirac delta function. Time integration of the distribution  $f v dv dt$  gives the energy spectrum of the beam  $N(E) dE = [n_0(x_0) / m_p] |dt/dv|_{v=v_0} dE$ . Here the Lagrange coordinate of the particle  $x_0$  and the Jacobian  $|dt/dv|_{v=v_0}$  are functions of the particle energy  $E$ . The Lagrange coordinate dependence on the energy  $x_0(E)$  is given implicitly by the integral of the particle motion:  $E(x, x_0) = E_0 + e[\varphi(x) - \varphi(x_0)]$ , with  $\varphi(x)$  the electrostatic potential. In the case under consideration, we have  $E_0 = 0$  and  $x = \infty$ . The Jacobian  $|dt/dv|_{v=v_0}$  is equal to the inverse of particle acceleration at  $t=0$ , i.e.,  $|dt/dv|_{v=v_0} = 1/eE_x(x_0)$ , and equal to  $|dx_0/dE|$ . Hence we obtain the expression for the energy spectrum

$$N(E) dE = \left[ n_0(x_0) \left| \frac{dx_0}{dE} \right| \right]_{x_0=x_0(E)} dE. \quad (93)$$

We note that this expression follows from the general condition of particle flux continuity in phase space.

As we can see, in the vicinity of the target on the axis the electric field is homogeneous. Therefore the form of the energy spectrum (93) is determined by the distribution of the proton density  $n_0[\varphi^{-1}(E)/e]$ . We see that, in general, a highly monoenergetic proton beam can be obtained when the function  $n_0(x_0)$  is a strongly localized function, i.e., when the thickness of the proton layer  $\Delta x_0$  is sufficiently small.

Here we discuss the possibility of ion acceleration, e.g., to that needed for the hadron therapy energy above 200 MeV using high-repetition-rate, moderate-intensity lasers. The regime of high-quality proton beam acceleration presented above requires a high enough laser pulse

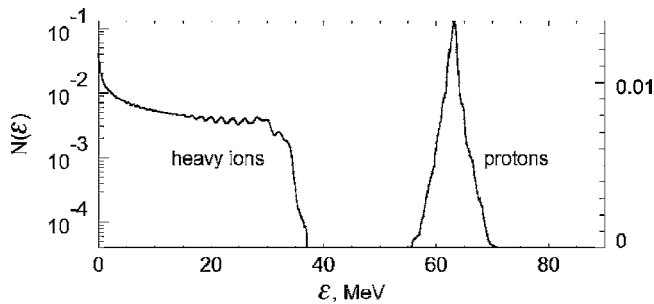


FIG. 35. The proton and the heavy-ion energy spectrum at  $t = 80$ .

intensity. The electric field in the laser pulse,  $E_{\text{las}} = \sqrt{4\pi I}/c$ , in order to expel almost all the electrons from the focus region must be larger than the electric field that is formed due to the electric charge separation  $E_0 \approx 2\pi en_0 Z_i I$ . Using the expression for the fast proton energy  $E_p \approx eE_0 R_{\perp}$ , we find a relationship between the proton energy and the laser power  $P_{\text{las}} = \pi R_{\perp}^2 I$  which reads  $E_p = \sqrt{4e^2 P_{\text{las}}}/c$ . In addition, the electron energy must be equal to or greater than the proton energy. In the optimal regime electrons are accelerated by the laser pulse up to the energy  $E_e \approx m_e c^2 a_0^2/2 \equiv (m_e c^2/2)(eE_{\text{las}}\lambda/2\pi m_e c^2)^2$ . The acceleration length of electrons  $l_{\text{acc}} \approx a_0 \lambda/2\pi$  should be of the order of  $R_{\perp}$ . Using these relations, we find the laser pulse power to be  $P_{\text{las}} = \pi I \lambda^2/4\pi^2 = (m_e^2 c^5/e^2) a_0^4/4 \approx 10(a_0^4/4)$  GW. We see that for the proton energy  $E_p \approx 200$  MeV one needs the laser power to be about 1.6 PW, i.e., a laser of the petawatt range.

In order to take into account the numerous nonlinear and kinetic effects as well as to extend consideration to multidimensional geometry, Esirkepov, Bulanov, *et al.* (2002) performed numerical simulations of the proton acceleration during the interaction of a short, high-power laser pulse with a two-layer target. In Figs. 34 and 35 we present the results of these simulations for a linearly polarized laser pulse with dimensionless laser amplitude  $a = 30$  interacting with a double-layer target. The first layer of the target (gold) has the form of a disk with diameter  $10\lambda$  and thickness  $0.5\lambda$ . The second layer (proton) also has the form of a disk with diameter  $5\lambda$  and thickness  $0.03\lambda$  and is placed at the rear of the first layer. The electron density in the heavy-ion layer corresponds to the ratio  $\omega_{pe}/\omega = 3$  between the plasma and the laser frequencies. For the proton layer it corresponds to  $\omega_{pe}/\omega = 0.53$ . The number of electrons in the first layer is 180 times larger than in the proton layer.

In Fig. 34 we show the densities of the plasma species inside the computation box at time  $t = 40$  (b) and  $t = 80$  (c). We see that the proton layer moves along the  $x$  axis and that the distance between the two layers increases. The heavy-ion layer expands due to Coulomb explosion and tends to become rounded. Part of the electrons are blown off by the laser pulse, while the rest form a hot cloud around the target. We notice that for the simulation parameters electrons do not completely abandon

the region irradiated by the laser light. Even if only a portion of the electrons are accelerated and heated by the laser pulse, the induced quasistatic electric field appears to be strong enough to accelerate the protons up to 65 MeV. The energy per nucleon acquired by the heavy ions is approximately 100 times smaller than the proton energy. In Fig. 35 we present the spectra of the proton energy and the energy per nucleon of the heavy ions. As can be seen, heavy ions have a wide energy spectrum while protons form a quasimonoenergetic bunch with  $\Delta E/E < 3\%$ . The proton beam remains localized in space for a while due to the bunching effect of the decreasing dependence of the electric field on the coordinate in the acceleration direction. The experimental proof of this ion acceleration mechanism is done by Schworer *et al.* (2006).

A regime of ion acceleration that exhibits very favorable properties has been identified by Bulanov *et al.* (2004), Esirkepov, Borghesi, *et al.* (2004), and Esirkepov, Bulanov, *et al.* (2004). In this regime the radiation pressure of the electromagnetic wave plays a dominant role in the interaction of an ultraintense laser pulse with a foil. In this radiation pressure dominant regime ion acceleration appears due to the radiation pressure of the laser light on the electron component with momentum transferred to ions through the electric field arising from charge separation. In this regime the proton component moves forward with almost the same velocity as the average longitudinal velocity of the electron component. Thus the proton kinetic energy is well above that of the electron component. In addition, in the radiation pressure dominant regime the ion acceleration mechanism is found to be highly efficient, and, as we shall explicitly show, the ion energy per nucleon is proportional to the laser-pulse energy. The main results of three-dimensional PIC simulations are shown in Fig. 36.

In this version of the numerical simulations, a linearly polarized laser pulse interacts with a thin film. The pulse is assumed to be Gaussian, with effective dimensions  $10\lambda_0 \times 10\lambda_0 \times 10\lambda_0$  and amplitude  $a_0 = 316$ . This amplitude corresponds to a pulse intensity of  $1.37 \times 10^{23}$  W/cm<sup>2</sup> at the wavelength  $\lambda_0 = 1$   $\mu\text{m}$ , in which case electrons in the wave are ultrarelativistic. The thickness of the foil is equal to  $l_0 = \lambda_0/4$ , and its density is 16 times the critical density  $n_0 = 16n_{\text{cr}}$ . The foil interacting with the laser pulse becomes deformed and changes into a “cocoon,” which in turn traps the electromagnetic wave [see Figs. 36(a) and 36(b)]. The leading edge of the cocoon moves at a relativistic speed. As a result of this process, a plasma layer with overcritical density and moving at nearly the speed of light interacts with the electromagnetic wave and reflects it. In other words, the electromagnetic radiation is reflected from a relativistic mirror. In the laboratory frame  $L$ , the electromagnetic pulse and the mirror move in the same direction. We denote the propagation velocity of the relativistic mirror by  $V$  and make the Lorentz transformation to the frame of reference  $M$  in which the mirror is at rest in the  $x' = 0$  plane. The time and coordinate  $(t', x')$  in the comov-

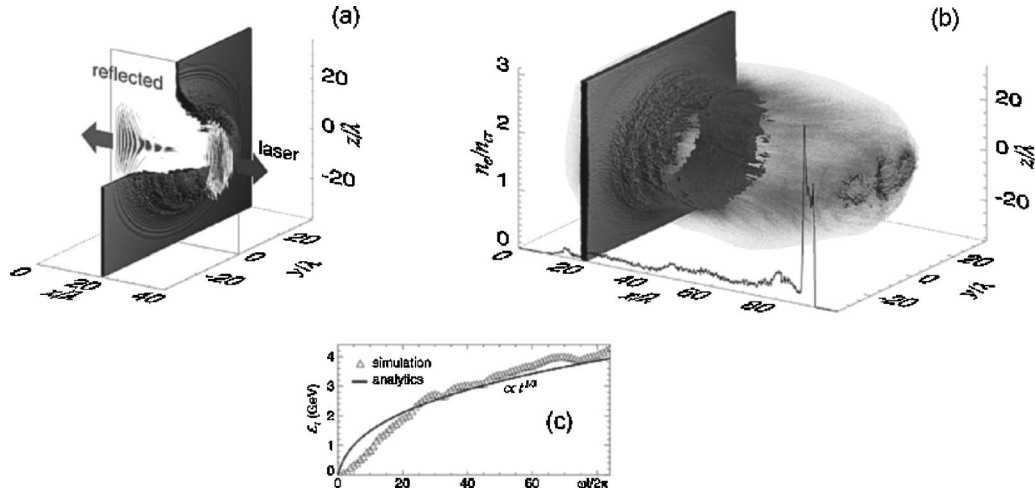


FIG. 36. High efficiency ion acceleration in the radiation pressure dominant (RPD) regime. (a) The ion density isosurface (a quarter removed to reveal the interior) and the  $x$  component of the normalized Poynting vector at  $t=40$ . (b) The isosurface of the ion density at  $t=100$ ; the black curve shows the ion density along the laser pulse axis. (c) The maximum ion kinetic energy vs time.

ing frame  $M$  are related to the time and coordinate  $(t, x)$  in the laboratory frame  $L$  by  $x' = \gamma_M(x - Vt)$  and  $t' = \gamma_M(t - Vx/c^2)$ , where  $\gamma_M = 1/\sqrt{1 - \beta_M^2}$  and  $\beta_M = V/c$ . In the comoving frame  $M$ , the wave frequency is  $\omega' = \omega_0 \sqrt{(1 - \beta_M)/(1 + \beta_M)} \approx \omega_0/2\gamma_M$ . In this frame the plasma density is higher than the critical density and the thickness of the plasma layer is larger than the collisionless skin depth. Thus the wave is totally reflected by the mirror with the resulting frequency seen in the laboratory frame of reference  $\omega'' \approx \omega_0/4\gamma_M^2$ . This is seen in Fig. 36(a) in the cross section of the Poynting vector where the thickness of the red stripes, corresponding to half of the radiation wavelength, increases from left to right (along the  $x$  axis).

In the Lorentz transformation to the comoving frame  $M$ , the electric field in the wave transforms according to the law  $E' = E_0(\omega'/\omega_0)$ . Consequently, the pressure (the force per unit area of the mirror) is  $E_0^2[(1 - \beta_M)/(1 + \beta_M)]$ . This pressure is relativistically invariant (Pauli, 1981) and the equation of motion of the leading edge of the cocoon in the laboratory frame  $L$  can be represented by

$$\frac{dp_{\parallel}}{dt} = \frac{E_0^2[t - x(t)/c] \sqrt{m_e^2 c^2 + p_{\parallel}^2} - p_{\parallel}}{2\pi n_0 l \sqrt{m_e^2 c^2 + p_{\parallel}^2}},$$

$$\frac{dx}{dt} = c \frac{p_{\parallel}}{\sqrt{m_e^2 c^2 + p_{\parallel}^2}}. \quad (94)$$

The solution of Eq. (94) for a constant laser-pulse amplitude can be cast in the form  $3p_{\parallel} + 2[p_{\parallel}^3 + (m_e^2 c^2 + p_{\parallel}^2)^{3/2}]/m_e^2 c^2 = 3E_0^2 t/2\pi n_0 l + C$ , where the constant  $C$  is determined by the initial condition. Asymptotically, as  $t \rightarrow \infty$ , the electron momentum grows as  $p_{\parallel} \approx (3E_0^2 t/4\pi n_0 l)^{1/3}$ , which is seen in Fig. 36(c). To find an upper limit for the energy  $E_p$  acquired by a proton after interacting with a finite-length laser pulse, i.e., with a finite-energy laser pulse  $E_{\text{las}}$ , we must take into account

the dependence of the laser radiation intensity on time  $t$  and coordinates  $x$ . We assume the pulse form to be a function of time and write  $w_0(\psi) = E_0^2(\psi)/2\pi n_0 l_0$ . We use the variables  $\psi = t - x/c$  and  $\tau = \int_{-\infty}^{\psi} w_0(\psi') d\psi' / m_p c$  and write the ion equation of motion in the form  $dp_{\parallel}/d\tau = m_p c \sqrt{m_p^2 c^2 + p_{\parallel}^2} / (\sqrt{m_p^2 c^2 + p_{\parallel}^2} + p_{\parallel})$ . Its solution for the initial condition  $p(\tau \rightarrow -\infty) = 0$  reads  $p = m_p c \tau(\tau + 2)/2(\tau + 1)$ . For a finite-length laser pulse the function  $\tau(\psi)$  tends to  $\tau_m = \int_{-\infty}^{+\infty} w_0(\psi') d\psi' / m_p c$ , which is proportional to the laser-pulse fluence. We obtain the maximum value of the fast proton momentum equal to  $p_m \approx m_p c \tau_m/2$ , i.e.,  $p_m \approx m_p c a_0^2 (\omega_0/\omega_{pe})^2 (m_e/m_p) L/l_0$ , where  $L$  is the laser-pulse length. We can rewrite this expression as a relationship between the final energy of fast protons  $E_p$  and the laser-pulse energy  $E_{\text{las}}$ :  $E_p = E_{\text{las}}/N$ , with  $N$  the total number of accelerated protons. For example, 1 MJ laser pulse can accelerate  $10^{14}$  protons up to energy of the order of 160 GeV per particle.

Esirkepov, Bulanov, *et al.* (2004) have noted that since the energy of the resulting ion bunch can be over 100 GeV per nucleon, this ion acceleration regime is suitable for quark-gluon plasma studies (see Ludlam and McLerran, 2003). In the paper by Bulanov *et al.* (2005), this regime was discussed in connection with an application to the investigation of neutrino oscillations.

## B. Laser-produced pions and muons

At much higher intensities,  $10^{23}$  W/cm<sup>2</sup>, 15 fs duration, a PIC simulation performed by Pukhov (2003) shows that the interaction with a 50- $\mu\text{m}$  solid target, with an electron density of  $n = 10^{22}$  cm<sup>3</sup>, leads to an electron beam of 5 GeV followed by a proton beam of 5 GeV. Let us note that the electrostatic field gradients involved are of the order of the laser transverse field gradients of 500 TeV/m at  $10^{23}$  W/cm<sup>2</sup>.

Bychenkov, Rozmus, *et al.* (2001) and Bychenkov, Sentoku, *et al.* (2001) carried out two-dimensional

particle-in-cell modeling to determine the laser intensity threshold for pion production by protons accelerated by the relativistically strong short laser pulses acting on a solid target. The pion production yield was determined as a function of laser intensity. It was shown that the threshold corresponds to the laser intensity above  $10^{21}$  W/cm<sup>2</sup>.

The pion has a rest mass of  $\sim 140$  MeV and a lifetime at rest of only 20 ns. This short lifetime prevents the acceleration of the low-energy pions since

$$\pi^+ \rightarrow \mu^+ + \nu_\mu. \quad (95)$$

At a 10 MeV/m acceleration, pions will disintegrate before they reach a significant energy. Prompt acceleration offers a completely new paradigm for high-energy physics. Over a distance of the order of only a millimeter pions can be accelerated to many times their mass, say 100 times (Bychenkov, Rozmus, *et al.*, 2001). At 15 GeV pions will have a lifetime of 2  $\mu$ s and can then be injected and accelerated to much higher energies using conventional means. At these energies in the laboratory frame the disintegration product, muons and neutrinos, will be emitted in a narrow cone angle of  $1/\gamma$  half angle. This represents an attractive new paradigm for a  $\mu$ - $\mu$  collider or the generation of neutrino beams that would avoid muon cooling. Pakhomov (2002) and Bulanov *et al.* (2005) have considered laser generation of controlled, high-flux pulses of neutrinos. The source will yield nanosecond-range pulses of muon neutrinos, with fluxes of  $\sim 10^{19}$   $\nu_\mu$  s<sup>-1</sup> sr<sup>-1</sup> and energies of  $\sim 20$  MeV or higher. The process assumes a driving laser with pulse energy  $\sim 8$  kJ, providing an irradiance of  $\sim 9 \times 10^{22}$  W/cm<sup>2</sup>. The study of neutrino oscillations would be a possible application of such a collider.

### C. Colliders

The next frontier in high-energy physics is the interaction at TeV center-of-mass energy. In this regime the electroweak symmetry is broken and is expected to reveal the microphysical meaning of mass and reach the limit of the standard model. To reach this regime, the Large Hadron Collider (LHC) (proton-proton) is being built at CERN. Parallel to this effort, there is also a strong motivation to build a lepton collider ( $e$ - $e$  or muon-muon) or a photon collider ( $\gamma$ - $\gamma$ ). Leptons, i.e., electrons and muons, have no structure, unlike hadrons (protons, neutrons, etc.). Therefore their interaction is clean and predictable, producing particles that can be unambiguously determined.

In this new high-energy physics adventure, ultrahigh intensity lasers may play an important role. They have the potential

- (1) to provide large field gradients,
- (2) to provide an efficient way to increase unstable particle lifetimes which are needed to make a muon-muon collider or neutrino beam,

- (3) to provide an efficient source of high-energy  $\gamma$  particles making possible a  $\gamma$ - $\gamma$  collider.

### 1. Laser-based colliders

In order to reduce the size (and possibly the cost) and/or to increase the final energy of particles, the high laser-induced accelerating gradient has been considered as a possible collider prospect.

The first such serious consideration may be found in the analysis by Xie *et al.* (1997). In this work all the known conditions required for achieving ultrahigh energy beyond the current linear collider energy frontier (such as 5 TeV) were incorporated. It is well known that for a collider to produce high-energy physics results (particularly that of particle physics), it needs to have not only sufficient energy but also sufficient luminosity so that enough relevant events may be observed in a given time. The number of events is given by  $\sigma L$ , where  $\sigma$  is the relevant event cross section and  $L$  the luminosity is defined as  $N^2 f/A$ , with  $N$ ,  $f$ , and  $A$  the number of particles in colliding bunches, the repetition rate of bunches, and the bunch cross section at collision point, respectively. Since  $\sigma$  is generally decreasing sharply as a function of energy  $E$  (in fact  $E^{-2}$  for high energies, except for resonances), the luminosity has to be increased proportionally to  $E^2$  for a fixed number of events in a given time (say a year, for example). This luminosity requirement is sometimes called the luminosity paradigm (of colliders). If one does not want to increase the total energy contained in bunches (i.e., power)  $NEf$ , in order to increase to increase the luminosity, one has to reduce the bunch cross section, for example. This, however, runs into some other collider conditions such as various beam instabilities.

Xie *et al.* (1997) showed the general strategy for optimizing collider design for ultrahigh energies. For example, one needs multiple stages of acceleration [and thus multiple stages of lasers aligned with spatial and temporal control (Chiu *et al.*, 2000; Cheshkov *et al.*, 2001)]. Such strategy generally calls for lasers of high efficiency, high fluence, high controllability much beyond what current solid-state laser technology allows, and substantial research and development of laser technology to meet those requirements. Ruth (1998) opted to use free-electron lasers (FEL) as the laser driver (the so-called two beam accelerator). A group at SLAC (Barnes *et al.*, 2002; Colby, 2002) is also designing a laser-based collider (without the use of gas).

We now comment on luminosity limitations in experiments on high-energy or fundamental physics. Contemporary high-energy collider experiments are driven by the desire to look at rarer events and ever smaller spatial volumes, requiring high luminosity. If instead one's desire is to investigate a violation of the Lorentz invariance (Sato, 2001) when the energy of the photon becomes large (perhaps PeV), the experiment needed is not luminosity dictated but mainly dictated by the energy itself (and the observable signal detectability of the particular process associated with their phenomenon,

such as the  $\gamma$  decay in a vacuum). For such a class of experiments, what we need is to accelerate particles to extremely high energies even though the number of such particles may be quite small. One notices that such experiments, though repeatable and entirely plausible, resemble the high-energy cosmic observation. In the latter, one would look for particles of extreme high energies (say  $10^{20}$  eV= $10^5$  PeV over an area as large as  $100 \times 100$  km<sup>2</sup> over more than a year). Other examples include a possible test of general relativity, such as the equivalence principle and some of its consequences. We address these in Sec. X.

The  $e$ - $e$  collider cannot exceed the TeV regime because of radiative effects known as beamsstrahlung. This effect scales inversely as the fourth power of the lepton mass and seriously impairs  $e$ - $e$  collider luminosity beyond the TeV level. The lightest lepton is the electron so one way to circumvent this limit is to choose the next lightest lepton, the muon, with a rest mass energy of 104 MeV or 200 times the electron mass. In a muon collider the beamsstrahlung would therefore be attenuated by almost ten orders of magnitude and completely eliminated. As seen earlier, Eq. (104), muons as well as neutrinos are produced by the decay of pions. Pions can be produced by the interaction of high-energy protons beam with a metallic target. As mentioned earlier, laser acceleration can accelerate pions to many times their mass in a fraction of a millimeter. This mass increase will be accompanied by a lifetime dilatation making it possible to inject pions into a conventional accelerator. Let us mention an additional expected benefit. As observed in a laser-accelerated electron beam, a prompt acceleration will produce a low emittance (high-quality) beam.

## 2. Increasing the $\tau$ -lepton lifetime

It is interesting to see that the next lepton observed will be the tau with a mass of 1784 MeV and a lifetime of 300 fs. Note that 300 fs corresponds to 100  $\mu$ m, a very short distance for conventional acceleration. This distance would in principle be sufficient for prompt acceleration of a  $\tau$  lepton to several times its mass and thus would increase its lifetime accordingly.

## 3. Photon-photon collider or $\gamma$ - $\gamma$ collider

The photon-photon collider is very complementary to the lepton collider. It is considered the best tool for addressing and discovering new physics: Higgs physics, extra dimensions, supersymmetry, and the top quark. In a photon collision any charged particles can be produced,

$$\gamma\gamma \rightarrow \text{Higgs}, \quad WW, \quad ZZ, \quad t\bar{t}. \quad (96)$$

The cross sections for pairs are significantly higher than in a  $e^+e^-$  collisions. The  $\gamma$ - $\gamma$  collider relies on the scattering of photons from a high-intensity laser by a super-relativistic electron beam. After scattering, photons have an energy close to the electron energy, as shown in

Eq. (97) below. The efficiency is excellent with one electron scattering one  $\gamma$  photon. The photon beams after focusing correspond approximately to the electron beam size.

The maximum energy of the scattered photons is

$$\hbar\omega_m = \frac{x}{x+1}E_0, \quad \text{with } x \approx \frac{E_0\hbar\omega_0}{m^2c^4} \text{ or } 19 \left[ \frac{E_0}{\text{TeV}} \right] \frac{\mu\text{m}}{\lambda}, \quad (97)$$

where  $E_0$  is the electron beam energy and  $\omega_0$  is the laser frequency.

These are additional meeting points of laser and high-energy charged particles. In some of these applications one can probe nonlinear QED (see Sec. XI) while others can yield large amounts of high-energy  $\gamma$ -gamma photons through the inverse Compton scattering process useful for high-energy and nuclear physics (Fujiwara, 2005). Tajima (2002) has suggested this process for realizing a possible nuclear transmutation (in combination with efficient lasers such as the free-electron laser; Minehara, 2002).

## IX. ASTROPHYSICS

The extreme magnitude of the accelerating gradient (and therefore the very short accelerating length) needed to reach ultrahigh energies is a unique feature of the acceleration mechanism associated with a laser. Because of this feature, it has been recognized that this mechanism (the wakefield excitation) is pivotal in the generation of ultrahigh-energy cosmic rays (Chen *et al.*, 2002). The recent observation of ultrahigh-energy cosmic rays indicates that cosmic rays exist beyond  $10^{20}$  eV and certainly beyond  $10^{19}$  eV [energies greater than the GZK cutoff (Greisen, 1966; Zatsepin and Kuzmin, 1966) due to the pionization loss of protons that decay by collision with cosmic microwave background photons]. This observation puts severe requirements on the acceleration mechanisms that have been proposed.

Ultrahigh-energy cosmic-ray events exceeding the Greisen-Zatsepin-Kuzmin cutoff ( $5 \times 10^{19}$  eV for protons originating from a distance larger than  $\sim 50$  Mps) have been found in recent years (Bird *et al.*, 1993; Hayashida *et al.*, 1994; Takeda *et al.*, 1998; Abu-Zayyad *et al.*, 1999). Observations also indicate a change of the power-law index in the ultrahigh-energy cosmic-ray spectrum [(events/energy)/(area/time)],  $f(E) \propto E^{-\alpha}$ , from  $\alpha \sim 3$  to a smaller value at energy around  $10^{18}$ - $10^{19}$  eV. These present an acute theoretical challenge regarding their composition as well as their origin (Olinto, 2000).

So far theories that attempt to explain the ultrahigh-energy cosmic rays can be largely categorized into the “top-down” and “bottom-up” scenarios. In addition to relying on exotic particle physics beyond the standard model, the main challenges of top-down scenarios are their difficulty complying with observed event rates and energy spectrum and the fine-tuning of particle lifetimes.

The main challenges of bottom-up scenarios, on the other hand, are the Greisen-Zatsepin-Kuzmin cutoff, as well as the lack of an efficient acceleration mechanism (Olinto, 2000). To circumvent the Greisen-Zatsepin-Kuzmin limit, several authors propose the “Z-burst” scenario (Weiler, 1999) in which neutrinos, instead of protons, are the actual messenger across the cosmos. For such a scenario to work, the original particle, say a proton, must be several orders of magnitude more energetic than the one that eventually reaches the Earth.

Even if the Greisen-Zatsepin-Kuzmin limit can be circumvented through the Z-burst scenario, the challenge for a viable acceleration mechanism remains. This is mainly because the existing paradigm for cosmic acceleration, namely, the Fermi mechanism (Fermi, 1949) and its variants, such as the diffusive shock acceleration (Krymsky, 1977; Axford *et al.*, 1978; Bell, 1978; Blandford and Osriker, 1978; Berezhinskii *et al.*, 1990; Achterberg *et al.*, 2001), are not effective in reaching ultrahigh energies (Achterberg, 1990). These acceleration mechanisms rely on the random collisions of high-energy particles against magnetic-field domains or the shock media, which induce severe energy losses at higher particle energies.

According to the conversion theory of protons  $\rightarrow$  neutrinos  $\rightarrow$  protons via Z bursts (Weiler, 1999), high-energy particles propagate through the cosmological distance as neutrinos and thus avoid pionization decay by photon collisions. They reach our galactic cluster and interact with gravitationally bound cosmic relic neutrinos. This theory allows sources of ultrahigh-energy cosmic rays to exist at cosmological distances. This is a much more likely possibility than finding sources in our own galactic cluster.

Nearly all astrophysical acceleration mechanisms for the bottom-up scenario have been based on the Fermi mechanism (Fermi, 1949) or its variants. Regardless of their details, all acceleration mechanisms based on the Fermi mechanism or its variants resort to momentum scattering by “collisions” with magnetic fields or other particles or fields. In ultrahigh energies such momentum scattering causes severe radiative energy losses even if scattered particles are protons in the regime beyond  $10^{19}$  eV. Chen *et al.* (2002) proposed that immense magnetic shocks created in the atmosphere of gamma-ray bursts can give rise to the excitation of large wakefields. These wakefields in the relativistically flowing plasma have properties that are convenient for ultrahigh-energy cosmic-ray generation. The wakefield, predominantly a longitudinal field, is Lorentz invariant. Thus even extreme high-energy particles (such as protons) see the same accelerating gradient, unlike transverse fields which decay as  $1/\gamma^2$ , where  $\gamma \geq O(10^{11})$ . The wakefields in the gamma-ray burst atmosphere amount to  $10^{16}$  eV/cm. The large rate of the gamma flux in this atmosphere causes collisional acceleration (the Eddington acceleration), which amounts to the value of Schwinger field. This is a part of the mechanism that constitutes the spectrum of gamma rays in the burst (Takahashi *et al.*, 2002). Another important feature of wake-

field acceleration in the gamma-ray burst atmosphere is their parallel directionality in successive acceleration. Even though the phase encounter of particles and wakefields is random and deceleration and acceleration are both possible, there are no overall momentum collisions as required in the Fermi mechanism. Thus the accumulation of stochastic momentum gain is possible for the wakefields (Chen *et al.*, 2002).

The laboratory laser acceleration, much more moderate in comparison with the gamma ray bursts, will demonstrate the fundamental properties of wakefield acceleration in ultrahigh-energy cosmic rays. In addition, this mechanism may be responsible for the electron acceleration in the jets of blazars. From blazars (Punch *et al.*, 1992) we observe very-high-energy gamma rays with a double-humped energy spectrum in which the higher energy is from the bremsstrahlung of high-energy electrons, while the lower one from synchrotron radiation from electrons in the magnetic field in the jet. The typical energy of gamma rays and thus that of high-energy electrons is on the order of TeV. If the central engine of the blazar, a massive galactic black hole, emits highly collimated high-energy electrons (and positrons), it is likely that the eruption of these jet particles accompanies disruptions (or modulations) of the electron (and positron) beam. Thus the lumpy electron beam carries large-amplitude plasma wakes, wakefields driven by the electron beam which can accelerate electrons in the jet plasma to high energies if they are trapped on such plasma waves. The energy gain of a trapped electron is typically  $\Gamma_p m_e c^2$ , where  $\Gamma_p$  is the Lorentz factor of the jet flow. Often the jet is seen to have highly relativistic flows with  $\Gamma_p$  as large as  $10^3$ . This amounts to an energy gain of TeV over the wakefield.

An Alfvén wave propagating in a stationary magnetized plasma has a velocity  $v_A = eB_0 / (4\pi m_e n_p)^{1/2}$ , which is typically much less than the speed of light. Here  $B_0$  is the magnetic field and  $n_p$  is the density of the plasma. The relative strength between the transverse field of the Alfvén wave is  $E_A/B_A = v_A/c$ . Although these two field components are unequal, being mutually perpendicular to the direction of propagation, they jointly generate a nonvanishing ponderomotive force that can excite a wakefield in the plasma, with phase velocity  $v_{ph} = v_A \ll c$ . Preliminary results from simulations indicate that such Alfvén waves can indeed excite plasma wakefields (Chen *et al.*, 2003). For ultrahigh-energy acceleration, such a slow wave would not be useful as the accelerating particle can quickly slip out of phase against the wakefield. In the frame where the plasma has a relativistic bulk flow, however, the dephasing length (thus the energy gain) can be enhanced. Furthermore, in this relativistic flow regime the excited wakefields are essentially unidirectional.

For astrophysical problems, the Alfvén-wave-plasma interaction relevant to us is in the nonlinear regime. The nonlinearity of the plasma wakefield is governed by the Lorentz-invariant normalized vector potential  $a_0 = eE/m_e c \omega$  of the driving em wave. When this parameter exceeds unity, nonlinearity is strong so that additional

important physics occurs. In the frame of a stationary plasma, the maximum field amplitude that the plasma wakefield can support is

$$E_{\max} \approx a_0 E_{\text{wb}} = m_e c \omega_p a_0 / c,$$

which is enhanced by a factor  $a_0$  beyond the cold wave-breaking limit, the Tajima-Dawson field  $E_{\text{wb}}$ , of the linear regime. Transform this to a frame of relativistic plasma flow and the cold wave-breaking field is reduced by a factor  $\Gamma_p^{1/2}$ , while  $a_0$  remains unchanged. The maximum “acceleration gradient”  $G$  experienced by a singly-charged particle on this plasma wakefield is

$$G = e E'_{\max} \approx a_0 m_e c^2 (4\pi r_e n_p / \Gamma_p)^{1/2}, \quad (98)$$

where  $r_e$  is the classical electron radius.

We now apply our acceleration mechanism to the problem of ultrahigh-energy cosmic rays. Gamma-ray bursts are the most violent release of energy in the Universe, second only to the big bang itself. Within seconds (for short bursts) about an erg of energy is released through gamma rays with a spectrum that peaks around several hundred keV. Existing models for gamma-ray bursts, such as the relativistic fireball model by Meszaros and Rees (1993), typically assume either neutron-star–neutron-star (NS-NS) coalescence or supermassive star collapse as the progenitor. The latter has been identified as the origin for long-burst gamma rays (with time duration  $\sim 10$ – $100$  s) from recent observations (Price *et al.*, 2002). The origin of short-burst gamma rays, however, is still uncertain, and NS-NS coalescence remains a viable candidate. While both candidate progenitors can in principle accommodate the plasma wakefield acceleration mechanism, the former is taken as an example. Neutron stars are known to be compact [ $R_{\text{ns}} \sim O(10)$  km] and carry intense surface magnetic fields ( $B_{\text{ns}} \sim 10^{12}$  G). Several generic properties are assumed when such compact objects collide. First, the collision creates a sequence of strong magnetoshocks (Alfvén shocks). Second, the tremendous release of energy creates a highly relativistic out-bursting fireball, most likely in the form of a plasma.

The fact that the gamma-ray burst prompt (photon) signals arrive within a brief time window implies that there must exist a threshold condition in the gamma-ray burst atmosphere where the plasma becomes optically transparent beyond some radius  $R_0$  from the NS-NS epicenter. Applying the collision-free threshold condition to the case of out-bursting gamma-ray photons, the optical transparency implies that  $\sigma_C \leq \Gamma_p / n_{p0} R_0$ , where  $\sigma_C \sim 2 \times 10^{-25}$  cm<sup>2</sup> is the Compton scattering cross section for  $\omega_{\text{grb}} \sim m_e c^2 / \hbar$ . Since  $\sigma_{pp} < \sigma_C$ , the ultrahigh-energy cosmic rays are also collision-free in the same environment.

The magnetoshocks are believed to constitute a substantial fraction, say  $\eta_a \sim 10^{-2}$ , of the total energy released from the gamma-ray burst progenitor. The energy Alfvén shocks carry is therefore  $\varepsilon_A \sim 10^{50}$  ergs. Due to the pressure gradient along the radial direction, the magnetic fields in Alfvén shocks that propagate outward from the epicenter will develop sharp discontinuities and

be compacted. The estimated shock thickness is  $\sim O(1)$  m at  $R_0$ (km). From this one can deduce the magnetic-field strength in the Alfvén shocks at  $R_0$ , which gives  $B_A \sim 10^{10}$  G. This leads to  $a_0 = e E_A / m_e \omega_A c$ . Under these assumptions, the acceleration gradient  $G$  is as large as

$$G \sim 10^{16} (a_0 / 10^9) (10^9 \text{ cm} / R_0)^{1/2} \text{ eV/cm}. \quad (99)$$

The wakefield acceleration, as considered above, provides an alternative mechanism to the Fermi acceleration (see Bell, 1978). Thus laboratory laser experiments may serve as a fascinating glimpse into cosmological processes of high-energy acceleration.

## X. ULTRAHIGH INTENSITY AND GENERAL RELATIVITY

The main postulate of general relativity is the Einstein principle of equivalence that states that the effect of a homogeneous gravitational field is equivalent to that of a uniform accelerated reference frame. In the past there have been experiments to test the equivalence principle in its weak limit in the laboratory using neutron beams with a spinning mirror (Bonse and Wroblewski, 1983). With the adoption of strong lasers, we may perhaps be able to test the equivalence principle in its strong limit.

Electrons subjected to a ultrahigh electric field can become relativistic in a time corresponding to a fraction of a femtosecond. In this case, the acceleration experienced by electrons is large and is given by

$$a_e = a_0 \omega c, \quad (100)$$

where  $a_e$  is the electron acceleration and  $\omega$  is the laser frequency. For  $a_0 = 1$ , we find  $a_e = 10^{25}$  g, and for  $a_0 = 10^5$ ,  $a_e = 10^{30}$  g.

This type of acceleration is found near the Schwarzschild radius of a black hole. The acceleration due to black-hole gravity is given by

$$a_e = \frac{GM}{R_s}. \quad (101)$$

Using the gravitational redshift expression at the Swartzschild radius

$$\frac{2GM}{R_s c^2} = 1. \quad (102)$$

An expression for the Swartzschild radius  $R_s$  and circumference  $C_{\text{BH}}$  of the equivalent black hole can be readily found:

$$R_s = \frac{1}{a_0} \frac{\lambda_{\text{laser}}}{2\pi}, \quad (103)$$

$$C_{\text{BH}} = \frac{\lambda_{\text{laser}}}{a_0}. \quad (104)$$

For  $a_0 = 1$ ,  $R_s = \lambda_{\text{laser}} = 1$   $\mu\text{m}$ , and mass  $M \sim M_{\text{Earth}}$ . For  $a_0 = 10^5$ ,  $R_s = 0.1$   $\text{\AA}$ . The black hole being very small will have a very high temperature. The Hawking tempera-

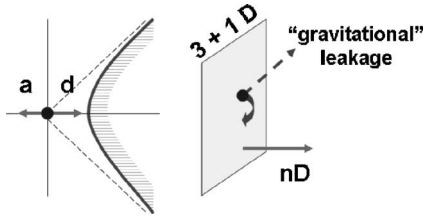


FIG. 37. Finite horizon and leakage of the wave function.

ture is given by the Hawking expression (Hawking, 1974)

$$T = \frac{\hbar c^3}{8\pi kGM}, \quad (105)$$

where we can easily find using Eqs. (101) and (105) the black-hole temperature:

$$kT = \frac{\hbar\omega}{8\pi a_0}. \quad (106)$$

For  $a_0 \sim 1$  the black-hole temperature is of the order of 1 eV or  $10^4$  °C. Note that this temperature is large compared to the 2.7-K cosmic background temperature, making the observation of this type of equivalent black hole observable.

The important point of the equivalence principle is that the effect of gravity is only felt by the particle which is accelerated. The inertial observer does not see the effect. The Unruh radiation (Unruh, 1976) may be the one which breaks this bind (Chen and Tajima, 1999). The signature of Unruh radiation may be buried under the noise of conventional radiation due to particle acceleration, i.e., the Larmor radiation. The ratio of the two is calculated (Chen and Tajima, 1999) as

$$P_U/P_L = \hbar\omega a_0/m_e c^2. \quad (107)$$

This ratio is 1 part in  $10^6$  at an intensity of  $10^{18}$  W/cm<sup>2</sup>. This ratio increases as a function of the square root of the laser intensity. Because of the pattern in radiation and the frequency band difference, it may be possible to observe this signal, according to Chen and Tajima (1999), in sufficiently intense laser regimes.

Let us also point out that large acceleration could lead to a large increase in proton decay as predicted by Ginzburg and Syrovatskii (1965a, 1965b). This process was studied in detail by Vanzella and Matsas (2001).

Another important implication of violent acceleration comes from the shrinking of the distance to the horizon from infinite to finite. The distance to the horizon is given by (Chen and Tajima, 1999)

$$d = c^2/a_e = \lambda/2\pi a_0, \quad (108)$$

using Eq. (100), where  $\lambda$  is the laser wavelength. This distance becomes substantially small for large  $a_0$ . Figure 37 illustrates the finite horizon and leakage of the wave function. The theory of quantum gravity has been recently advanced (Akama, 1983; Rubakov and Shaposhnikov, 1983; Amelino-Camelio *et al.*, 1998; Arkani-Hamed *et al.*, 1999; Arkani-Hamed, Dimopoulos, and

Dvali, 2000; Arkani-Hamed, Dimopoulos, Dvali, and Kaloper, 2000; Giddings and Thomas, 2002; Rubakov, 2003), stating that gravitational effects having extra dimensions could be observed over macrodistances. Our ultraintense lasers could provide a new way to test extra-dimensional effects. It is possible that for a sufficiently intense laser field the distance of the electron to its horizon might become on the order of or smaller than the distance  $r_n$  over which the effects of extra dimensions could be observed. According to the quantum gravity theory of Arkani-Hamed *et al.* (1998, 2002),

$$r_n \sim 10^{32/n-17} \text{ cm}. \quad (109)$$

Here  $n$  is the extra dimension beyond 4. If this is the case we expect that the wave function of the electron may begin to feel the different gravitational law and subsequent consequences for values of  $n$  up to 3 corresponding to  $r \sim 10^{-6}$  cm in Eq. (109). The possibility of exploring quantum gravity represents an exciting opportunity for the ultraintense laser field.

## XI. NONLINEAR QED

In a strong electromagnetic field the vacuum behaves similarly to a birefracting and a medium with a dichroism, i.e., an anisotropic medium (Klein and Nigam, 1964a, 1964b; Heyl and Hernquist, 1997). This has been known for about 70 years, since the papers published by Halpern (1933), Euler (1936), and Heisenberg and Euler (1936). After discovering pulsars and with the emergence of lasers able to generate relativistically strong electromagnetic fields, it has become clear that the effects of vacuum polarization can be observed in the cosmos and under laboratory conditions (see, for example, Ginzburg, 1989). A measure of the electromagnetic-field strength in quantum electrodynamics is given by the field

$$E_{\text{Schw}} = m_e^2 c^3 / e\hbar = 1.3 \times 10^{16} \text{ V/cm}, \quad (110)$$

which is known as the Schwinger critical field. This is the field necessary for the electron to gain an energy corresponding to  $m_e c^2$  over the Compton length  $\lambda_C = \hbar/m_e c$ .

Heisenberg and Euler (1936) obtained the Lagrangian valid for an arbitrarily strong free electromagnetic field. The Heisenberg-Euler Lagrangian contains corrections due to photon-photon scattering mediated by a true exchange of virtual electron-positron pairs. Quantum effects become of the order of  $\alpha = e^2/\hbar c = 1/137$  when the field strength approaches  $E_{\text{Schw}}$ . This Lagrangian has both real and imaginary parts which describe the vacuum polarization and it is exponentially small in the probability limit  $E/E_{\text{Schw}} \ll 1$  of the  $e^-, e^+$  pair creation (see Ritus, 1979; Itzykson and Zubar, 1980; Berestetskii, Lifshitz, and Pitaevskii, 1982). In the limit  $E/E_{\text{Schw}} \ll 1$ , electron-positron pair creation can occur just as a result of quantum tunneling, and its rate is exponentially small,  $W \propto \exp(-\pi E_{\text{Schw}}/E)$ , as follows from the results by

Klein (1929) and Sauter (1931) (see also Krekora *et al.*, 2004). Bunkin and Tugov (1970) and Aleksandrov *et al.* (1985) first attracted attention to the question of whether high-power lasers might provide a new way to approach the critical field  $E_{\text{Schw}}$  to create pairs in a vacuum. Zel'dovich and Popov (1972) studied the problem of pair creation in the Coulomb field of colliding heavy ions with  $Z_1 + Z_2 > 137$ . X-ray lasers were considered for generating a much higher electric field than could be generated in the optical range because of the ability to focus the beam over a tighter spot ( $\sim 0.1$  nm in size; see Zhang *et al.*, 1997; Chen and Pelligrini, 1999; Chen and Tajima, 1999; Melissinos, 1999; Ringwald, 2001; Roberts *et al.*, 2002; Tajima, 2002).

Spontaneous particle creation from a vacuum is one of the most important problems in quantum-field theory. The mechanism of particle-antiparticle pair creation has been applied to various problems that range from black-hole evaporation (Hawking, 1975) to nuclear physics (Fradkin *et al.*, 1985) and particle creation in the Universe (Parker, 1969).

Theoretically, the process of  $e^-, e^+$  pair creation resembles that of tunneling ionization of the atom. Atom ionization achieved by alternating the electric field was considered by Keldysh (1965) and electron-positron pair creation by Brezin and Itzykson (1970). In both cases we discuss the breakdown of either an initially neutral gas or of a vacuum in the alternating electric field. The formalism used to calculate the probability of  $e^-, e^+$  pair creation in a vacuum by the alternating electric field is similar to the formalism developed for the description of ionization by Perelomov, Popov, and Terentiev (1966) (see also Popov, 2001, 2002a, 2002b; Popov and Marinov, 1973; Narozhny and Nikishov, 1974).

In strong laser fields, the vacuum is no longer inert. The vacuum nonlinear susceptibilities appear due to the interaction between two photons via production of virtual  $e^-, e^+$  pairs. An effective Euler-Heisenberg Lagrangian for light-light scattering has been determined for the process  $\gamma + \gamma \rightarrow \gamma + \gamma$  in the limit of a relatively weak electric and magnetic field ( $E/E_{\text{Schw}} \ll 1$  and  $B/B_{\text{Schw}} \ll 1$ ) and is given by  $L = L_0 + L'$ . Here  $L_0$  is the Lagrangian of a free electromagnetic field. It describes the linear electrodynamics of a vacuum.

The nonlinear quantum electrodynamics correction is described by  $L'$  and  $L = L_0 + L'$  has the form

$$L = \frac{1}{16\pi} F_{\alpha\beta} F^{\alpha\beta} - \frac{\kappa}{64\pi} [5(F_{\alpha\beta} F^{\alpha\beta})^2 - 14F_{\alpha\beta} F^{\beta\gamma} F_{\gamma\delta} F^{\delta\mu}] \quad (111)$$

(see Itzykson and Zubar, 1980; Berestetskii, Lifshitz, and Pitaevskii, 1982). Here  $\kappa = e^4 \hbar / 45 \pi m_e^4 c^7$  and  $F_{\alpha\beta} = \partial_\alpha A_\beta - \partial_\beta A_\alpha$  is the four-tensor of the electromagnetic field. A ratio of nonlinear terms to the linear part of the Lagrangian is of the order of  $L'/L_0 \approx 10^{-4} (E/E_{\text{Schw}})^2$ . In the case of the petawatt laser focused onto a spot with a size equal to the laser light wavelength ( $\lambda = 1 \mu\text{m}$ ), the electric field is equal to  $\approx 4.5 \times 10^{12}$  v/cm and  $L'/L_0 \approx 10^{-14}$ .

By finding an extremum of the Hamiltonian function with respect to the variations of the four-potential  $A_\alpha$ , one obtains the usual set of Maxwell's equations with the following material equations:

$$D_i = \varepsilon_{ij} E_j = (\delta_{ij} + \varepsilon'_{ij}) E_j, \quad (112)$$

$$H_i = \mu_{ij} B_j = (\delta_{ij} + \mu'_{ij}) B_j, \quad (113)$$

where

$$\varepsilon'_{ij} = \frac{\kappa}{4\pi} [2(E^2 - B^2)\delta_{ij} + 7B_i B_j], \quad (114)$$

and

$$\mu'_{ij} = \frac{\kappa}{4\pi} [2(E^2 - B^2)\delta_{ij} - 7E_i E_j]. \quad (115)$$

The nonlinear dependence of the vacuum susceptibilities on the electromagnetic-field amplitude results in the birefringence of the vacuum (Klein and Nigam, 1964a, 1964b), in the scattering of light by light (McKenna and Platzman, 1963), Čerenkov radiation in vacuum (Dremin, 2002), photon splitting (Akhmedaliev *et al.*, 2002), in the parametric four-wave processes (Rozanov, 1993), in the soliton formation (Soljacic and Segev, 2000; Shukla *et al.*, 2004), and to the nonlinear phase shift of the counterpropagating electromagnetic waves (Rozanov, 1993, 1998; Andreev, Komarov, *et al.*, 2002; Andreev, Zhidkov, *et al.*, 2002). Klein and Nigam (1964a, 1964b) estimated the Kerr constant of the vacuum to be

$$K = \frac{7}{90\pi} \left( \frac{e^2}{\hbar c} \right)^2 \left( \frac{\hbar}{m_e c} \right)^3 \frac{1}{m_e c^2 \lambda}. \quad (116)$$

Here  $\lambda$  is the wavelength of the electromagnetic wave. The Kerr constant in the vacuum for  $\lambda = 1 \mu\text{m}$  is of the order of  $10^{-27}$  cm<sup>2</sup>/erg, which is a factor  $\approx 10^{20}$  smaller than for water. Above we used a definition of the Kerr constant when the refraction index  $n$  dependence on the electric field is given by  $n = n_0 + \lambda K |E|^2$ .

The Kerr nonlinearity results in the limit of moderate intensity to the self-focusing of the laser light propagating in media. As shown by Rozanov (1993), in a QED nonlinear vacuum two counterpropagating electromagnetic waves mutually focus each other. The critical power  $P_c = cE^2 d^2 / 4\pi$ , where  $d$  is the laser beam waist, for the mutual self-focusing can be found by using Eq. (116). We obtain  $P_c = (90/28) c E_{\text{Schw}}^2 \lambda^2 / \alpha$ . For  $\lambda \approx 1 \mu\text{m}$  it yields  $P_c \approx 2.5 \times 10^{24}$  W. Within the framework of the relativistic engineering concept, we have demonstrated (Bulanov, Esirkepov, and Tajima, 2003) that the wavelength of the laser pulse, which has been reflected and focused at the wake plasma wave, becomes shorter by a factor  $4\gamma_{\text{ph}}^2$  and its power increases by a factor  $2\gamma_{\text{ph}}$ . From this it follows that nonlinear QED vacuum polarization effects are expected to be observable for 50 PW 1- $\mu\text{m}$  lasers.

As is known (see Berestetskii, Lifshitz, and Pitaevskii, 1982), the Lagrangian  $L'$  has an exponentially small imaginary part, which corresponds to electron-positron pair creation in vacuum.

In 1951, Julian Schwinger calculated in detail the probability of the process when a static electric field breaks down a vacuum to produce  $e^-$ ,  $e^+$  pairs:

$$W = \frac{c}{4\pi^3 l_c^4} \left( \frac{E}{E_{\text{Schw}}} \right)^2 \sum_{n=1}^{\infty} \frac{1}{n^2} \exp\left(-\frac{\pi n E_{\text{Schw}}}{E}\right). \quad (117)$$

It reaches its optimal value at  $E/E_{\text{Schw}} \approx 1$  approximately equal to  $c/\lambda_c^4 \approx 10^{53} \text{ cm}^{-3} \text{ s}^{-1}$ .

According to Brezin and Itzykson (1970) the transition probability per unit time to spontaneously produce pairs is given by

$$W \approx \frac{c}{4\pi^3 l_c^4} \begin{cases} \frac{\pi a_0}{2 \ln(4/a_0)} \left( \frac{\hbar\omega}{m_e c^2} \right)^2 \left( \frac{e a_0}{4} \right)^{4m_e c^2/\hbar\omega}, & a_0 \ll 1 \\ \left( \frac{E}{E_{\text{Schw}}} \right)^2 \exp\left(-\frac{\pi E_{\text{Schw}}}{E}\right), & a_0 \gg 1. \end{cases} \quad (118)$$

The nonlinear corrections to Maxwell equations (112)–(115) depend on two scalar Poincaré invariants of the field:  $B^2 - E^2 = \text{inv}$  and  $\mathbf{E} \cdot \mathbf{B} = \text{inv}$ . It means that no pairs are produced in the field of a plane wave. The counterpropagating waves indeed have nonzero Lorentz invariants and the pairs can be generated. In the field produced by focused laser beams there are also regions near the focus where  $E^2 \neq B^2$  (see Bunkin and Tugov, 1970; Melissinos, 1998; Ringwald, 2001). Electron-positron pair production from a vacuum in an electromagnetic field created by two counterpropagating focused laser pulses interacting with each other has been analyzed by Narozhny *et al.* (2004a). It has been shown that  $e^+e^-$  pair production can be experimentally observed when the intensity of each beam is  $I \sim 10^{26} \text{ W/cm}^2$ , which is two orders of magnitude lower than that for a single pulse (see Narozhny *et al.*, 2004b).

We see that the presence of high-energy electrons acts as a catalyst for spontaneous pair creation by the laser, while also providing the necessary energy-momentum balance. A standing wave field, for which  $E \neq 0$  but  $B = 0$ , can lead to pair creation without the need of a catalyst provided  $E \geq E_{\text{Schw}}$ . The probability for  $a_0 \geq 1$  is given by Eq. (128) within a factor of order unity. When the field is weak ( $a_0 < 1$ ), the probability increases rapidly as the field intensity increases toward the critical field, as shown by Eq. (128). When it exceeds the critical field, however, the quantum effect sets in and the probability is exponentially suppressed. When we consider radiation (synchrotron radiation) with a high-energy electron beam, it is customary to introduce a dimensionless parameter  $Y$ , the beamsstrahlung parameter, to describe pair creation due to the collision between electron (with Lorentz factor  $\gamma$ ) and field (often created by the other beam) as

$$Y = \gamma E / E_{\text{Schw}}. \quad (119)$$

Here if the electron has a large energy ( $\gamma \gg 1$ ), the necessary threshold ( $Y > 1$ ) to create pairs is much lowered:

$$E = E_{\text{Schw}} / \gamma. \quad (120)$$

In a collider application the beamsstrahlung is related to the beam parameters as

$$Y = \frac{5r_e^2 \gamma N}{6\alpha \sigma \sigma_z (\sigma_x + \sigma_y)}. \quad (121)$$

Because of threshold lowering, the collider can be corrupted by copious pair generation as  $Y$  approaches unity. On the other hand, if  $Y$  becomes large, the conditions might improve (Xie *et al.*, 1997). This is because the number of photons generated from an  $e^-e^+$  collision in the large- $Y$  regime scales as

$$n_\gamma \propto Y^{-1/3}. \quad (122)$$

However, in a real collision, there is an overlap of the tails that makes the value of  $Y$  at that portion of the beams of order unity, which causes a substantial emission of photons. In the case of a hard photon turning into an  $e^-e^+$  pair in an external field, the rate of such pair production is

$$\frac{dn}{dt} = \frac{\alpha m_e}{\omega} \begin{cases} 0.23 \exp(-8/3\Omega), & \Omega \ll 1 \\ 0.38\Omega^{2/3}, & \Omega \gg 1, \end{cases} \quad (123)$$

where  $\Omega = Y\hbar\omega/m_e c^2 \gamma$ . In this case the total energy of the produced pair is equal to that of the initial photon. This process has been called the “stimulated” process by Chen and Pellegrini (1999).

$e^-e^+$  pair creation was already observed in a scattering experiment of high-energy electrons by intense lasers (Bula *et al.*, 1996; Burke *et al.*, 1997; Bamber *et al.*, 1999). In these references, measurements of quantum electrodynamic processes in an intense electromagnetic wave, where nonlinear effects (both multiphoton and vacuum polarization) prevail, were reported. Nonlinear Compton scattering and electron-positron pair production have been observed in collisions of 46.6 and 49.1 GeV electrons in the final focus test beam at SLAC with terawatt pulses of 1053 and 527 nm wavelengths from a Nd:glass laser. Peak laser intensities of  $\approx 5 \times 10^{18} \text{ W/cm}^2$  have been achieved, corresponding to a value of 0.4 for the parameter  $a_0$  and to a value of 0.25 for the parameter  $Y = \gamma E / E_{\text{Schw}}$ . Data are presented on the scattered electron spectra arising from nonlinear Compton scattering with up to four photons absorbed from the field. The observed positron production rate depends on the fifth power of the laser intensity, as expected for a process in which five photons are absorbed from the field. The positrons are interpreted as arising from the collision of a high-energy Compton-scattered photon with the laser beam. The results are found to be in agreement with theoretical predictions.

Tajima (2001) suggested using a high-energy electron ring (such as the Spring-8 accelerator) and a high-intensity laser to provide conditions appropriate for

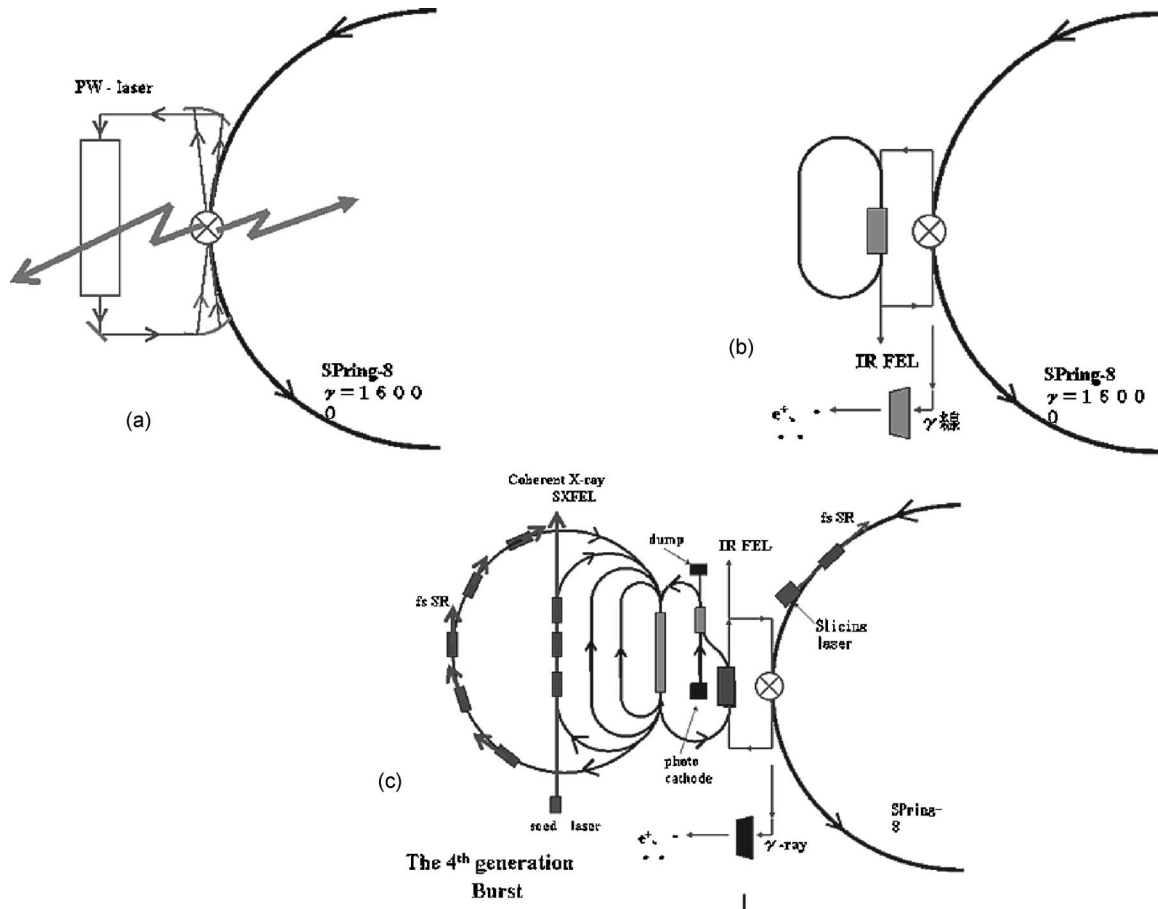


FIG. 38. Use of a high-energy electron ring and a high-intensity laser to provide the conditions appropriate for nonlinear QED experiments.

nonlinear QED experiments. In this case the parameter  $Y$  becomes greater than unity while obtaining a large event number based on a high-repetition-rate laser and ring electron bunches; see Fig. 38(a). This is an example of multiplying the two technologies, the laser and the (conventional) accelerator, as mentioned earlier. In this scheme, if one replaces the high-intensity laser, such as the solid-state Ti:sapphire petawatt laser at APRC-JAERI (Yamakawa *et al.*, 2002), by a high-fluence free-electron laser (in a ring or in a supercavity), one can also obtain a high-fluence  $\gamma$ -ray generator. As an example, a 100- $\mu\text{m}$  free-electron laser turns up  $\gamma$  rays of 10 MeV if scattered off the Spring-8 ring electron (8 GeV) beam; see Fig. 38(b). The scattering of the electron momentum (10 MeV/ $c$ ) barely changes its ring orbit, continuing its circulation. Such  $\gamma$  rays may be of use in photonuclear physics. For example, such a photon interacting with nuclear matter may lead to a new field of investigation which relies on the coupling between weak and strong interactions (Fujiwara *et al.*, 2005). Polarized  $\gamma$  photons may be used to create a large flux of polarized positrons, which may be important in future collider-beam sources to enhance the signal-to-noise ratio of desired events (Omori *et al.*, 2003). Further creative combinations of lasers and electron rings [see Fig. 38(c)] may lead to a brand new generation of light source, such as femtosecond synchrotron x rays and coherent soft x rays.

## XII. CONCLUSIONS

With the possibility of increasing laser intensities to a new height, the field of optics, until now confined to the eV–sub-eV regime, has abruptly moved to the present MeV–GeV and likely TeV regime in the near future. At relativistic intensities the laser-matter interaction is dominated by the relativistic character of the electron and has led to novel applications. In this regime the dynamics are dictated by relativistic dynamics of (essentially) free electrons in rigidly prescribed laser fields, which provide an immense opportunity and controllability. We have described some of these applications in nuclear physics, astrophysics, high-energy physics, general relativity, and nonlinear QED. Relativistic lasers have introduced the possibility that many subdisciplines that we have seen bifurcated may now be woven into an integrated larger field. We have tried to show the parallel between bound-electron nonlinear optics and relativistic optics. We have shown applications in high-energy photon generation, electron and proton acceleration, radioisotope production, and thermonuclear fast ignition. Looking into the future, one of the most intriguing applications of relativistic optics is producing an attosecond laser with reasonable efficiency. This should lead to the generation of pulses with much higher intensities and confirm the unproven rule that the generation of

higher intensities generally leads to shorter pulse duration. If we follow this rule, it suggests that in the next ten years or so we shall be able to approach the Schwinger intensity corresponding to  $10^{30}$  W/cm<sup>2</sup> with pulse duration in the zeptosecond regime. In this case the new non-linear medium will be just a vacuum. Immense technical challenges in controlling the laser and optics lie ahead for such tasks.

We also anticipate that future applications will come from the union between high-energy accelerators and relativistic intensity lasers. By pairing these two technologies we should be able to access unheralded regimes. This could take the scientific community beyond what we currently know. Finally, the large scientific effort in relativistic optics should lead to engineering applications called relativistic engineering, relativistic optoelectronics, or relativistic photonics, in which micrometer-integrated devices driven by well-controlled relativistic lasers will efficiently produce high-energy photons and particles in the attosecond-zeptosecond scale.

#### ACKNOWLEDGMENTS

We are grateful to a number of our colleagues: C. Barty, M. Campbell, A. Chao, S. Chattopadhyay, P. Chen, T. Cowan, T. Ditmire, M. Downer, J. Dunn, E. Esarey, T. Zh. Esirkepov, D. Farina, M. Kando, Y. Kato, M. Key, Y. Kishimoto, J. Koga, K. Ledingham, M. Lontano, C. Ma, K. Mima, K. Nakajima, N. M. Naumova, J. Nees, A. Ogata, F. Pegoraro, R. Pitthan, B. Rau, M. Roth, R. Ruth, I. V. Sokolov, P. Sprangle, Y. Takahashi, H. Takuma, V. V. Telnov, M. Xie, and K. Yamakawa. This work was supported by the National Science Foundation under Grant No. STC PHY-8920108, National Foundation, Frontier of Physics Program FOCUS #PHYS-011 4336.

#### REFERENCES

- Abu-Zayyad, T., *et al.*, 1999, in *Proceedings of the 26th International Cosmic Ray Conference (ICRC)*, Salt Lake City, 1999 (University of Utah, Salt Lake City), Vol. 3, p. 125.
- Achterberg, A., 1990, *Astron. Astrophys.* **231**, 251.
- Achterberg, A., Y. A. Gallant, J. G. Kirk, and A. W. Guthmann, 2001, *Mon. Not. R. Astron. Soc.* **328**, 393.
- Agostini, P., G. Barjot, J. F. Bonnafant, G. Mainfray, and C. Manus, 1968, *IEEE J. Quantum Electron.* **QE-4**, 667.
- Akama, K., 1983, in *Gauge Theory and Gravitation: Proceedings of the International Symposium, Nara, Japan*, Lecture Notes in Physics No. 176, edited by K. Kikkawa, N. Nakanishi, and H. Nariai (Springer-Verlag, Berlin), p. 267.
- Akhiezer, A. I., and R. V. Polovin, 1956, *Sov. Phys. JETP* **30**, 915.
- Akhmadaliev, Sh. Zh., *et al.*, 2002, *Phys. Rev. Lett.* **89**, 061802.
- Albert, O., H. Wang, D. Liu, Z. Chang, and G. Mourou, 2000, *Opt. Lett.* **25**, 1125.
- Albrecht, G., A. Antonetti, and G. Mourou, 1981, *Opt. Commun.* **40**, 59.
- Aleksandrov, E. B., A. A. Ansel'm, and A. N. Moskalev, 1985, *Sov. Phys. JETP* **62**, 680.
- Altucci, C., *et al.*, 1999, *Phys. Rev. A* **61**, 021801(R).
- Amelino-Camelia, G., J. Ellis, N. E. Mavromatos, D. V. Nanopoulos, and S. Sarkar, 1998, *Nature (London)* **393**, 763.
- Amiranoff, F., 2001, *Meas. Sci. Technol.* **12**, 1795.
- Amiranoff, F., S. Baton, D. Bernard, *et al.*, 1998, *Phys. Rev. Lett.* **81**, 995.
- Andreev, A. A., V. M. Komarov, A. V. Charukhev, I. M. Litvinenko, and K. U. Platonov, 2002, *Zh. Eksp. Teor. Fiz.* **121**, 266 [*JETP* **94**, 222 (2002)].
- Andreev, A. A., A. G. Zhidkov, A. Sasaki, and K. Yu. Platonov, 2002, *Plasma Phys. Controlled Fusion* **44**, 1.
- Andreev, N. E., L. M. Gorbunov, V. I. Kirsanov, A. A. Pogosova, and R. R. Ramazashvili, 1992, *Pis'ma Zh. Eksp. Teor. Fiz.* **55**, 551 [*JETP Lett.* **55**, 571 (1992)].
- Antonsen, T., Jr., and P. Mora, 1992, *Phys. Rev. Lett.* **69**, 2204.
- Aoyama, A., J. Ma, Y. Akahane, N. Inoue, H. Ueda, H. Kiriyama, K. Yamakawa, 2002, in *Technical Digest of Conference on Lasers and Electro-Optics (CLEO) 2002* (Optical Society of America), p. 109.
- Apollonov, V. V., A. I. Artem'ev, Y. L. Kalachev, A. M. Prokhorov, and M. V. Fedorov, 1998, *JETP Lett.* **47**, 91.
- Arkani-Hamed, N., S. Dimopoulos, and G. Dvali, 1998, *Phys. Lett. B* **429**, 263.
- Arkani-Hamed, N., S. Dimopoulos, and G. Dvali, 1999, *Phys. Rev. D* **59**, 086004.
- Arkani-Hamed, N., S. Dimopoulos, and G. Dvali, 2000, *Sci. Am. (Int. Ed.)* **283** (8), 62.
- Arkani-Hamed, N., S. Dimopoulos, and G. Dvali, 2002, *Phys. Today* **55** (2), 35.
- Arkani-Hamed, N., S. Dimopoulos, G. Dvali, and N. Kaloper, 2000, *Phys. Rev. Lett.* **84**, 586.
- Arutyunian, F. R., and V. A. Tumanian, 1963, *Phys. Lett.* **4**, 176.
- Ashour-Abdalla, M., J. N. Leboeuf, T. Tajima, J. M. Dawson, and C. F. Kennel, 1981, *Phys. Rev. A* **23**, 1906.
- Askar'yan, G. A., 1962, *Sov. Phys. JETP* **15**, 8.
- Askar'yan, G. A., and S. V. Bulanov, 1983, *Sov. Tech. Phys. Lett.* **9**, 533.
- Askar'yan, G. A., S. V. Bulanov, F. Pegoraro, and A. M. Pukhov, 1994, *JETP Lett.* **60**, 251.
- Askar'yan, G. A., S. V. Bulanov, F. Pegoraro, and A. M. Pukhov, 1995, *Comments Plasma Phys. Controlled Fusion* **17**, 35.
- Askar'yan, G. A., M. S. Rabinovich, A. D. Smirnova, and V. B. Studenov, 1967, *JETP Lett.* **5**, 93.
- Assamagan, K. A., W. W. Buck, S.-Y. Chen, R. Ent, R. N. Green, P. Gueye, C. Keppel, G. Mourou, D. Umstadter, and R. Wagner, 1999, *Nucl. Instrum. Methods Phys. Res. A* **438**, 265.
- Atzeni, S., 1999, *Phys. Plasmas* **6**, 3316.
- Atzeni, S., M. Temporal, and J. J. Honrubia, 2002, *Nucl. Fusion* **42**, L1.
- Auston, D. H., 1971, *Opt. Commun.* **3**, 272.
- Axford, W. I., E. Leer, and G. Skadron, 1978, in *15th International Cosmic Ray Conference*, Plovdiv, Bulgaria, 1977 (B'lgarska Akademiia na Naukite, Sofia), Vol. 11, pp. 132–137.
- Backus, S., C. Durfee, G. Mourou, H. C. Kapteyn, and M. M. Murnane, 1997, *Opt. Lett.* **22**, 1256.
- Backus, S., C. G. Durfee III, M. Murnane, and H. G. Kapteyn, 1998, *Rev. Sci. Instrum.* **69**, 1207.
- Backus, S., H. C. Kapteyn, M. M. Murnane, D. M. Gold, H. Nathel, and W. White, 1993, *Opt. Lett.* **18**, 134.

- Badziak, J., H. Hora, E. Woryna, J. Jablonski, L. Laska, P. Parys, K. Rohlena, and J. Wolowski, 2003, *Phys. Lett. A* **315**, 452.
- Badziak, J., E. Woryna, P. Parys, K. Y. Platanov, S. Jablonski, L. Ryć, A. B. Vankov, and J. Wolowski, 2001, *Phys. Rev. Lett.* **87**, 215001.
- Bahk, S.-W., *et al.*, 2004, *Opt. Lett.* **29**, 2837.
- Bakunov, M. I., V. B. Gildenburg, Y. Nishida, and N. Yugami, 2001, *Phys. Plasmas* **8**, 2987.
- Baltuska, A., *et al.*, 2003, *Nature (London)* **421**, 611.
- Bamber, C., *et al.*, 1999, *Phys. Rev. D* **60**, 092004.
- Banerjee, S., S. Sepke, R. Shah, A. Valenzuela, A. Maksimchuk, and D. Umstadter, 2005, *Phys. Rev. Lett.* **95**, 035004.
- Barnes, C. D., E. C. Colby, and T. Plettner, 2002, in *Advanced Accelerator Concepts: Tenth Workshop*, edited by C. E. Clayton and P. Muggli, AIP Conf. Proc. No. 647 (AIP, Melville, NY), p. 294.
- Barnes, D. C., T. Kurki-Suonio, and T. Tajima, 1987, *IEEE Trans. Plasma Sci.* **PS-15**, 154.
- Barty, C. P. J., C. L. Gordon III, and B. E. Lemoff, 1994, *Opt. Lett.* **19**, 1442.
- Barut, A. O., 1980, *Electrodynamics and Classical Theory of Fields and Particles* (Dover, New York).
- Bass, M., P. A. Franken, J. F. Ward, and G. Weinreich, 1962, *Phys. Rev. Lett.* **9**, 446.
- Bauer, D., R. Salomaa, and P. Mulser, 1998, *Phys. Rev. E* **58**, 2436.
- Bayer, R., 2002, private communication.
- Beaud, P., M. Richardson, E. Miesak, and B. T. Chai, 1993, *Opt. Lett.* **18**, 1550.
- Beg, F., A. R. Bell, A. E. Dangor, C. N. Danson, A. P. Fews, M. E. Glinsky, B. A. Hammel, P. Lee, P. A. Norreys, and M. Tatarakis, 1997, *Phys. Plasmas* **4**, 447.
- Bell, A. R., 1978, *Mon. Not. R. Astron. Soc.* **182**, 147.
- Bell, A. R., 1994, *Phys. Plasmas* **1**, 1643.
- Berestetskii, V. B., E. M. Lifshitz, and L. P. Pitaevskii, 1982, *Quantum Electrodynamics* (Pergamon, New York).
- Berezhiani, V. I., S. M. Mahajan, and N. L. Shatashvili, 1997, *Phys. Rev. E* **55**, 995.
- Berezhiani, V. I., and I. G. Murusidze, 1990, *Phys. Lett. A* **148**, 338.
- Berezinskii, V. S., S. V. Bulanov, V. A. Dogiel, V. L. Ginzburg, and V. S. Ptuskin, 1990, *Astrophysics of Cosmic Rays* (Elsevier, Amsterdam).
- Bespalov, V. I., and V. I. Talanov, 1966, *JETP Lett.* **3**, 307.
- Bestle, J., V. M. Akulin, and W. P. Schleich, 1993, *Phys. Rev. A* **48**, 746.
- Bingham, R., 1994, *Nature (London)* **368**, 496.
- Bingham, R., J. T. Mendonça, and P. K. Shukla, 2004, *Plasma Phys. Controlled Fusion* **46**, R1.
- Bird, D., *et al.*, 1993, *Phys. Rev. Lett.* **71**, 3401.
- Blandford, R. D., and J. P. Ostriker, 1978, *Astrophys. J., Lett. Ed.* **221**, L29.
- Bloembergen, N., 1965, *Nonlinear Optics* (Addison-Wesley, Reading, MA).
- Bloembergen, N., 1974, *IEEE J. Quantum Electron.* **10**, 375.
- Bloembergen, N., and P. Lallemand, 1966, *Phys. Rev. Lett.* **16**, 81.
- Bonse, U., and T. Wroblewski, 1983, *Phys. Rev. Lett.* **51**, 1401.
- Borghesi, M., S. Bulanov, *et al.*, 2002, *Phys. Rev. Lett.* **88**, 135002.
- Borghesi, M., D. H. Campbell, *et al.*, 2002, *Phys. Plasmas* **9**, 2214.
- Borghesi, M., A. Mackinnon, and D. H. Campbell, 2004, *Phys. Rev. Lett.* **92**, 055003.
- Borghesi, M., A. Mackinnon, R. Gaillard, O. Will, A. Pukhov, and J. Meyer-ter-vehn, 1998, *Phys. Rev. Lett.* **80**, 5137.
- Borghesi, M., *et al.*, 2005, *Phys. Rev. Lett.* **94**, 195003.
- Borisov, A. B., A. V. Borovskiv, O. B. Shiryaev, V. V. Korobkin, A. M. Prokhorov, J. C. Solem, T. S. Luk, K. Boryer, and C. K. Rhodes, 1992, *Phys. Rev. A* **45**, 5830.
- Born, M., and E. Wolf, 1964, *Principles of Optics* (Pergamon, New York).
- Bourdier, A., 1983, *Phys. Fluids* **26**, 1804.
- Boyd, R. W., 1992, *Nonlinear Optics* (Academic, San Diego).
- Brabec, T., and F. Krausz, 2000, *Rev. Mod. Phys.* **72**, 545.
- Brezin, E., and C. Itzykson, 1970, *Phys. Rev. D* **2**, 1191.
- Brunel, F., 1987, *Phys. Rev. Lett.* **59**, 52.
- Budker, G. I., 1956, *Atomic Energy* **1**, 673.
- Bula, C., K. T. McDonald, E. I. Prebys, *et al.*, 1996, *Phys. Rev. Lett.* **76**, 3116.
- Bulanov, S. V., F. Califano, *et al.*, 2001, in *Reviews of Plasma Physics*, edited by V. D. Shafranov (Kluwer Academic, Plenum, New York), Vol. 22, p. 227.
- Bulanov, S. V., T. Esirkepov, J. Koga, and T. Tajima, 2004, *Plasma Phys. Rep.* **30**, 196.
- Bulanov, S. V., T. Esirkepov, P. Migliozzi, F. Pegoraro, T. Tajima, and F. Terranova, 2005, *Nucl. Instrum. Methods Phys. Res. A* **540**, 25.
- Bulanov, S. V., T. Zh. Esirkepov, F. Califano, *et al.*, 2000, *JETP Lett.* **71**, 407.
- Bulanov, S. V., T. Zh. Esirkepov, N. M. Naumova, F. Pegoraro, and V. A. Vshivkov, 1999, *Phys. Rev. Lett.* **82**, 3440.
- Bulanov, S. V., T. Zh. Esirkepov, N. M. Naumova, and I. V. Sokolov, 2003, *Phys. Rev. E* **67**, 016405.
- Bulanov, S. V., T. Zh. Esirkepov, and T. Tajima, 2003, *Phys. Rev. Lett.* **91**, 085001; **92**, 159901(E) (2004).
- Bulanov, S. V., I. N. Inovenkov, V. I. Kirsanov, N. M. Naumova, and A. S. Sakharov, 1992, *Phys. Fluids B* **4**, 1935.
- Bulanov, S. V., I. N. Inovenkov, V. I. Kirsanov, *et al.*, 1991, *Bull. Lebedev Phys. Inst.* **6**, 9.
- Bulanov, S. V., and V. S. Khoroshkov, 2002, *Plasma Phys. Rep.* **28**, 453.
- Bulanov, S. V., V. I. Kirsanov, and A. S. Sakharov, 1989, *JETP Lett.* **50**, 176.
- Bulanov, S. V., M. Lotano, T. Zh. Esirkepov, F. Pegoraro, and A. M. Pukhov, 1996, *Phys. Rev. Lett.* **76**, 3562.
- Bulanov, S. V., A. Macchi, and F. Pegoraro, 1998, *Phys. Lett. A* **245**, 439.
- Bulanov, S. V., N. M. Naumova, and F. Pegoraro, 1994, *Phys. Plasmas* **1**, 745.
- Bulanov, S. V., N. M. Naumova, F. Pegoraro, and J.-I. Sakai, 1998, *Phys. Rev. E* **58**, R5257.
- Bulanov, S. V., F. Pegoraro, A. M. Pukhov, and A. S. Sakharov, 1997, *Phys. Rev. Lett.* **78**, 4205.
- Bulanov, S. V., and A. S. Sakharov, 1991, *JETP Lett.* **54**, 203.
- Bulanov, S. V., and T. Tajima, 2005, *J. Part. Accel. Soc. Jpn.* **2**, 35.
- Bulanov, S. V., M. Yamagiwa, T. Zh. Esirkepov, *et al.*, 2005, *Phys. Plasmas* **12**, 073103.
- Bunkenburg, J., *et al.*, 1985, *IEEE J. Quantum Electron.* **QE-17**, 1620.
- Bunkin, F. V., and I. I. Tugov, 1970, *Sov. Phys. Dokl.* **14**, 678.
- Burger, S., K. Bongs, S. Dettmer, W. Ertmer, K. Sengstock, A. Sanpera, G. V. Shlyapnikov, and M. Lewenstein, 1999, *Phys. Rev. Lett.* **83**, 5198.

- Burke, D. L., *et al.*, 1997, *Phys. Rev. Lett.* **79**, 1626.
- Burnett, K., M. Edwards, and C. W. Clark, 1999, *Phys. Today* **52** (12), 37.
- Bychenkov, V. Yu., W. Rozmus, A. Maksimchuk, D. Umstadter, and C. E. Capjack, 2001, *Plasma Phys. Rep.* **27**, 1017.
- Bychenkov, V. Yu., Y. Sentoku, S. V. Bulanov, K. Mima, G. Mourou, and S. V. Tolokonnikov, 2001, *JETP Lett.* **74**, 664.
- Bychenkov, V. Yu., V. P. Silin, and V. T. Tikhonchuk, 1990, *Sov. Phys. JETP* **71**, 79.
- Califano, F., N. Attico, F. Pegoraro, G. Bertin, and S. V. Bulanov, 2001, *Phys. Rev. Lett.* **86**, 5293.
- Carman, R. L., R. F. Benjamin, and C. K. Rhodes, 1981, *Phys. Rev. A* **24**, 2649.
- Cattani, F., A. Kim, D. Andersson, and M. Lisak, 2000, *Phys. Rev. E* **62**, 1234.
- Chandrasekhar, S., 1961, *Hydrodynamic and Hydromagnetic Stability* (Cambridge University Press, Cambridge, England).
- Chao, A., R. Pitthan, T. Tajima, and D. Yermian, 2003, *Phys. Rev. ST Accel. Beams* **6**, 024201.
- Chen, P., and C. Pellegrini, 1999, in *Proceedings of the 15th Advanced ICFA Beam Dynamics Workshop on Quantum Aspects of Beam Physics*, Monterey, CA, 1998, edited by P. Chen (World Scientific, Singapore), p. 571.
- Chen, P., and T. Tajima, 1999, *Phys. Rev. Lett.* **83**, 256.
- Chen, P., T. Tajima, and Y. Takahashi, 2002, *Phys. Rev. Lett.* **89**, 161101.
- Chen, S.-Y., M. Krishnan, A. Maksimchuk, *et al.*, 1999, *Phys. Plasmas* **6**, 4739.
- Chen, S.-Y., A. Maksimchuk, and D. Umstadter, 1998, *Nature (London)* **396**, 653.
- Chen, S.-Y., G. S. Sarkisov, A. Maksimchuk, *et al.*, 1998, *Phys. Rev. Lett.* **80**, 2610.
- Cherepenin, V. A., and V. V. Kulagin, 2004, *Phys. Lett. A* **321**, 103.
- Cheriaux, G., P. Rousseau, F. Salin, *et al.*, 1996, *Opt. Lett.* **21**, 414.
- Cheshkov, S., T. Tajima, W. Horton, and K. Yokoya, 2001, *Phys. Rev. ST Accel. Beams* **3**, 071301.
- Chessa, P., and P. Mora, 1998, *Phys. Plasmas* **5**, 3451.
- Chian, A. C.-L., 1981, *Phys. Rev. A* **24**, 2773.
- Chiao, R. Y., 1993, *Phys. Rev. A* **48**, R34.
- Chiao, R. Y., E. Garmire, and C. H. Townes, 1964, *Phys. Rev. Lett.* **13**, 479.
- Chiao, R. Y., C. H. Townes, and B. P. Stoicheff, 1964, *Phys. Rev. Lett.* **12**, 592.
- Chirila, C. C., *et al.*, 2002, *Phys. Rev. A* **66**, 063411.
- Chiu, C., S. Cheshkov, and T. Tajima, 2000, *Phys. Rev. ST Accel. Beams* **3**, 101301.
- Clark, E. L., K. Krushelnick, J. R. Davies, *et al.*, 2000, *Phys. Rev. Lett.* **84**, 670.
- Clark, E. L., K. Krushelnick, M. Zepf, F. N. Beg, M. Tatarakis, A. Machacek, M. I. Santala, I. Watts, P. A. Norreys, and A. E. Dangor, 2000, *Phys. Rev. Lett.* **85**, 1654.
- Clayton, C. E., K. A. Marsh, A. Dyson, M. Everett, A. Lal, W. P. Leemans, R. Williams, and C. Joshi, 1993, *Phys. Rev. Lett.* **70**, 37.
- Colby, E. R., 2002, in *Advanced Accelerator Concepts: Tenth Workshop*, edited by C. E. Clayton and P. Muggli, AIP Conf. Proc., No. 647 (AIP, Melville, NY), p. 39.
- Collier, J., C. Hernandez-Gomez, I. N. Ross, P. Matousek, C. N. Danson, and J. Walczak, 1999, *Appl. Opt.* **38**, 7486.
- Collier, J. L., *et al.*, 2004, unpublished.
- Corkum, P., 1993, *Phys. Rev. Lett.* **71**, 1994.
- Cowan, T. E., *et al.*, 2000a, in *High Field Science*, edited by T. Tajima, K. Mima, and H. Baldis (Kluwer, New York), p. 145.
- Cowan, T. E., *et al.*, 2000b, *Nucl. Instrum. Methods Phys. Res. A* **445**, 130.
- Cowan, T. E., *et al.*, 2000c, *Phys. Rev. Lett.* **84**, 903.
- Daido, H., F. Miki, K. Mima, *et al.*, 1986, *Phys. Rev. Lett.* **56**, 846.
- Dalla, S., and M. Lontano, 1994, *Phys. Rev. E* **49**, R1819.
- Darmanyan, S., A. Kamchatnov, and F. Lederer, 1998, *Phys. Rev. E* **58**, R4120.
- Davydovskii, V. Ya., 1963, *Sov. Phys. JETP* **16**, 629.
- Dawson, J. M., 1959, *Phys. Rev.* **113**, 383.
- Dawson, J. M., and A. T. Lin, 1984, in *Basic Plasma Physics*, edited by M. N. Rosenbluth and R. Z. Sagdeev (North-Holland, Amsterdam), Vol. 2, p. 555.
- Denavit, J., 1992, *Phys. Rev. Lett.* **69**, 3052.
- Dias, J. M., N. C. Lopes, L. O. Silva, G. Figueira, and J. T. Mendonca, 2002, *Phys. Rev. E* **65**, 036404.
- Dietrich, P., N. H. Burnett, M. Ivanov, and P. B. Corkum, 1994, *Phys. Rev. A* **50**, R3585.
- Disdier, L., J. P. Garconnet, G. Malka, and J. L. Miquel, 1999, *Phys. Rev. Lett.* **82**, 1454.
- Ditmire, T., T. Donnelly, A. M. Rubenchik, R. W. Falcone, and M. D. Perry, 1996, *Phys. Rev. A* **53**, 3379.
- Ditmire, T., and M. D. Perry, 1993, *Opt. Lett.* **18**, 426.
- Ditmire, T., R. A. Smith, J. W. G. Tisch, and M. H. R. Hutchinson, 1997, *Phys. Rev. Lett.* **78**, 3121.
- Ditmire, T., E. Springate, J. W. G. Tisch, *et al.*, 1998, *Phys. Rev. A* **57**, 369.
- Ditmire, T., J. W. G. Tisch, E. Springate, M. B. Mason, *et al.*, 1997, *Nature (London)* **386**, 54.
- Ditmire, T., J. Zweiback, V. P. Yanovsky, *et al.*, 1999, *Nature (London)* **398**, 6727.
- Ditmire, T., J. Zweiback, V. P. Yanovsky, *et al.*, 2000, *Phys. Plasmas* **7**, 1993.
- Doumy, G., F. Quere, O. Gobert, *et al.*, 2004, *Phys. Rev. E* **69**, 026402.
- Drake, J. F., Y. C. Lee, K. Nishikawa, and N. L. Tsingzadze, 1976, *Phys. Rev. Lett.* **36**, p. 196.
- Dremin, I. M., 2002, *JETP Lett.* **76**, 151.
- Dromley, B., S. Kar, M. Zepf, and P. S. Foster, 2003, *Central Laser Facility Annual Report, RAL*, unpublished, p. 76.
- Dubietis, A., G. Jonusauskas, and A. Piskarskas, 1992, *Opt. Commun.* **88**, 437.
- Dudnikova, G. I., V. Yu. Bychenkov, A. Maksimchuk, *et al.*, 2003, *Phys. Rev. E* **67**, 026416.
- D'yachenko, V. F., and V. S. Imshennik, 1979, *Sov. J. Plasma Phys.* **5**, 413.
- Eberly, J., 1969, *Prog. Opt.* **7**, 361.
- Eloy, M., R. Azambuja, J. T. Mendonca, and R. Bingham, 2001, *Phys. Plasmas* **8**, 1084.
- Endoh, A., M. Watanabe, N. Sarukura, and S. Watanabe, 1989, *Opt. Lett.* **14**, 353.
- Esarey, E., and M. Pilloff, 1995, *Phys. Plasmas* **2**, 1432.
- Esarey, E., C. B. Schroeder, W. Leemans, and B. Hafizi, 1999, *Phys. Plasmas* **6**, 2262.
- Esirkepov, T. Zh., 2001, *Comput. Phys. Commun.* **135**, 144.
- Esirkepov, T., M. Borghesi, S. V. Bulanov, G. Mourou, and T. Tajima, 2004, *Phys. Rev. Lett.* **92**, 175003.
- Esirkepov, T. Zh., S. Bulanov, H. Daido, Y. Kato, V. S. Khoroshkov, Y. Kitagawa, K. Mima, K. Nagai, K. Nishihara, S. Sakabe, F. Pegoraro, and T. Tajima, 2002, *Phys. Rev. Lett.* **89**, 175003.

- Esirkepov, T. Zh., S. V. Bulanov, K. Nishihara, and T. Tajima, 2004, *Phys. Rev. Lett.* **92**, 255001.
- Esirkepov, T. Zh., F. F. Kamenets, *et al.*, 1998, *JETP Lett.* **68**, 36.
- Esirkepov, T. Zh., K. Nishihara, S. V. Bulanov, and F. Pegoraro, 2002, *Phys. Rev. Lett.* **89**, 275002.
- Esirkepov, T. Zh., F. Sentoku, F. Califano, *et al.*, 1999, *JETP Lett.* **70**, 82.
- Euler, H., 1936, *Ann. Phys.* **26**, 398.
- Farina, D., and S. V. Bulanov, 2001, *Phys. Rev. Lett.* **86**, 5289.
- Farina, D., and S. V. Bulanov, 2005, *Plasma Phys. Controlled Fusion* **47**, A73.
- Farina, D., *et al.*, 2000, *Phys. Rev. E* **62**, 4146.
- Faure, J., *et al.*, 2004, *Nature (London)* **431**, 541.
- Fedorov, M. V., and A. M. Movsesian, 1989, *J. Opt. Soc. Am. B* **6**, 928.
- Feldman, J. E., and R. Y. Chiao, 1971, *Phys. Rev. A* **4**, 352.
- Fermi, E., 1949, *Phys. Rev.* **75**, 1169.
- Fisher, D. L., and T. Tajima, 1993, *Phys. Rev. Lett.* **71**, 4338.
- Forsslund, D. W., J. M. Kindel, W. Mori, *et al.*, 1985, *Phys. Rev. Lett.* **54**, 558.
- Fourkal, E., J. S. Li, W. Xiong, *et al.*, 2003, *Phys. Med. Biol.* **48**, 3977.
- Fourkal, E., B. Shahine, M. Ding, J. S. Li, T. Tajima, and C.-M. Ma, 2002, *Med. Phys.* **29**, 2788.
- Fradkin, D., 1980, *Phys. Rev. D* **22**, 1018.
- Fradkin, E. S., D. M. Gitman, and Sh. M. Shvartsman, 1985, *Quantum Electrodynamics with Unstable Vacuum* (Springer-Verlag, Berlin).
- Franken, P. A., A. Hill, C. Peters, and G. Weinreich, 1961, *Phys. Rev. Lett.* **7**, 118.
- Fritzier, S., Z. Najmudin, V. Malka, *et al.*, 2002, *Phys. Rev. Lett.* **89**, 165004.
- Fuchs, J., J. C. Adam, F. Amiranoff, *et al.*, 1997, *Phys. Rev. Lett.* **80**, 2326.
- Fuchs, J., G. Malka, J. C. Adam, *et al.*, 1998, *Phys. Rev. Lett.* **80**, 1658.
- Fujiwara, M., *et al.*, 2005, in *Exotic Nuclear Systems*, edited by Z. Gasci, Zs. Dombardi, and A. Krasznahorkay, AIP Conf. Proc. No. 802 (AIP, Melville, NY), p. 246.
- Fukuda, Y., K. Yamakawa, Y. Akahane, *et al.*, 2003, *Phys. Rev. A* **67**, 061201.
- Gahn, C., *et al.*, 2000, *Appl. Phys. Lett.* **77**, 2662.
- Geddes, C. G. R., 2004, *Nature (London)* **431**, 538.
- Gerstein, J. I., and N. Tzoar, 1975, *Phys. Rev. Lett.* **35**, 934.
- Gibbon, P., 1996, *Phys. Rev. Lett.* **76**, 50.
- Gibbon, P., and E. Förster, 1996, *Plasma Phys. Controlled Fusion* **38**, 769.
- Gibbon, P., P. Monot, T. August, and G. Mainfray, 1995, *Phys. Plasmas* **2**, 1304.
- Giddings, S. B., and S. Thomas, 2002, *Phys. Rev. D* **65**, 056010.
- Ginzburg, V. L., 1964, *The Propagation of Electromagnetic Waves in Plasmas* (Pergamon, New York).
- Ginzburg, V. L., 1989, *Applications of Electrodynamics in Theoretical Physics and Astrophysics* (Gordon and Breach, New York).
- Ginzburg, V. L., and S. I. Syrovatskii, 1965a, *Cosmic Magnetobremsstrahlung (Synchrotron Radiation)*, in *Annu. Rev. Astron. Astrophys.* **3**, 297.
- Ginzburg, V. L., and S. I. Syrovatskii, 1965b, *Usp. Fiz. Nauk* **87**, 65.
- Gitomer, S. G., R. D. Jones, F. Begay, *et al.*, 1986, *Phys. Fluids* **29**, 2679.
- Giulietti, D., L. A. Ghizzi, A. Giulietti, *et al.*, 1997, *Phys. Rev. Lett.* **79**, 3194.
- Gold, D. M., H. Nathel, P. R. Bolton, W. E. White, and L. D. V. Woerkom, 1991, *Proc. SPIE* **1413**, 41.
- Goloviznin, V. V., and T. Schep, 1999, *JETP Lett.* **70**, 450.
- Gorbunov, L. M., and V. I. Kirsanov, 1987, *Zh. Eksp. Teor. Fiz.* **93**, 509.
- Gorbunov, L. M., P. Mora, and T. M. Antonsen, Jr., 1996, *Phys. Rev. Lett.* **76**, 2495.
- Gorbunov, L. M., P. Mora, and R. Ramazashvili, 2002, *Phys. Rev. E* **65**, 036401.
- Gorbunov, L. M., P. Mora, and A. A. Solodov, 2003, *Phys. Plasmas* **10**, 1124.
- Gorbunov, L. M., and R. R. Ramazashvili, 1998, *JETP* **87**, 461.
- Gordeev, A. V., and T. V. Losseva, 1999, *JETP Lett.* **70**, 684.
- Gordon, D., K. C. Tzeng, C. E. Clayton, *et al.*, 1998, *Phys. Rev. Lett.* **80**, 2133.
- Greisen, K., 1966, *Phys. Rev. Lett.* **16**, 748.
- Grimes, M. K., Y. S. Lee, A. R. Rundquist, *et al.*, 1999, *Phys. Rev. Lett.* **82**, 4010.
- Gunn, J. E., and J. P. Ostriker, 1969, *Phys. Rev. Lett.* **22**, 728.
- Gurevich, A., L. Pariskaya, and L. Pitaevskii, 1966, *Sov. Phys. JETP* **22**, 449.
- Gurevich, A., L. Pariskaya, and L. Pitaevskii, 1972, *Sov. Phys. JETP* **36**, 274.
- Hadzievski, Lj., M. S. Jovanovic, M. M. Skoric, and K. Mima, 2002, *Phys. Plasmas* **9**, 2569.
- Halpern, O., 1933, *Phys. Rev.* **44**, 855.
- Hartemann, F. V., S. N. Fochs, G. P. Le Sage, *et al.*, 1995, *Phys. Rev. E* **51**, 4833.
- Hartemann, F. V., J. R. Van Meter, A. L. Troha, *et al.*, 1998, *Phys. Rev. E* **58**, 5001.
- Hawking, S. W., 1974, *Nature (London)* **248**, 30.
- Hawking, S. W., 1975, *Commun. Math. Phys.* **43**, 199.
- Hayashida, N., *et al.*, 1994, *Phys. Rev. Lett.* **73**, 3491.
- Heaviside, O., 1902, *Electromagnetic Theory*, 3 Vols. (Benn, London, 1983–1912).
- Heisenberg, W., and H. Euler, 1936, *Z. Phys.* **98**, 714.
- Hellwarth, R. W., 1961, *Advances in Quantum Electronics* (Columbia University Press, New York), p. 34.
- Hemker, R. G., N. M. Hafz, and M. Uesaka, 2002, *Phys. Rev. ST Accel. Beams* **5**, 041301.
- Henneberger, W. C., 1968, *Phys. Rev. Lett.* **21**, 838.
- Hentschel, M., R. Kienberger, Ch. Spielmann, G. A. Reider, N. Milosevic, T. Brabec, P. Corkum, U. Heinzmann, M. Drescher, and F. Krausz, 2001, *Nature (London)* **414**, 509.
- Heyl, J. S., and L. Hernquist, 1997, *J. Phys. A* **30**, 6485.
- Homoelle, D., A. L. Gaeta, V. Yanovsky, and G. Mourou, 2002, *Opt. Lett.* **27**, 1646.
- Honda, M., 2004, *Phys. Rev. E* **69**, 016401.
- Honda, M., J. Meyer-ter-Vehn, and A. M. Pukhov, 2000, *Phys. Rev. Lett.* **85**, 2128.
- Honda, T., K. Nishihara, T. Okamoto, *et al.*, 1999, *J. Plasma Fusion Res.* **75**, 219.
- Hosokai, T., K. Kinoshita, A. Zhidkov, *et al.*, 2003, *Phys. Rev. E* **67**, 036407.
- Il'in, A. S., V. V. Kulagin, and V. A. Cherepenin, 1999, *J. Commun. Technol. Electron.* **44**, 389.
- Itatani, J., *et al.*, 1998, *Opt. Commun.* **148**, 70.
- Itzykson, C., and J.-B. Zubar, 1980, *Quantum Field Theory* (McGraw-Hill, New York).
- Ivanenko, D. D., and I. Ya. Pomeranchuk, 1944, *Phys. Rev.* **65**, 343.

- Jackson, J. D., 1998, *Classical Electrodynamics* (John Wiley, New York).
- Joachain, C. J., *et al.*, 2000, *Adv. At., Mol., Opt. Phys.* **42**, 225.
- Joglekar, A. P., H. Liu, G. J. Spooner, E. Meyhofer, G. Mourou, and A. J. Hunt, 2003, *Appl. Phys. B: Lasers Opt.* **77**, 25.
- Joshi, C. J., and P. B. Corkum, 1995, *Phys. Today* **48** (1), 36.
- Jullien, A., O. Albert, F. Burgy, G. Hamoniaux, J.-P. Rousseau, J.-P. Chambaret, F. Angé-Rochereau, G. Chériaux, J. Etchepare, N. Minkovski, and S. M. Saltiel, 2005, *Opt. Lett.* **30**, 920.
- Jung, I. D., F. X. Kärtner, N. Matuschek, D. H. Sutter, F. Morier-Genoud, G. Zhang, U. Keller, V. Scheuer, M. Tilsch, and T. Tschudi, 1997, *Opt. Lett.* **22**, 1009.
- Kando, M., K. Nakajima, M. Arinaga, *et al.*, 1997, *J. Nucl. Mater.* **248**, 405.
- Kaplan, A., B. Dubetsky, and P. Shkolnikov, 2003, *Phys. Rev. Lett.* **91**, 143401.
- Kaplan, A. E., and P. L. Shkolnikov, 2002, *Phys. Rev. Lett.* **88**, 074801.
- Kaptein, H., M. Murnane, A. Skoze, and R. W. Falcone, 1991, *Opt. Lett.* **16**, 490.
- Katsouleas, T., and W. B. Mori, 1988, *Phys. Rev. Lett.* **61**, 90.
- Kaw, P., and J. Dawson, 1970, *Phys. Fluids* **13**, 472.
- Kaw, P. K., A. Sen, and T. Katsouleas, 1992, *Phys. Rev. Lett.* **68**, 3172.
- Keitel, C. H., 2001, *Contemp. Phys.* **42**, 353.
- Keldysh, L. V., 1965, *Sov. Phys. JETP* **20**, 1307.
- Key, M. H., E. M. Campbell, T. E. Cowan, *et al.*, 1999, in *First International Conference on Inertial Fusion Sciences and Applications, Bordeaux, France*, edited by C. Labaune, W. J. Hogan, and K. A. Tanaka (Elsevier, New York), p. 392.
- Khachatryan, A. G., 1998, *Phys. Rev. E* **58**, 7799.
- Khachatryan, A. G., 2000, *Phys. Plasmas* **7**, 5252.
- Khachatryan, V. S., and E. I. Minakova, 1998, *Eur. J. Phys.* **19**, 523.
- Kieffer, J. C., J. P. Matte, H. Pépin, *et al.*, 1992, *Phys. Rev. Lett.* **68**, 480.
- Kienberger, R., F. Krausz, *et al.*, 2004, *Nature (London)* **427**, 817.
- Kishimoto, Y., T. Masaki, and T. Tajima, 2002a, *Phys. Plasmas* **9**, 589.
- Kishimoto, Y., T. Masaki, and T. Tajima, 2002b, in *Proceedings of the 7th International Symposium of the Graduate University for Advanced Studies on Science of Superstrong Field Interactions*, Shonan Village, Hayama, Japan, 2002, edited by K. Nakajima and M. Deguchi, AIP Conf. Proc. No. 634 (AIP, Melville, NY), p. 147.
- Kishimoto, Y., K. Mima, T. Watanabe, and K. Nishikawa, 1983, *Phys. Fluids* **26**, 2308.
- Kishimoto, Y., and T. Tajima, 1999, in *High Field Science*, edited by T. Tajima, K. Mima, and H. Baldis (Plenum, New York), p. 85.
- Kivshar, Yu. S., and B. Luther-Davies, 1998, *Phys. Rep.* **298**, 8.
- Kivshar, Yu. S., and D. P. Pelinovsky, 2000, *Phys. Rep.* **331**, 117.
- Klein, O., 1929, *Z. Phys.* **53**, 157.
- Klein, J. J., and B. P. Nigam, 1964a, *Phys. Rev.* **135**, B1279.
- Klein, J. J., and B. P. Nigam, 1964b, *Phys. Rev.* **136**, B1540.
- Kmetec, J. D., C. L. Gordon III, J. J. Macklin, *et al.*, 1992, *Phys. Rev. Lett.* **68**, 1527.
- Kmetec, J. D., J. J. Macklin, and J. F. Young, 1991, *Opt. Lett.* **16**, 1001.
- Kodama, R., K. A. Tanaka, Y. Sentoku, *et al.*, 2000, *Phys. Rev. Lett.* **84**, 674.
- Kodama, R., *et al.*, 2001, *Nature* **412**, 798.
- Koga, J., K. Nakajima, M. Yamagiwa, and A. G. Zhidkov, 2002, in *Proceedings of the 7th International Symposium of the Graduate University for Advanced Studies on Science of Superstrong Field Interactions*, Shonan Village, Hayama, Japan, 2002, edited by K. Nakajima and M. Deguchi, AIP Conf. Proc. No. 634 (AIP, Melville, NY), p. 50.
- Kolomenskii, A. A., and A. N. Lebedev, 1963, *Sov. Phys. JETP* **17**, 179.
- Kong, Q., S. Miyazaki, S. Kawata, *et al.*, 2003, *Phys. Plasmas* **10**, 4605.
- Korobkin, V. V., and R. V. Serov, 1966, *JETP Lett.* **4**, 70.
- Kovalev, V. E., and V. Yu. Bychenkov, 2003, *Phys. Rev. Lett.* **90**, 185004.
- Kozaki, Y., *et al.*, 1998, *Proceedings of the 17th IAEA Fusion Energy Conference*, Yokohama.
- Kozlov, V. A., A. G. Litvak, and E. V. Suvorov, 1979, *Sov. Phys. JETP* **49**, 75.
- Krainov, V. P., and M. B. Smirnov, 2000, *Phys. Usp.* **43**, 901.
- Krainov, V. P., and M. B. Smirnov, 2002, *Phys. Rep.* **370**, 237.
- Krall, J., A. Ting, E. Esarey, and P. Sprangle, 1993, *Phys. Rev. E* **48**, 2157.
- Krekora, P., Q. Su, and R. Grobe, 2004, *Phys. Rev. Lett.* **92**, 040406.
- Kruer, W. L., 1988, *The Physics of Laser Plasma Interactions* (Addison-Wesley, New York).
- Krushelnick, K., E. Clark, R. Allot, *et al.*, 2000, *IEEE Trans. Plasma Sci.* **28**, 1184.
- Krushelnick, K., E. L. Clark, Z. Najmudin, M. Salvati, M. I. K. Santala, M. Tatarakis, A. E. Dangor, V. Malka, D. Neely, R. Allot, and C. Danson, 1999, *Phys. Rev. Lett.* **83**, 737.
- Krushelnick, K., E. L. Clark, M. Zepf, *et al.*, 2000, *Phys. Plasmas* **7**, 2055.
- Krymskii, G. F., 1977, *Dokl. Akad. Nauk SSSR* **234**, 1306.
- Kumarappan, V., M. Krishnamurthy, and D. Mathur, 2001, *Phys. Rev. Lett.* **87**, 085005.
- Kumarappan, V., M. Krishnamurthy, and D. Mathur, 2002, *Phys. Rev. A* **66**, 033203.
- Kuznetsov, E. A., 1996, *Chaos* **6**, 381.
- Kuznetsov, A., T. Esirkepov, F. Kamenets, *et al.*, 2001, *Plasma Phys. Rep.* **27**, 211.
- Kuznetsov, E. A., A. M. Rubenchik, and V. E. Zakharov, 1986, *Phys. Rep.* **142**, 105.
- Lai, H. M., 1980, *Phys. Fluids* **23**, 2373.
- Lamb, H., 1932, *Hydrodynamics* (Cambridge University Press, Cambridge, England).
- Landau, L. D., and E. M. Lifshitz, 1980, *The Classical Theory of Fields* (Pergamon Press, Oxford).
- Landau, L. D., and E. M. Lifshitz, 1984, *Electrodynamics of Continuous Media* (Pergamon Press, Oxford).
- Landecker, K., 1952, *Phys. Rev.* **86**, 852.
- Larsson, J., P. A. Heimann, A. M. Lindenberg, P. J. Schuk, P. H. Bucksbaum, R. W. Lee, H. A. Padmore, J. S. Wark, and R. W. Falcone, 1998, *Appl. Phys. A: Mater. Sci. Process.* **66**, 587.
- Last, I., and J. Jortner, 2001, *Phys. Rev. A* **66**, 063201.
- Last, I., I. Schek, and J. Jortner, 1997, *J. Chem. Phys.* **107**, 6685.
- Lawson, J. D., 1979, *IEEE Trans. Nucl. Sci.* **NS-26**, 4217.
- Ledingham, K. W., I. Spencer, T. McCanny, *et al.*, 2000, *Phys. Rev. Lett.* **84**, 899.
- Ledingham, K. W. D., P. McKenna, and R. P. Singhal, 2003, *Science* **300**, 1107.

- Leemans, W. P., P. Catravas, E. Esarey, C. G. R. Geddes, C. Toth, R. Trines, C. B. Schroeder, B. A. Shudwick, J. van Tilborg, and J. Faure, 2002, *Phys. Rev. Lett.* **89**, 174802.
- Leemans, W. P., D. Rodgers, P. E. Catravas, *et al.*, 2001, *Phys. Plasmas* **8**, 2510.
- Lemoff, B. E., and C. P. Barty, 1993, *Opt. Lett.* **18**, 1651.
- Lezius, M., S. Dobosz, D. Normand, and M. Schmidt, 1998, *Phys. Rev. Lett.* **80**, 261.
- L'Huillier, A., P. Balcou, S. Candel, *et al.*, 1992, *Phys. Rev. A* **46**, 2778.
- Li, Y., Z. Huang, M. D. Borland, and S. Milton, 2002, *Phys. Rev. ST Accel. Beams* **5**, 044701.
- Liang, E. P., S. C. Wilks, and M. Tabak, 1998, *Phys. Rev. Lett.* **81**, 4887.
- Lichters, R., *et al.*, 1996, *Phys. Plasmas* **3**, 3425.
- Lindl, J. D., 1998, *Inertial Fusion Energy* (Springer-Verlag, New York).
- Lindl, J. D., P. Amendt, R. Berger, *et al.*, 2004, *Phys. Plasmas* **11**, 339.
- Lindman, E. L., 1977, *J. Phys. (Paris)* **38**, 6.
- Liseikina, T. V., F. Califano, V. A. Vshivkov, F. Pegoraro, and S. V. Bulanov, 1999, *Phys. Rev. E* **60**, 5991.
- Litvak, A. G., 1969, *Sov. Phys. JETP* **30**, 344.
- Lontano, M., *et al.*, 2001, *Phys. Plasmas* **8**, 5113.
- Lontano, M., *et al.*, 2002, *Phys. Plasmas* **9**, 2562.
- Lontano, M., *et al.*, 2003, *Phys. Plasmas* **10**, 639.
- Ludlam, T., and L. McLerran, 2003, *Phys. Today* **56** (10), 48.
- Luk, T. S., A. McPherson, G. Gibson, K. Boyer, and C. Rhodes, 1989, *Opt. Lett.* **14**, 1113.
- Macchi, A., F. Cornolti, and F. Pegoraro, 2002, *Phys. Plasmas* **9**, 1704.
- Macchi, A., *et al.*, 2001, *Phys. Rev. Lett.* **87**, 205004.
- Mackinnon, A. J., M. Borghesi, S. Hatchett, *et al.*, 2001, *Phys. Rev. Lett.* **86**, 1769.
- Mackinnon, A. J., Y. Sentoku, P. K. Patel, *et al.*, 2002, *Phys. Rev. Lett.* **88**, 215006.
- Maine, P., and G. Mourou, 1988, *Opt. Lett.* **13**, 467.
- Maine, P., D. Strickland, P. Bado, M. Pessot, and G. Mourou, 1987, *Rev. Phys. Appl.* **22**, 1657.
- Maine, P., D. Strickland, P. Bado, M. Pessot, and G. Mourou, 1988, *IEEE J. Quantum Electron.* **24**, 398.
- Maksimchuk, A., V. Yu. Bychenkov, K. Flippo, *et al.*, 2004, *Plasma Phys. Rep.* **30**, 473.
- Maksimchuk, A., S. Gu, K. Flippo, D. Umstadter, *et al.*, 2000, *Phys. Rev. Lett.* **84**, 4108.
- Mako, F., and T. Tajima, 1984, *Phys. Fluids* **27**, 1815.
- Malka, G., E. Lefebvre, and J. L. Miquel, 1997, *Phys. Rev. Lett.* **78**, 3314.
- Malka V., J. Faure, and F. Amiranoff, 2001, *Phys. Plasmas* **8**, 2605.
- Malka, V., *et al.*, 2002, *Science* **298**, 1596.
- Malkin, V. M., G. Shvets, and N. J. Fisch, 1999, *Phys. Rev. Lett.* **82**, 4448.
- Mangles, S. P. D., *et al.*, 2004, *Nature (London)* **431**, 535.
- Maquet, A., and R. Grobe, 2002, *J. Mod. Opt.* **49**, 2001.
- Marburger, J. H., and R. F. Tooper, 1975, *Phys. Rev. Lett.* **35**, 1001.
- Martinez, O. E., 1987, *IEEE J. Quantum Electron.* **23**, 1385.
- Matsukado, K., *et al.*, 2003, *Phys. Rev. Lett.* **91**, 215001.
- Mayer, G., and F. Gires, 1964, *Compt. Rend.* **258**, 2039.
- Max, C., J. Arons, and B. Langdon, 1974, *Phys. Rev. Lett.* **33**, 209.
- McCall, S. L., and E. L. Hahn, 1969, *Phys. Rev.* **183**, 457.
- McKenna, J., and P. M. Platzman, 1963, *Phys. Rev.* **129**, 2354.
- Melissinos, A. C., 1998, in *Proceedings of International Conference "Frontier Tests of QED and Physics of the Vacuum,"* edited by E. Zavattini, D. Bakalov, and C. Rizzo (Heron Press, Sofia), p. 236.
- Melissinos, A. C., 1999, in *Proceedings of the 15th Advanced ICFA Beam Dynamics Workshop on Quantum Aspects of Beam Physics*, Monterey, CA, 1998, edited by P. Chen (World Scientific, Singapore), p. 564.
- Meszáros, P., and M. J. Rees, 1993, *Astrophys. J.* **405**, 278.
- Migus, A., C. V. Shank, E. P. Ippen, and R. L. Fork, 1982, *IEEE J. Quantum Electron.* **QE-18**, 101.
- Mikhailovskii, A. B., 1992, *Electromagnetic Instabilities in an Inhomogeneous Plasma* (Consultant Bureau, New York).
- Milosevic, N., P. B. Corkum, and T. Brabec, 2003, *Phys. Rev. Lett.* **92**, 013002.
- Mima, K., W. Horton, T. Tajima, and A. Hasegawa, 1991, *Power-Law Energy Spectrum and Orbital Stochasticity* (AIP, New York), p. 27.
- Mima, K., M. S. Jovanovic, Y. Sentoku, *et al.*, 2001, *Phys. Plasmas* **8**, 2349.
- Mima, K., T. Ohsuga, H. Takabe, K. Nishihara, T. Tajima, E. Zaidman, and W. Horton, 1986, *Phys. Rev. Lett.* **57**, 1421.
- Minehara, E. J., 2002, *Nucl. Instrum. Methods Phys. Res. A* **483**, 8.
- Miura, E., K. Koyama, S. Kato, *et al.*, 2005, *Appl. Phys. Lett.* **86**, 251501.
- Miyamoto, S., S. Kato, K. Mima, *et al.*, 1997, *J. Plasma Fusion Res.* **73**, 343.
- Mocken, G. R., and C. H. Keitel, 2003, *Phys. Rev. Lett.* **91**, 173202.
- Mocker, H. W., and R. J. Collins, 1965, *Appl. Phys. Lett.* **7**, 270.
- Modena, A., Z. Najmudin, A. E. Dangor, *et al.*, 1995, *Nature (London)* **337**, 606.
- Monot, P., T. Auguste, P. Gibbon, F. Jakober, and G. Mainfray, 1995, *Phys. Rev. Lett.* **74**, 2953.
- Mora, P., 2003, *Phys. Rev. Lett.* **90**, 185002.
- Mori, W., T. Katsouleas, J. Dawson, and C. Lai, 1995, *Phys. Rev. Lett.* **74**, 542.
- Mori, W. B., 1991, *Phys. Rev. A* **44**, 5118.
- Mourou, G., 1997, *Appl. Phys. B: Lasers Opt.* **65**, 205.
- Mourou, G., Z. Chang, A. Maksimchuk, *et al.*, 2002, *Plasma Phys. Rep.* **28**, 12.
- Mourou, G. A., C. P. J. Barty, and M. D. Perry, 1998, *Phys. Today* **51** (1), 22.
- Mourou, G. A., N. M. Naumova, I. V. Sokolov, B. Hou, and J. A. Nees, 2004, in *Ultrafast Optics IV*, Vol. 95 of Springer Series in Optical Sciences, edited by F. Krausz, G. Korn, P. Corkum, and I. A. Walmsley (Springer-Verlag, Berlin), p. 305.
- Nagashima, K., Y. Kishimoto, and H. Takuma, 1999, *Phys. Rev. E* **59**, 1263.
- Najmudin, Z., *et al.*, 2001, *Phys. Rev. Lett.* **87**, 215004.
- Nakajima, K., 2002, in *Proceedings of the 2nd International Conference on Superstrong Fields in Plasmas*, Varenna, 2001, edited by M. Lontano, G. Mourou, O. Svelto, and T. Tajima, AIP Conf. Proc. No. 611 (AIP, Melville, NY), p. 447.
- Nakajima, K., D. Fisher, T. Kawakubo, *et al.*, 1995, *Phys. Rev. Lett.* **74**, 4428.
- Nakamura, T., and S. Kawata, 2003, *Phys. Rev. E* **67**, 026403.
- Nakanishi, T., *et al.*, 2001, *Jpn. J. Appl. Phys., Part 2* **46**, L555.
- Nantel, M., *et al.*, 1998, *IEEE J. Sel. Top. Quantum Electron.* **4**, 449.

- Narozhny, N. B., and M. S. Fofanov, 2000, JETP **90**, 753.
- Narozhny, N. B., and A. I. Nikishov, 1974, Sov. Phys. JETP **38**, 427.
- Narozhny, N. B., *et al.*, 2004a, JETP Lett. **80**, 382.
- Narozhny, N. B., *et al.*, 2004b, Phys. Lett. A **330**, 1.
- Naumova, N., I. Sokolov, J. Nees, A. Maksimchuk, V. Yanovsky, and G. Mourou, 2004, Phys. Rev. Lett. **93**, 195003.
- Naumova, N. M., S. V. Bulanov, T. Z. Esirkepov, D. Farina, K. Nishihara, F. Pegoraro, H. Ruhl, and A. S. Sakharov, 2001, Phys. Rev. Lett. **87**, 185004.
- Naumova, N. M., J. Koga, K. Nakajima, *et al.*, 2001, Phys. Plasmas **8**, 4149.
- Naumova, N. M., J. A. Nees, B. Hou, G. A. Mourou, and I. V. Sokolov, 2004, Opt. Lett. **29**, 778.
- Naumova, N. M., J. A. Nees, and G. A. Mourou, 2005, Phys. Plasmas **12**, 056707.
- Naumova, N. M., J. A. Nees, I. V. Sokolov, B. Hou, and G. A. Mourou, 2004, Phys. Rev. Lett. **92**, 063902.
- Naumova, N. M., *et al.*, 2002a, Phys. Rev. E **65**, 045402.
- Naumova, N. M., *et al.*, 2002b, in *Proceedings of 2nd International Conference on Superstrong Fields in Plasmas*, edited by M. Lontano, G. Mourou, O. Svelto, and T. Tajima, AIP Conf. Proc. No. 611 (AIP, Melville, NY), p. 170.
- Nees, J., S. Biswal, F. Druon, J. Faure, M. Nantel, and G. Mourou, 1998, IEEE J. Sel. Top. Quantum Electron. **4**, 376.
- Nees, J., N. Naumova, E. Power, V. Yanovsky, I. Sokolov, A. Maksimchuk, S. Bahk, V. Chvykov, G. Kalintchenko, B. Hou, and G. Mourou, 2005, J. Mod. Opt. **52**, 305.
- Nemoto, K., A. Maksimchuk, S. Banerjee, *et al.*, 2001, Appl. Phys. Lett. **78**, 595.
- Nikishov, A. I., and V. I. Ritus, 1964, Sov. Phys. JETP **19**, 529.
- Nishihara, K., *et al.*, 2001, Nucl. Instrum. Methods Phys. Res. A **464**, 98.
- Nishioka, H., K. Kimura, K. Ueda, and H. Takuma, 1993, IEEE J. Quantum Electron. **29**, 2251.
- Norreys, P., *et al.*, 1999, Phys. Plasmas **6**, 2150.
- Norris, T., 1992, Opt. Lett. **17**, 1009.
- Okihara, S., T. Zh. Esirkepov, K. Nagai, *et al.*, 2004, Phys. Rev. E **69**, 026401.
- Olinto, A. V., 2000, Phys. Rep. **333**, 329.
- Omori, T., T. Aoki, K. L. Dobashi, T. Hirose, Y. Kurihara, T. Okugi, I. Sakai, A. Tsunemi, J. Urakawa, M. Washio, and K. Yokoya, 2003, Nucl. Instrum. Methods Phys. Res. A **500**, 232.
- Ostrovskii, L. A., 1976, Sov. Phys. Usp. **116**, 315.
- Pakhomov, A., 2002, J. Phys. G **28**, 1469.
- Pang, J., Y. K. Ho, X. Q. Yuan, *et al.*, 2002, Phys. Rev. E **66**, 066501.
- Parker, J., Jr., and C. R. Stroud, 1990, Phys. Rev. A **41**, 1602.
- Parker, L., 1969, Phys. Rev. **183**, 1057.
- Parks, P. B., T. E. Cowan, R. B. Stephens, and E. M. Campbell, 2001, Phys. Rev. A **63**, 063203.
- Pashinin, P. P., 1987, *Formation and Control of Optical Wavefronts*, Proceedings of the Institute of General Physics of the Academy of Sciences of the USSR (Nauka, Moscow), Vol. 7.
- Passoni, M., V. T. Tikhonchuk, M. Lontano, and V. Yu. Bychenkov, 2004, Phys. Rev. E **69**, 026411.
- Paul, A., R. A. Bartels, R. Tobey, H. Green, S. Weiman, I. P. Christov, M. M. Murnane, H. C. Kapteyn, and S. Backus, 2003, Nature (London) **421**, 51.
- Pauli, W., 1981, *Theory of Relativity* (Dover, New York).
- Pegoraro, F., *et al.*, 1996, Phys. Scr., T **63**, 262.
- Pegoraro, F., *et al.*, 1997, Plasma Phys. Controlled Fusion **39**, B261.
- Perelomov, A. M., V. S. Popov, and M. V. Terent'ev, 1966, Sov. Phys. JETP **23**, 924.
- Perry, M., P. Pennington, B. C. Stuart, *et al.*, 1999, Opt. Lett. **24**, 160.
- Pessot, M., J. Squier, and G. Mourou, 1989, Opt. Lett. **14**, 797.
- Pessot, M., *et al.*, 1987, Opt. Commun. **62**, 419.
- Ping, Y., I. Geltner, N. J. Fisch, G. Shvets, and S. Suckewer, 2000, Phys. Rev. E **62**, R4532.
- Pirozhkov, A. S., S. V. Bulanov, T. Zh. Esirkepov, M. Mori, A. Sagisaka, and H. Daido, 2005, Phys. Lett. A **349**, 256.
- Plaja, L., and E. C. Jarque, 1998, Phys. Rev. E **58**, 3977.
- Poornakala, S., A. Das, A. Sen, and P. K. Kaw, 2002, Phys. Plasmas **9**, 1820.
- Popov, V. S., 2001, JETP Lett. **74**, 133.
- Popov, V. S., 2002a, Phys. Lett. A **298**, 83.
- Popov, V. S., 2002b, JETP **94**, 1057.
- Popov, V. S., 2004, Phys. Usp. **47**, 855.
- Popov, V. S., and M. S. Marinov, 1973, Sov. J. Nucl. Phys. **16**, 449.
- Popov, V. S., V. D. Mur, and B. M. Karnakov, 1997, JETP Lett. **66**, 229.
- Pretzler, G., A. Saemann, A. Pukhov, *et al.*, 1998, Phys. Rev. E **58**, 1165.
- Price, A., *et al.*, 2002, e-print astro-ph/0203467.
- Pukhov, A., and J. Meyer-Ter-Vehn, 2002, Appl. Phys. B: Lasers Opt. **74**, 355.
- Pukhov, A. M., 2001, Phys. Rev. Lett. **86**, 3562.
- Pukhov, A. M., 2003, Rep. Prog. Phys. **66**, R47.
- Pukhov, A. M., and J. Meyer-ter-Vehn, 1996, Phys. Rev. Lett. **76**, 3975.
- Pukhov, A. M., and J. Meyer-ter-Vehn, 1998, Phys. Plasmas **5**, 1860.
- Punch, M., *et al.*, 1992, Nature (London) **358**, 477.
- Quesnel, B., and P. Mora, 1998, Phys. Rev. E **58**, 3719.
- Rau, B., and T. Tajima, 1998, Phys. Plasmas **5**, 3575.
- Rau, B., T. Tajima, and H. Hojo, 1997, Phys. Rev. Lett. **78**, 3310.
- Reiss, H., 1962, J. Math. Phys. **3**, 59.
- Reitsma, A. J. W., V. V. Goloviznin, L. P. J. Kamp, and T. J. Schep, 2002, Phys. Rev. Lett. **88**, 014802.
- Ringwald, A., 2001, Phys. Lett. B **510**, 107.
- Ritus, V. I., 1979, *Proceedings of the P. N. Lebedev Physics Institute of Acad. Sci. USSR* (Nauka, Moscow), Vol. 111, p. 5.
- Roberts, C. D., S. M. Schmidt, and D. V. Vinnik, 2002, Phys. Rev. Lett. **89**, 153901.
- Roberts, C. S., and S. J. Buchsbaum, 1964, Phys. Rev. **135**, A381.
- Roso, L., L. Plaja, K. Rzazewski, and D. von der Linde, 2000, Laser Part. Beams **18**, 467.
- Ross, I. N., J. L. Collier, P. Matousek, *et al.*, 2000, Appl. Opt. **39**, 2422.
- Ross, I. N., P. Matousek, G. H. C. New, and K. Osvay, 2002, J. Opt. Soc. Am. B **19**, 12, 2945.
- Ross, I. N., *et al.*, 1997, Opt. Commun. **144**, 125.
- Roth, M., *et al.*, 2001, Phys. Rev. Lett. **86**, 436.
- Roth, M., *et al.*, 2002, in *Proceedings of the 2nd International Conference on Superstrong Fields in Plasmas*, Varenna, 2001, edited by M. Lontano, G. Mourou, O. Svelto, and T. Tajima, AIP Conf. Proc. No. 611 (AIP, Melville, NY), p. 199.
- Rouyer, C., *et al.*, 1993, Opt. Lett. **18**, 214.
- Rozañov, N. N., 1993, JETP **76**, 991.
- Rozañov, N. N., 1998, JETP **86**, 284.
- Rubakov, V. A., 2003, Usp. Fiz. Nauk **173**, 219.

- Rubakov, V. A., and M. E. Shaposhnikov, 1983, *Phys. Lett.* **125B**, 136.
- Ruhl, H., Y. Sentoku, K. Mima, *et al.*, 1999, *Phys. Rev. Lett.* **82**, 743.
- Ruhl, H., *et al.*, 2001, *Plasma Phys. Rep.* **27**, 411.
- Ruth, R. D., 1998, *Phys. Today* **51** (2), 98.
- Sagdeev, R. Z., 1966, in *Reviews of Plasma Physics*, edited by M. A. Leontovich (Consultant Bureau, New York), Vol. 4, p. 23.
- Sakabe, S., *et al.*, 2004, *Phys. Rev. A* **69**, 023203.
- Sakai, J. I., *et al.*, 2002, *Phys. Plasmas* **9**, 2959.
- Salamin, Y. I., and F. H. M. Faisal, 1997, *Phys. Rev. A* **55**, 3678.
- Salamin, Y. I., and C. H. Keitel, 2002 *Phys. Rev. Lett.* **88**, 095005.
- Salières, P., and M. Lewenstein, 2001, *Meas. Sci. Technol.* **12**, 1818.
- Salières, P., *et al.*, 2001, *Science* **292**, 902.
- Sarachik, E., and G. Schappert, 1970, *Phys. Rev. D* **1**, 2738.
- Sarkisov, G. S., *et al.*, 1999, *Phys. Rev. E* **59**, 7042.
- Satoh, H., 2001, *Kagaku* (Kyoto, Jpn.) **71**, 183.
- Sauter, F., 1931, *Z. Phys.* **69**, 742.
- Savage, R., C. Joshi, and W. Mori, 1992, *Phys. Rev. Lett.* **68**, 946.
- Schaechter, L., 1999, *Phys. Rev. Lett.* **83**, 92.
- Schaechter, L., R. L. Byer, and R. H. Siemann, 2002, in *Advanced Accelerator Concepts*, edited by C. E. Clayton and P. Muggli, AIP Conf. Proc. No. 647 (AIP, Melville, NY), p. 310.
- Schafer, K. J., and K. C. Kulander, 1997, *Phys. Rev. Lett.* **78**, 638.
- Schafer, K. J., *et al.*, 2004, *Phys. Rev. Lett.* **92**, 023003.
- Scharf, W. H., 1994, *Biomedical Particle Accelerators* (AIP, Woodbury, NY).
- Schmidt, G., and W. Horton, 1985, *Comments Plasma Phys. Controlled Fusion* **9**, 85.
- Schoenlein, R. W., S. Chattopadhyay, H. H. W. Chong, *et al.*, 2000, *Science* **287**, 2237.
- Schwinger, J., 1951, *Phys. Rev.* **82**, 664.
- Schwoerer, C., *et al.*, 2006, *Nature* **439**, 445.
- Sekikawa, T., S. Watanabe, *et al.*, 2004, *Nature* (London) **432**, 605.
- Semenova, V. I., 1967, *Radiophys. Quantum Electron.* **10**, 599.
- Sentoku, Y., *et al.*, 1999a, *Phys. Plasmas* **6**, 2855.
- Sentoku, Y., *et al.*, 1999b, *Phys. Rev. Lett.* **83**, 3434.
- Sentoku, Y., *et al.*, 2000, *Phys. Rev. E* **62**, 7271.
- Sentoku, Y., *et al.*, 2002, *Appl. Phys. B: Lasers Opt.* **74**, 207215.
- Shao, Y. L., T. Ditmire, J. W. G. Tisch, *et al.*, 1996, *Phys. Rev. Lett.* **77**, 3343.
- Shearer, J. W., J. Garrison, J. Wong, and J. E. Swain, 1972, *Phys. Rev. A* **8**, 1582.
- Sheehy, B., J. D. D. Martin, L. F. Di Mauro, *et al.*, 1999, *Phys. Rev. Lett.* **83**, 5270.
- Shen, B., and J. Meyer-ter-Vehn, 2002, *Phys. Rev. E* **65**, 016405.
- Shen, Y. R., 1984, *The Principles of Nonlinear Optics* (Wiley, New York).
- Shizuma, T., T. Hayakawa, and K. Nishio, 2002, in *Proceedings of the Workshop on Applications of IRFEL and Nuclear Isomers 2002*, edited by T. Yamauchi (JAERI, Tokai).
- Shukla, P. K., M. Marklund, D. D. Tskhakaya, and B. Eliasson, 2004, *Phys. Plasmas* **11**, 3767.
- Shukla, P. K., N. N. Rao, M. Y. Yu, and N. L. Tsintsadze, 1986, *Phys. Rep.* **138**, 1.
- Shvets, G., N. J. Fisch, A. Pukhov, and J. Meyer-ter-Vehn, 1998, *Phys. Rev. Lett.* **81**, 4879.
- Shvets, G., N. J. Fisch, A. Pukhov, and J. Meyer-ter-Vehn, 1999, *Phys. Rev. E* **60**, 2218.
- Siegman, A. E., 1986, *Lasers* (University Science Books, Mill Valley, CA), p. 362.
- Singh, K. P., and V. K. Tripathi, 2004, *Phys. Plasmas* **11**, 743.
- Smetanin, I. V., T. Esirkepov, D. Farina, *et al.*, 2004, *Phys. Lett. A* **320**, 438.
- Snively, R., M. H. Key, S. P. Hatchett, *et al.*, 2000, *Phys. Rev. Lett.* **85**, 2945.
- Sokolov, A. A., and I. M. Ternov, 1968, *Synchrotron Radiation* (Akademie Verlag, Berlin/Pergamon Press, New York).
- Sokolov, A. A., I. M. Ternov, and Yu. M. Loskutov, 1962, *Phys. Rev.* **125**, 731.
- Soljagic, M., and M. Segev, 2000, *Phys. Rev. A* **62**, 043817.
- Spence, D. E., P. N. Kean, and W. Sibbett, 1991, *Opt. Lett.* **6**, 42.
- Sprangle, P., E. Esarey, A. Ting, and G. Joyce, 1988, *Appl. Phys. Lett.* **53**, 2146.
- Sprangle, P., C. M. Tang, and E. Esarey, 1987, *IEEE Trans. Plasma Sci.* **PS-15**, 145.
- Springate, E., N. Hay, J. W. Tisch, *et al.*, 2000, *Phys. Rev. A* **61**, 063201.
- Squier, J., F. Salin, G. Mourou, and D. Harter, 1991, *Opt. Lett.* **16**, 324.
- Stamper, J., K. Papadopoulos, R. N. Sudan, *et al.*, 1971, *Phys. Rev. Lett.* **26**, 1012.
- Steiger, A. D., and C. H. Woods, 1971, *Phys. Rev. A* **5**, 1467.
- Strickland, A. D., and G. Mourou, 1985, *Opt. Commun.* **56**, 212.
- Sudan, R. N., 1993, *Phys. Rev. Lett.* **70**, 3075.
- Sullivan, A., *et al.*, 1991, *Opt. Lett.* **16**, 1406.
- Suk, K., N. Barov, J. Rosenzweig, and E. Esarey, *et al.*, 2001, *Phys. Rev. Lett.* **86**, 1011.
- Sun, G.-Z., *et al.*, 1987, *Phys. Fluids* **30**, 526.
- Tabak, M., J. Hammer, M. E. Glinsky, *et al.*, 1994, *Phys. Plasmas* **1**, 1626.
- Tajima, T., 1985, *Laser Part. Beams* **3**, 351.
- Tajima, T., 1987, *Nature* (London) **327**, 285.
- Tajima, T., 1998, *J. Jpn. Soc. Ther. Radio-Oncol.* **9**, 83.
- Tajima, T., 1989, *Computational Plasma Physics* (Addison-Wesley, Reading, MA).
- Tajima, T., 2001, in *Advanced Accelerator Concepts*, edited by P. Colestock *et al.* (AIP, Melville, NY), p. 77.
- Tajima, T., 2002, *Proceedings of the Japan-Hungary Seminar* (IIAS, Kyoto).
- Tajima, T., 2003, *Plasma Phys. Rep.* **29**, 207.
- Tajima, T., and J. M. Dawson, 1979, *Phys. Rev. Lett.* **43**, 267.
- Tajima, T., Y. Kishimoto, and M. C. Downer, 1999, *Phys. Plasmas* **6**, 3759.
- Tajima, T., and G. Mourou, 2002, *Phys. Rev. ST Accel. Beams* **5**, 031301.
- Tajima, T., K. Soyama, J. K. Koga, and H. Takuma, 2000, *J. Phys. Soc. Jpn.* **69**, 3840.
- Tajima, T., and T. Taniuti, 1990, *Phys. Rev. A* **42**, 3587.
- Takahashi, Y., L. Hillman, and T. Tajima, 2000, in *High-Field Science*, edited by T. Tajima, K. Mima, and H. Baldis (Kluwer, New York), p. 171.
- Takeda, M., *et al.*, 1998, *Phys. Rev. Lett.* **81**, 1163.
- Tamaki, Y., K. Midorikawa, *et al.*, 1999, *Phys. Rev. Lett.* **82**, 1422.
- Tapié, J.-L., 1991, Ph.D. thesis (Université de Paris-Sud).
- Tapié, J.-L., and G. Mourou, 1992, *Opt. Lett.* **17**, 136.
- Tarasevitch, A., A. Orisch, D. von der Linde, *et al.*, 2000, *Phys. Rev. E* **62**, 023816.

- Tatarakis, M., I. Watts, F. N. Beg, *et al.*, 2002, *Nature (London)* **415**, 280.
- Telnov, V. I., 1990, *Nucl. Instrum. Methods Phys. Res. A* **294**, 72.
- Telnov, V. I., 2000, *Int. J. Mod. Phys. A* **15**, 2577.
- Telnov, V. I., 2001, *Nucl. Instrum. Methods Phys. Res. A* **472**, 43.
- Temporal, M., J. J. Honrubia, and S. Atzeni, 2002, *Phys. Plasmas* **9**, 3098.
- Ter-Aoetisyan, S., *et al.*, 2004, *Phys. Rev. Lett.* **93**, 155006.
- Thompson, M., J. B. Rosenzweig, and H. Suk, 2004, *Phys. Rev. ST Accel. Beams* **7**, 011301.
- Timofeev, A. V., 1979, *Sov. J. Plasma Phys.* **5**, 705.
- Tochitsky, S. Ya., *et al.*, 2004, *Phys. Rev. Lett.* **92**, 095004.
- Tomassini, P., M. Galimberti, A. Giulietti, *et al.*, 2003, *Phys. Rev. ST Accel. Beams* **6**, 121301.
- Tournois, P., 1993, *Electron. Lett.* **29**, 1414.
- Tournois, P., 1997, *Opt. Commun.* **140**, 245.
- Treacy, E. B., 1969, *IEEE J. Quantum Electron.* **5**, 454.
- Trines, R., V. Goloviznin, L. Kamp, and T. Schep, 2001, *Phys. Rev. E* **63**, 026406.
- Troha, A. L., J. R. Van Meter, E. C. Landahl, *et al.*, 1999, *Phys. Rev. E* **60**, 926.
- Tsintsadze, N. L., and D. D. Tskhakaya, 1977, *Sov. Phys. JETP* **45**, 252.
- Tzeng, K-C., and W. B. Mori, 1998, *Phys. Rev. Lett.* **81**, 104.
- Tzeng, K-C., W. B. Mori, and C. D. Decker, 1996, *Phys. Rev. Lett.* **76**, 3332.
- Tzeng, K-C., W. B. Mori, and T. Katsouleas, 1997, *Phys. Rev. Lett.* **79**, 5258.
- Ueda, K., H. Nishioka, K. Kimura, and H. Takuma, 1993, *Laser Part. Beams* **11**, 22.
- Ueshima, Y., Y. Kishimoto, A. Sasaki, and T. Tajima, 1999, *Laser Part. Beams* **17**, 45.
- Ueshima, Y., Y. Sentoku, and Y. Kishimoto, 2000, *Nucl. Instrum. Methods Phys. Res. A* **455**, 181.
- Umstadter, D., 2003, *J. Phys. D* **36**, R151.
- Umstadter, D., S.-Y. Chen, A. Maksimchuk, G. Mourou, and R. Wagner, 1996, *Science* **273**, 472.
- Umstadter, D., E. Esarey, and J. Kim, 1994, *Phys. Rev. Lett.* **72**, 1224.
- Umstadter, D., J. K. Kim, and E. Dodd, 1996, *Phys. Rev. Lett.* **76**, 2073.
- Unruh, W., 1976, *Phys. Rev. D* **14**, 870.
- Vaillancourt, T. G., B. Norris, J. S. Coe, and G. A. Mourou, 1990, *Opt. Lett.* **15**, 317.
- Van Meter, J. R., S. Carlip, and F. V. Hartemann, 2001, *Am. J. Phys.* **69**, 783.
- Vanzella, D., and G. Matsas, 2001, *Phys. Rev. Lett.* **87**, 151301.
- Vázquez de Aldana, J. R., N. J. Kylstra, L. Roso, *et al.*, 2001, *Phys. Rev. A* **64**, 013411.
- Veksler, V. I., 1957, *Atomic Energy* **2**, 427.
- Vekstein, G. E., 1998, *Am. J. Phys.* **66**, 886.
- Villorosi, P., *et al.*, 2000, *Phys. Rev. Lett.* **85**, 2494.
- Von der Linde, D., 1998, *Superstrong Fields in Plasmas*, edited by M. Lontano, G. Mourou, F. Pegoraro, and E. Sindoni, AIP Conf. Proc. No. 426 (AIP, Woodbury, NY), p. 221.
- Von der Linde, D., and K. Rzàzewski, 1996, *Appl. Phys. B: Lasers Opt.* **63**, 499.
- Voronov, G. S., and N. B. Delone, 1965, *JETP Lett.* **1**, 66.
- Vshivkov, A. V., *et al.*, 1998a, *Nucl. Instrum. Methods Phys. Res. A* **410**, 493.
- Vshivkov, A. V., *et al.*, 1998b, *Phys. Plasmas* **5**, 2752.
- Wagner, R., S.-Y. Chen, A. Maksimchuk, and D. Umstadter, 1997, *Phys. Rev. Lett.* **78**, 3125.
- Waltz, R. E., and O. P. Manley, 1978, *Phys. Fluids* **21**, 808.
- Watts, I., M. Zepf, E. Clark, *et al.*, 1999, *Central Laser Facility Annual Report*, RAL, unpublished, p. 24.
- Weibel, E. W., 1959, *Phys. Rev. Lett.* **2**, 83.
- Weiler, T. J., 1999, *Astropart. Phys.* **11**, 303.
- Weinacht, T. C., J. Ahn, and P. H. Bucksbaum, 1998, *Phys. Rev. Lett.* **80**, 5508.
- White, W. E., F. G. Patterson, R. L. Combs, D. F. Price, and R. L. Shepherd, 1993, *Opt. Lett.* **18**, 1343.
- Whitham, G. B., 1974, *Linear and Nonlinear Waves* (Wiley, New York).
- Wilks, S. C., *et al.*, 1989, *Phys. Rev. Lett.* **62**, 2600.
- Wilks, S. C., *et al.*, 2001, *Phys. Plasmas* **8**, 542.
- Woodbury, E. J., and W. K. Ng, 1962, *Proc. IRE* **50**, 2367.
- Woodward, P. M., 1947, *J. IEEE* **93**, Part III A, 1554.
- Wulff, M., D. Bourgeois, T. Ursby, L. Goir, and G. Mourou, 1997, in *Time Resolved Diffraction*, edited by J. R. Helliwell and P. M. Rentzepis (Clarendon Press, Oxford), pp. 195–228.
- Xie, M., T. Tajima, K. Yokoya, and S. Chattopadhyay, 1997, in *Advanced Accelerator Concepts*, edited by S. Chattopadhyay, J. McCullough, and P. Dahl, AIP Conf. Proc. No. 398 (AIP, Woodbury, NY), p. 233.
- Yamagiwa, M., and J. Koga, 1999, *J. Phys. D* **32**, 2526.
- Yamakawa, K., Y. Akahane, M. Aoyama, Y. Fukuda, N. Inoue, J. Ma, and H. Ueda, 2002, *Superstrong Fields in Plasmas*, edited by M. Lontano, G. Mourou, O. Svelto, and T. Tajima, AIP Conf. Proc. No. 611 (AIP, Melville, NY), p. 385.
- Yamakawa, K., H. Shiraga, and Y. Kato, 1991, *Opt. Lett.* **16**, 1593.
- Yamazaki, A., H. Kotaki, I. Daito, *et al.*, 2005, *Phys. Plasmas* **12**, 093101.
- Yokoya, K., 2000, *Nucl. Instrum. Methods Phys. Res. A* **455**, 25.
- Zakharov, V. E., 1972, *Sov. Phys. JETP* **35**, 908.
- Zatsepin, G., and V. Kuzmin, 1966, *JETP Lett.* **4**, 78.
- Zel'dovich, Ya. B., 1975, *Sov. Phys. Usp.* **18**, 79.
- Zel'dovich, Ya. B., and Yu. P. Raizer, 1967, *Physics of Shock Waves and High-Temperature Hydrodynamic Phenomena* (Academic Press, New York).
- Zel'dovich, Ya. B., and V. S. Popov, 1972, *Sov. Phys. Usp.* **14**, 673.
- Zepf, M., G. D. Tsakiris, G. Pretzler, *et al.*, 1998, *Phys. Rev. E* **58**, R5253.
- Zhang, J., A. G. MacPhee, J. Lin, *et al.*, 1997, *Science* **276**, 1097.
- Zhidkov, A., J. Koga, A. Sasaki, and M. Uesaka, 2002, *Phys. Rev. Lett.* **88**, 185002.
- Zhidkov, A., J. Koga, K. Kinoshita, and M. Uesaka, 2004, *Phys. Rev. E* **69**, 035401(R).
- Zhidkov, A. G., A. Sasaki, and T. Tajima, 2000, *Phys. Rev. E* **61**, R2224.
- Zhidkov, A. G., A. Sasaki, T. Tajima, *et al.*, 1999, *Phys. Rev. E* **60**, 3273.
- Zhou, J., J. Peatross, M. M. Murnane, *et al.*, 1996, *Phys. Rev. Lett.* **76**, 752.
- Ziener, C., *et al.*, 2003, *J. Appl. Phys.* **93**, 768.
- Zweiback, J., T. E. Cowan, R. A. Smith, *et al.*, 2000, *Phys. Rev. Lett.* **85**, 3640.
- Zweiback, J., and T. Ditmire, 2001, *Phys. Plasmas* **8**, 4545.